

Aus dem Berlin-Brandenburger Centrum für
Regenerative Therapien (BCRT)
der Medizinischen Fakultät Charité – Universitätsmedizin Berlin

DISSERTATION

„Optimizing culture conditions for hepatic differentiation of human
induced pluripotent stem cells: from 3D culture systems to co-
cultures”

zur Erlangung des akademischen Grades
Doctor rerum medicinalium (Dr. rer. medic.)

vorgelegt der Medizinischen Fakultät
Charité – Universitätsmedizin Berlin

von
Nora Freyer
aus Jena

Datum der Promotion: 16.06.2018

INHALTSVERZEICHNIS

ZUSAMMENFASSUNG DER PUBLIKATIONSPROMOTION	1
ABSTRACT (deutsch)	1
ABSTRACT (englisch)	2
INTRODUCTION.....	3
<i>Scientific background</i>	3
<i>Aim of the thesis</i>	4
METHODS.....	6
<i>Culture of undifferentiated hiPSC</i>	6
<i>Hepatic differentiation of hiPSC in 2D cultures</i>	6
<i>Hepatic differentiation of hiPSC in perfused 3D bioreactors</i>	7
<i>Culture of primary human hepatocytes (PHH)</i>	7
<i>Co-culture with HUVEC during hepatic differentiation of hiPSC</i>	7
<i>Analysis of metabolic parameters and protein secretion</i>	8
<i>Gene expression analysis of stage specific markers</i>	8
<i>Immunofluorescence studies</i>	9
<i>Measurement of cytochrome P450 (CYP) isoenzyme activities</i>	9
<i>Statistical evaluation</i>	10
RESULTS.....	10
<i>Hepatic differentiation of hiPSC in 3D bioreactors or 2D cultures (Freyer et al., 2016)</i>	10
<i>Hepatic differentiation of hiPSC in 3D cultures: a comparative study (Meier et al., 2017)</i>	12
<i>Hepatic differentiation of hiPSC in co-culture with HUVEC using optimized culture media (Freyer et al., 2017)</i>	13
DISCUSSION	15
REFERENCES.....	18
EIDESSTATTLICHE VERSICHERUNG	21
ANTEILSERKLÄRUNG AN DEN ERFOLGTEN PUBLIKATIONEN	22
ORIGINALARBEITEN ALS PROMOTIONSLEISTUNG.....	23
LEBENS LAUF	71
KOMPLETTE PUBLIKATIONS LISTE	73
DANKSAGUNG.....	74

ZUSAMMENFASSUNG DER PUBLIKATIONSPROMOTION

ABSTRACT (deutsch)

Die Differenzierung von humanen induzierten pluripotenten Stammzellen (hiPSC) zu Hepatozyten stellt eine vielversprechende Alternative zu primären humanen Hepatozyten (PHH) dar, die in Zelltherapien oder in der Medikamententestung mit *in vitro* Modellen Anwendung finden könnte. Bisher zeigen aus hiPSC gewonnene Hepatozyten im Vergleich zu PHH allerdings einen unreifen Phänotyp.

Das Ziel dieser Promotion war die Optimierung der Kulturbedingungen für die hepatische Differenzierung von hiPSC, um deren Funktionalität zu verbessern. Im ersten Schritt wurde die hepatische Differenzierung auf einen perfundierten 3D-Bioreaktor übertragen, um physiologischere Kulturbedingungen zu schaffen. Dafür wurden zwei unterschiedliche Differenzierungsprotokolle und hiPSC-Linien verwendet und das Differenzierungsergebnis mit statischen 3D-Sphroiden und 2D-Kulturen verglichen. Der Ausreifungsgrad wurde anhand der Gen- und Proteinexpression hepatischer Marker und der Aktivität verschiedener pharmakologisch relevanter Cytochrom-P450-Isoenzyme (CYP) im Vergleich zu PHH beurteilt. Die im 3D-Bioreaktor differenzierten hiPSC wiesen mit beiden Differenzierungsprotokollen und hiPSC-Linien eine erhöhte Sekretion hepatischer Exportproteine wie Albumin oder Alpha-1-Antitrypsin auf. Außerdem wurden gesteigerte Aktivitäten von Enzymen des Arzneimittelstoffwechsels wie CYP1A2 oder CYP2B6 im Vergleich zu 3D-Sphroiden und 2D-Kulturen gemessen. Mittels immunhistochemischer Untersuchungen wurde die Bildung gewebส์ähnlicher Strukturen im 3D-Bioreaktor gezeigt. Allerdings war die Funktionalität auch der im 3D-Bioreaktor differenzierten hiPSC geringer als die der PHH.

Im zweiten Schritt wurde der Einfluss einer Kokultur mit humanen Endothelzellen auf die hepatische Ausreifung der hiPSC untersucht, da Endothelzellen bereits vor der Vaskularisierung entscheidend für die embryonale Leberentwicklung sind. Zu diesem Zweck wurde die hepatische Differenzierung von hiPSC in 2D-Kulturen mit oder ohne Zugabe von *human umbilical vein endothelial cells* (HUVEC) durchgeführt. Dabei wurden verschiedene Mischungen aus endothelzell- und hepatozytenspezifischen Kulturmedien verwendet. Die Zugabe der optimierten Kokulturmedien führte zu einer deutlichen Erhöhung der CYP-Aktivitäten und der mRNA-Expression hepatischer Marker wie *hepatocyte nuclear factor 4 alpha*, unabhängig davon, ob HUVEC dazugegeben wurden oder nicht.

Die Ergebnisse lassen den Schluss zu, dass der Bioreaktor die hepatische Ausreifung der aus hiPSC generierten Hepatozyten unterstützt. Die Untersuchungen zur Kokultur mit Endothelzellen in 2D-Kulturen zeigten, dass der positive Effekt der optimierten Kokulturmedien den Effekt der HUVEC-Kokultur selbst übertraf.

Der nächste logische Schritt, um die drei hier beschriebenen Studien zu verbinden, wäre daher die Untersuchung einer Kokultur mit hiPSC und Endothelzellen während der hepatischen Differenzierung im 3D-Bioreaktor.

ABSTRACT (englisch)

The derivation of hepatocytes from human induced pluripotent stem cells (hiPSC) represents a promising alternative to primary human hepatocytes (PHH) for potential applications in cell therapies or drug toxicity testing using *in vitro* models. To date, hiPSC-derived hepatocytes still show an immature phenotype when compared to PHH.

The aim of this thesis was to optimize culture conditions for the hepatic differentiation of hiPSC to improve their functionality. In the first step the hepatic differentiation was transferred to a perfused 3D bioreactor to create a more physiological culture environment. Therefore, two different differentiation protocols and hiPSC lines were applied and the differentiation outcome was compared to static 3D spheroids and 2D cultures. The maturation state was analyzed with respect to gene and protein expression of hepatic markers as well as activity of different pharmacologically relevant cytochrome P450 (CYP) isoenzymes, using PHH as reference cells. The results of both differentiation protocols and cell lines indicate a higher maturation of hiPSC-derived hepatocytes in 3D bioreactors compared with 2D cultures or 3D spheroids regarding secretion of hepatic export proteins such as albumin or alpha-1-antitrypsin. In addition increased activities of drug-metabolizing enzymes such as CYP1A2 or CYP2B6 were shown. Immunohistochemical studies revealed the formation of tissue-like structures. However, the functionality of the differentiated cells from the 3D bioreactor was still lower than in PHH cultures.

In the second step the effect of a co-culture with human endothelial cells on the hepatic maturation of hiPSC-derived hepatocytes was investigated, since it was observed that endothelial cells are important for the embryonic liver development prior to vascularization. For this purpose, hepatic differentiation of hiPSC was performed in 2D cultures in the presence or absence of human umbilical vein endothelial cells (HUVEC) using culture media mixtures based on endothelial cell and hepatocyte growth media. The use of the optimized co-culture media

resulted in distinctly increased CYP activities and mRNA expression of hepatic markers such as hepatocyte nuclear factor 4 alpha regardless whether HUVEC were present or not.

In conclusion, the results emphasize the potential of the bioreactor technology to support the hepatic maturation of hiPSC-derived hepatocytes. The positive effect of a co-culture with endothelial cells investigated in 2D cultures was outweighed by the effect of the optimized co-culture media.

Hence, the next logical step to combine the three studies of the present thesis would be the investigation of HUVEC-hiPSC co-cultures during hepatic differentiation in the 3D bioreactors.

INTRODUCTION

Scientific background

The derivation of hepatocytes from human pluripotent stem cells represents a promising alternative to primary human hepatocytes (PHH) for applications in cell therapies, but also in disease research and drug toxicity testing using *in vitro* models.

The liver represents the central organ involved into drug metabolism and is therefore a major target of drug-associated toxicity. For this reason, human hepatocytes, the parenchymal cells of the liver, are of special interest for toxicological investigations during pre-clinical drug testing. PHH, although considered as the current gold-standard for *in vitro* investigations, are only scarcely available and show a high inter-donor variability leading to unpredictable fluctuations in cell quality. Thus, there is a hitherto unmet need for alternative human cell sources for *in vitro* hepatic drug studies.

Pluripotent stem cells can differentiate into any cell type of the three germ layers (endoderm, mesoderm, ectoderm) and can be easily obtained in sufficient numbers due to their high proliferative capacities. Human pluripotent stem cells have first been obtained in the form of human embryonic stem cells (hESC) that are derived from the inner cell mass of a blastocyst [1]. More recently the derivation of human induced pluripotent stem cells (hiPSC) by reprogramming somatic cell types with pluripotency and proliferation genes was described [2]. They have the same characteristics as hESC but are not subject of ethical concerns. Current differentiation protocols into hepatocytes were initially developed for hESC and consist of a three-step procedure mimicking the embryonic development of the liver: i) induction of definitive endoderm (DE), ii) differentiation into hepatoblasts and iii) final maturation into hepatocytes [3-6]. Studies investigating the potentials of hiPSC-derived hepatocytes for cell therapies, disease modeling and drug toxicity testing showed promising results [7]. Despite these encouraging

results the functionality of hiPSC-derived hepatocytes remains low – they are commonly called hepatocyte-like cells (HLC) and their characteristics are more comparable to fetal rather than to adult PHH [8]. Attempts to further improve the maturation of HLC include the transfer of the differentiation process from conventional 2D cultures to a 3D culture environment to provide more physiological culture conditions. Thereby the cultivated cells are able to form more cell-cell contacts important for the maintenance of a mature hepatic phenotype. A 3D culture can be realized either scaffold free by self-aggregation of the cells or based on scaffolds such as collagen or hollow-fibers [9]. Furthermore, perfused culture systems have been developed to provide an even better approximation of the *in vivo* situation by enhancing oxygenation and medium supply of the cultured cells [9]. The perfused 3D bioreactor applied in the present thesis has been originally developed as an extracorporeal liver support system and was down-scaled for *in vitro* applications [10]. In this bioreactor cells are growing in the extra-capillary space of hollow-fiber membranes that are perfused with medium and air [10]. There is also increasing evidence that, next to a 3D culture environment, the co-culture with non-parenchymal cells could also improve the hepatic functionality of hiPSC-derived HLC [11]. It has been shown that endothelial cells play a role during embryonic liver development prior to the formation of a functional vasculature [12]. Thus, the development of co-culture approaches could further advance the maturity of hiPSC-derived hepatic cells.

Aim of the thesis

The aim of this thesis was to optimize culture conditions for hepatic differentiation of hiPSC-derived HLC to be used in preclinical drug research.

In the first step the hepatic differentiation was transferred to a perfused 3D bioreactor. Two different differentiation protocols and hiPSC lines were applied and the differentiation outcome was compared to static 3D spheroids and 2D cultures both being differentiated with the same protocols. The maturation state of the HLC derived in the different culture systems was analyzed with respect to gene and protein expression of hepatic markers as well as functionality of pharmacological relevant cytochrome P450 (CYP) isoenzymes, using PHH as reference cells (Freyer *et al.*, 2016; Meier *et al.*, 2017).

In the second step the effect of a co-culture with human umbilical vein endothelial cells (HUVEC) on the hepatic maturation of hiPSC-derived HLC was investigated using optimized co-culture media. For this purpose, hepatic differentiation of hiPSC was performed in 2D cultures in the presence or absence of HUVEC and with culture media mixtures based on endothelial cell and hepatocyte growth media. The differentiation outcome was evaluated on the

basis of gene and protein expression of stage-specific markers as well as CYP activities. This allowed judging not only the effect of HUVEC co-culture but also those of culture media adapted for co-culture purposes (Freyer *et al.*, 2017).

The objectives of this thesis and the corresponding publications that address these questions are summarized graphically in Figure 1.

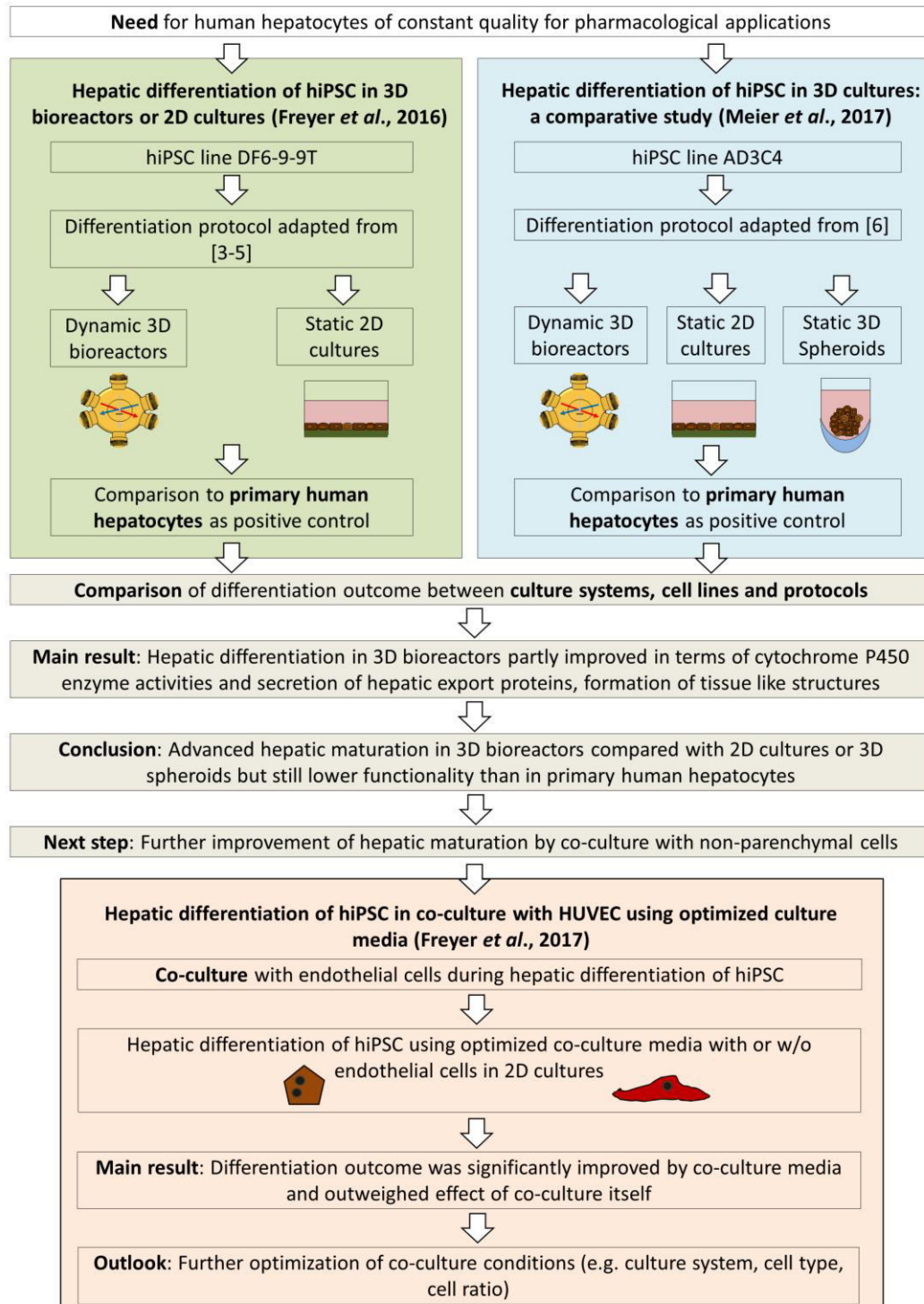


Figure 1: Schematic outline of the present thesis comprising of three publications (illustrations of culture systems from (Meier *et al.*, 2017, Int J of Mol Med, 40:1759-1771)).

METHODS

Culture of undifferentiated hiPSC

For the present thesis the hiPSC lines DF6-9-9T (WiCell Research Institute, Madison, WI, USA) [13] and SB Adult 3 clone 4 (AD3C4) [14] were applied. The cells were expanded on six-well cell culture plates coated with 8.68 $\mu\text{g}/\text{cm}^2$ Matrigel (growth factor reduced, Corning, NY, USA) using mTeSRTM1 medium (Stemcell Technologies, Vancouver, BC, Canada) containing 0.05 mg/ml gentamycin (Merck, Darmstadt, Germany) or 100,000 U/l penicillin and 100 mg/l streptomycin (Life Technologies, Carlsbad, CA, USA). The cells were passaged after reaching a confluency of around 70% using 2 mg/ml dispase or 0.5 mM EDTA (both Life Technologies). Medium was exchanged daily and hiPSC were maintained at 37°C and 5% CO₂.

Hepatic differentiation of hiPSC in 2D cultures

Two protocols for hepatic differentiation were applied, both of them consisting of three steps as compared in Table 1. Cytokines were all purchased from Peprotech (London, UK), except for Wnt3a from R&D Systems (Minneapolis, MN, USA). Sodium butyrate, DMSO and hydrocortisone were obtained from Sigma Aldrich (St. Louis, MO, USA). RPMI 1640 culture medium was from Merck and hepatocyte culture medium HCM from Lonza (Walkersville, MD, USA). All other media and supplements were purchased from Life Technologies.

Table 1: Protocols for hepatic differentiation of hiPSC as applied in the present thesis.

Differentiation Stage	Freyer <i>et al.</i>, 2016 and 2017 (adapted from [3-5]), hiPSC line DF6-9-9T	Meier <i>et al.</i>, 2017 (adapted from [6]), hiPSC line AD3C4
Step 1: Definitive endoderm	RPMI 1640 culture medium supplemented with 100 ng/ml activin A, 50 ng/ml Wnt3a, 1 μM sodium butyrate and 2% (v/v) B27 supplements without insulin Duration: 3 days (d0-d3)	STEMdiff TM Definitive Endoderm Kit (Stemcell Technologies) according to the manufacturer's instructions Duration: 5 days (d0-d5)
Step 2: Hepatoblasts	Hepatocyte culture medium with single quotes supplemented with 10 ng/ml hepatocyte growth factor (HGF) (HCM-I) Duration: 10 days (d3-d13)	Knockout DMEM with 20% Knockout Serum Replacement, 0.5% GlutaMAX, 1% Non-Essential Amino Acids, 0.1 mM β -Mercaptoethanol and 1% DMSO Duration: 4 days (d5-d9)
Step 3: Hepatocyte-like cells	Hepatocyte culture medium with single quotes supplemented with 10 ng/ml HGF and 10 ng/ml oncostatin M (OSM) (HCM-II) Duration: 4 days (d13-d17)	Hepatocyte maturation medium with 1% GlutaMAX, 10 μM hydrocortisone, 10 ng/ml HGF and 20 ng/ml OSM Duration: 9 days (d9-d18)

Hepatic differentiation of hiPSC in perfused 3D bioreactors

The here applied 3D bioreactors (StemCell Systems, Berlin, Germany) had a cell compartment volume of 2 ml. They were connected to a tubing system for medium perfusion (StemCell Systems) and integrated into a perfusion device (StemCell Systems) consisting of two modular pump units, a heating chamber and an electronically controlled gas mixing unit (Vögtlin Instruments, Aesch, Switzerland). Prior to cell inoculation the cell compartment was coated with 3 mg Matrigel (Corning) for 1 h at room temperature. Afterwards a number of 100×10^6 cells were inoculated into each bioreactor. The temperature was kept at 37°C, the medium recirculation rate was 10 ml/min, the initial feed rate was 1 ml/h and air containing 5% CO₂ was supplied at a flow rate of 20 ml/min. Perfusion rates of medium and amount of CO₂ were adjusted, if necessary, to maintain sufficient glucose levels of at least 25 mg/dl and a pH of 7.2 to 7.4. After an adaptation phase of 2 days (Meier *et al.*, 2017) resp. 3 days (Freyer *et al.*, 2016) in mTeSRTM1 medium hepatic differentiation was conducted by perfusion of the bioreactors with the different differentiation media as indicated in Table 1. Between each differentiation step, the bioreactor was flushed with 60 ml of the next medium to remove the medium used in the previous step.

Culture of primary human hepatocytes (PHH)

PHH were isolated from macroscopically healthy tissue from resected human liver with informed consent of the patients and approval by the Ethical Committee of the Charité - Universitätsmedizin Berlin (EA2/026/09). Cell isolation was performed according to Pfeiffer *et al.* [15]. A number of 2.0×10^5 cells/cm² were seeded onto rat-tail collagen coated cell culture plates using Heparmed Vito 143 supplemented with 0.8 mg/l insulin, 5 mg/l transferrin, 0.003 mg/l glucagon (ITG), 100,000 U/l penicillin and 100 mg/l streptomycin (all Merck, Darmstadt, Germany) and 10% fetal calf serum (PAA, Dartmouth, MA, USA).

Co-culture with HUVEC during hepatic differentiation of hiPSC

Prior to co-culture, cells of the hiPSC line DF6-9-9T (WiCell Research Institute) were differentiated into DE cells according to the protocol adapted from Hay and colleagues (Table 1) [3-5]. Afterwards HUVEC (PromoCell GmbH, Heidelberg, Germany) were added at a ratio of 1:2 (5×10^5 HUVEC + 1×10^6 DE cells). Further differentiation was carried out using i) a 1:1 mixture of the differentiation medium (HCM-I/II, Table 1) and endothelial cell growth medium (PromoCell GmbH), consisting of basal medium and supplements (EGM complete), or ii) HCM-I/II enriched with endothelial cell growth supplements (EGM supplements). In parallel, DE cells

were differentiated without HUVEC applying the described medium mixtures or pure HCM-I/II for control.

Analysis of metabolic parameters and protein secretion

Measurement of metabolic parameters was performed at defined time-intervals in samples from 3D or 2D cultures. Parameters and measurement methods are listed in Table 2.

Table 2: Analysis of secreted proteins and metabolites during hepatic differentiation of hiPSC

Parameter	Freyer <i>et al.</i> 2016 and 2017	Meier <i>et al.</i> 2017
Glucose and lactate	Blood gas analyzer (ABL 700, Radiometer, Copenhagen, Denmark)	Blood gas analyzer (ABL 700, Radiometer, Copenhagen, Denmark)
Lactate dehydrogenase (LDH)	clinical chemistry analyzer (Cobas® 8000; Roche Diagnostics, Mannheim, Germany)	Not analyzed
Alpha-1-antitrypsin (A1AT)	Not analyzed	ELISA protocol as described by Dakocytomation (Glostrup, Denmark)
α -fetoprotein (AFP)	clinical chemistry analyzer (Cobas® 8000; Roche Diagnostics)	ELISA protocol as described by Dakocytomation (Glostrup, Denmark)
Urea	clinical chemistry analyzer (Cobas® 8000; Roche Diagnostics)	QuantiChrom™ Urea Assay Kit (BioAssay Systems, Hayward, CA, USA)
Albumin (ALB)	ELISA Quantitation kit (Bethyl Laboratories, Montgomery, TX, USA)	ELISA protocol as described by Dakocytomation (Glostrup, Denmark)

Gene expression analysis of stage specific markers

Isolation of RNA and subsequent cDNA synthesis was performed using PureLink™ RNA Mini Kit (Life Technologies) and High Capacity cDNA Reverse Transcription Kit (Applied Biosystems, Foster City, CA) as described previously [16]. The cDNA was mixed with PCR Master mix (Applied Biosystems) and human-specific primers and probes (TaqMan GeneExpression Assay system, Life Technologies). Quantitative real-time PCR (qRT-PCR) was carried out with the Mastercycler ep Realplex 2 (Eppendorf, Hamburg, Germany). The expression of analyzed genes was normalized to that of the housekeeping gene glyceraldehyde-3-phosphate dehydrogenase (*GAPDH*). Fold changes of expression levels relative to undifferentiated hiPSC were calculated using the $\Delta\Delta C_t$ method. The mRNA expression of the following genes was analyzed: *AFP*, *ALB*, *CYP1A2*, *CYP2B6*, *CYP2C9*, *CYP3A4*, cytokeratin 18 (*KRT18* alias CK18), GATA binding protein 2 (*GATA2*), hepatocyte nuclear factor 4 alpha (*HNF4A*), Neurofilament, light polypeptide (*NEFL*), platelet and endothelial cell adhesion molecule 1 (*PECAM1*), POU domain, class 5, transcription factor 1 (*POU5F1* alias Oct-3/4), Nanog homeobox (*NANOG*), SRY-box 7 (*SOX7*) and SRY-box 17 (*SOX17*).

Immunofluorescence studies

All samples were fixed with 4% formaldehyde solution (Herbeta Arzneimittel, Berlin, Germany). 2D cultures were permeabilized with ice-cold 80% (v/v) methanol (J.T. Baker, Deventer, The Netherlands) whereas bioreactor and tissue samples were dehydrated, paraffinized, and cut into slides of 2.5 μm thickness. Then, the slides were deparaffinized and rehydrated. Antigen retrieval was performed by boiling the samples in citrate buffer (pH 6.0) for 15 min. Antibody staining was performed for all samples as described previously [16]. Samples were incubated with primary antibodies for the following antigens: ALB, AFP, cytokeratin 18 (KRT18 alias CK18), cytokeratin 19 (KRT19, alias CK19), CYP1A2, CYP2B6, HNF4A, Ki-67, multidrug resistance-associated protein 2 (MRP2), POU domain, class 5, transcription factor 1 (POU5F1, alias Oct-3/4), stage-specific embryonic antigen 4 (SSEA-4) and tight junction protein 1 (TJP1). The following secondary antibodies were used: Alexa Fluor® 488 anti-mouse and Alexa Fluor® 594 anti-rabbit (Life Technologies).

Measurement of cytochrome P450 (CYP) isoenzyme activities

Determination of CYP activities was performed by incubating the cultures with a drug cocktail containing substrates for pharmacological relevant CYP isoenzymes (Table 3). Phenacetin and diclofenac were purchased from Sigma Aldrich, bupropion from Toronto Research Chemicals (North York, ON, Canada) and midazolam from Roche (Basel, Switzerland). Concentrations of specific products were measured in samples taken from culture supernatants/perfusates at predefined time intervals. Analyses were performed by means of LC-MS by cooperation partners at Janssen Research and Development or at Boehringer Ingelheim Pharma GmbH & Co.KG.

Table 3: Analyzed CYP isoenzymes, their substrates with applied final concentrations and resulting products

Enzyme	Freyer <i>et al.</i> 2016 and 2017	Meier <i>et al.</i> 2017
CYP1A2	Substrate: 100 μM phenacetin Product: Acetaminophen	Substrate: 25 μM phenacetin Product: Acetaminophen
CYP2B6	Substrate: 500 μM bupropion Product: 6-Hydroxybupropion	Substrate: 75 μM bupropion Product: 6-Hydroxybupropion
CYP2C9	Substrate: 25 μM diclofenac Product: 4'-Hydroxydiclofenac	Not analyzed
CYP3A4/5	Substrate: 10 μM midazolam Product: 1'-Hydroxymidazolam	Substrate: 25 μM midazolam Product: 1'-Hydroxymidazolam

Statistical evaluation

Data evaluation and graphical illustration were performed with GraphPad Prism 5.0 and 7.0 (GraphPad Software, SanDiego, CA, USA). Experiments were performed at least in triplicates, and results are presented as mean \pm standard error of the mean or as median \pm interquartile range. The area under curve (AUC) was calculated for time courses of biochemical parameters and differences between culture systems or culture conditions were detected with an unpaired, two-tailed Student's t-test or one-way analysis of variance (ANOVA). Differences were judged as significant, if the p-value was less than 0.05.

RESULTS

Hepatic differentiation of hiPSC in 3D bioreactors or 2D cultures (Freyer et al., 2016)

In this study, the hepatic differentiation of the hiPSC line DF6-9-9T was comparatively investigated in 3D bioreactors and conventional 2D cultures, using a range of markers on metabolic, protein and gene expression level. Differentiation of hiPSC into HLC was performed applying the same protocol for both culture systems: i) differentiation into DE cells was induced using activin A, Wnt3a and sodium butyrate, ii) afterwards HGF was added to drive further differentiation and iii) final maturation was achieved with HGF and OSM.

The metabolic activity, integrity and differentiation behavior of hiPSC was assessed by daily measurement of parameters in the culture perfusate resp. supernatants. The energy metabolism was assessed by measuring glucose consumption and lactate production, which increased over time in both, 2D cultures and 3D bioreactors, during hepatic differentiation. In 2D cultures average glucose consumption rates per cell were significantly higher than in 3D bioreactors. Lactate production rates mirrored those of glucose consumption. The cell integrity was monitored by measuring LDH release into the culture medium. In 2D cultures a significantly higher LDH liberation than in 3D bioreactors was observed during the first 3 days of differentiation, which decreased to basal levels afterwards. Furthermore the differentiation process was constantly monitored by measuring the secretion of liver-specific proteins and metabolites into the culture supernatant. Secretion of the albumin precursor protein AFP, indicating the presence of hepatoblasts, increased in 2D cultures from day 7 onwards and in 3D bioreactors from day 9 onwards, but in 2D cultures the increase was significantly higher than in 3D bioreactors. Albumin secretion, indicating the presence of mature hepatocytes, was detected in both culture systems from day 12 onwards. Maximum values achieved at the end of differentiation on day 17 were thrice as high in 3D bioreactors compared to 2D cultures. Urea

secretion rates showed a constant increase in 3D bioreactors over the whole differentiation period whereas in 2D cultures a fluctuating time course was observed with peaks at the beginning of differentiation and between day 9 and 13.

CYP activities of the obtained HLC were analyzed by their ability to metabolize various substrates into products specific for different pharmacologically relevant CYP isoenzymes. Activities of CYP1A2 and CYP2B6 were higher in 3D bioreactors as compared with 2D cultures, with a generally higher activity of CYP1A2. In contrast, CYP3A4/5 activity was higher in 2D cultures. All CYP activities were significantly lower in HLC cultures as compared to those detected in PHH.

At the end of differentiation, both culture systems were compared regarding the gene expression of stage specific markers relative to undifferentiated hiPSC. The expression of the pluripotency genes *POU5F1* and *NANOG* was downregulated in both culture systems compared to undifferentiated hiPSC, with 2D cultures showing a significantly stronger down-regulation than HLC differentiated in 3D bioreactors. The endodermal markers *AFP* and *SOX17* showed a 60,000-fold resp. 20-fold increased gene expression in both culture systems, whereas PHH showed no relevant expression of these markers. In addition, a 100-fold increased expression of the mesodermal marker *GATA2* was observed in 3D bioreactor cultures. Among the markers for mature hepatocytes, *ALB* showed the highest up-regulation in HLC cultures. In 3D bioreactors *ALB* expression was twice as high as in 2D cultures being in line with the results from albumin secretion. Gene expression of *CYP1A2* and *CYP2B6* was downregulated in both culture systems relative to undifferentiated hiPSC, but 3D bioreactors still showed a higher expression of these markers than 2D cultures. For *CYP2C9* and *CYP3A4/5* an increased gene expression of 40-fold resp. five-fold was detected showing no distinct differences between the two culture systems. PHH showed a distinctly higher gene expression of all markers for mature hepatocytes compared to HLC from both culture systems.

In addition, the protein expression of stage specific markers was analyzed before and after hepatic differentiation of hiPSC by means of immunofluorescence staining performed in comparison to native human liver tissue. In cultures of undifferentiated hiPSC almost all cells were positive for the pluripotency markers *POU5F1* and *SSEA-4*, whereas HLC and native human liver tissue were devoid of these markers. Vice versa, markers for mature hepatocytes such as albumin and *HNF4A* were observed in both HLC cultures and native liver tissue but not in undifferentiated cells. In 3D bioreactors the double-staining of *KRT18* and *KRT19* revealed ring-shaped cell arrangements lined with stained cells indicating the formation of bile-duct like

structures similar to native liver tissue. The tight junction protein TJP1 and the transporter MRP2 could not be detected in 2D cultures, while in 3D bioreactors thin fluorescent borders between the cells were observed indicating the presence of TJP1. In the native liver tissue, the majority of the cells were double positive for MRP2 and TJP1. Furthermore, most of the cells in 2D cultures and 3D bioreactors were positive for CYP1A2, but negative for CYP2B6, which is in line with the functional analysis showing higher activities for CYP1A2. In 3D bioreactors, the inner ring of tubular-like structures lacked CYP1A2 immunoreactivity confirming the presence of bile duct cells. In native human liver tissue, most cells were positive for both CYP isoenzymes.

To assure that normalization of secretion rates and activities to the initial cell number did not falsify the comparison of the two culture models, the amount of proliferating cells was detected before, during and after hepatic differentiation applying immunofluorescence staining of the proliferation marker Ki-67. In cultures of undifferentiated hiPSC, almost all cells showed immunoreactivity for Ki-67. In 2D cultured DE cells, the amount of proliferating cells was lowered to two thirds and after hepatic differentiation around one third of the cells were still proliferating in both culture systems. In native human liver tissue, no Ki-67 positive cells could be detected.

In summary, the results indicate a higher maturation of HLC in 3D bioreactors compared with 2D cultures regarding albumin secretion, activity of CYP1A2 and 2B6 as well as formation of tissue-like structures. However, full hepatic functionality was not yet achieved; for example, the albumin precursor-protein AFP was still expressed, and the activity of CYP2C9 and expression of the biliary transporter MRP2 could not be detected.

Hepatic differentiation of hiPSC in 3D cultures: a comparative study (Meier et al., 2017)

In this study, the hepatic differentiation of hiPSC in 3D bioreactors was evaluated using a different cell line and protocol. The differentiation outcome in the bioreactor system was compared to that in 2D cultures and 3D spheroids, which were differentiated by the co-authors of this study applying the same differentiation protocol. The hiPSC line AD3C4 was differentiated into HLC in 3D bioreactors applying a modified three-step differentiation protocol: i) differentiation into DE cells was induced using a commercial available kit purchased from Stemcell Technologies, ii) afterwards hepatoblast differentiation was induced with DMSO and iii) final maturation was achieved with HGF and OSM.

To monitor the differentiation process daily measurements of secreted proteins and metabolites were performed similar to the study with the hiPSC line DF6-9-9T (Freyer et al., 2016). AFP secretion was detected at a similar range in all culture systems from day 10 or 11 of

differentiation onwards and increased until day 13 or 15. Afterwards AFP secretion distinctly decreased to almost zero until the last day of differentiation (d18). The magnitude of AFP secretion rates was around 20 to 40-fold lower when compared to secretion rates of this protein observed for the hiPSC line DF6-9-9T (Freyer *et al.*, 2016). ALB secretion could only be observed in 3D bioreactors but not in 2D cultures or 3D spheroids and was in a similar range as compared to secretion rates observed for the hiPSC line DF6-9-9T by Freyer *et al.* (2016). Additionally, the secretion of A1AT was determined, since this protein is also secreted by mature hepatocytes. Similar to ALB, A1AT was only secreted by 3D bioreactor cultures. In contrast, urea production was observed in all culture systems from day 11 on with the 3D spheroids showing a strong peak at day 13, which was three- to five-fold higher than rates in 2D cultures and 3D bioreactors on that day. Afterwards, urea production of 3D spheroids decreased rapidly down to zero on day 18. In 2D cultures urea production rates also showed a moderate increase until day 15 followed by decreasing values until day 18 reaching similar ranges as observed in the 3D bioreactors. Values for urea production in the bioreactor system were comparable to those observed for the hiPSC line DF6-9-9T by Freyer *et al.* (2016).

Activities of pharmacologically relevant CYP isoenzymes were analyzed by measuring the conversion of drugs into isoenzyme specific products. Among the hiPSC-derived HLC cultures only the 3D bioreactors showed CYP1A2 activity. Activity of CYP2B6 could not be detected in any of the culture systems, which is in contrast to the findings from the hiPSC line DF6-9-9T by Freyer *et al.* (2016), showing CYP2B6 activities at least in 3D bioreactor cultures. The isoenzyme CYP3A4 showed the highest activity in 3D spheroids followed by 3D bioreactors and 2D cultures. Cultures of PHH used as reference cells showed distinctly higher values compared to hiPSC-derived HLC cultures.

In summary, the study confirms an advanced hepatic maturation of HLC in dynamic 3D bioreactors as compared to static 3D spheroids or 2D cultures. However, the results also showed that the functionality of the differentiated cells was still lower than in PHH cultures.

Hepatic differentiation of hiPSC in co-culture with HUVEC using optimized culture media (Freyer et al., 2017)

In this study, co-culture of HUVEC with hiPSC-derived DE cells during hepatic differentiation was investigated aiming to further improve hepatic maturation of HLC. In a further aspect of the study, the effect of optimized co-culture media on the differentiation outcome was analyzed in HLC cultures maintained with or without HUVEC addition. Experiments were performed in 2D cultures with two different media, i) a 1:1 mixture of the differentiation medium (HCM-I/II,

Table 1) and the endothelial cell growth medium EGM complete, or ii) HCM-I/II enriched with EGM supplements. These media were applied during hepatic differentiation of hiPSC (cell line DF6-9-9T) in the presence or absence of HUVEC and in comparison with hiPSC mono-cultures differentiated in pure HCM-I/II medium.

The secretion of stage-specific proteins and metabolites was measured over the whole differentiation period. Secretion rates of AFP were significantly increased in hiPSC mono-cultures differentiated with the optimized co-culture media compared to HCM-I/II medium while addition of HUVEC did not further increase AFP secretion. For albumin secretion the results were similar although the differences were not significant due to large variances. Results for urea secretion were different: here, the HCM-I/II cultures showed similar values as the co-cultures and the mono-cultures using HCM-I/II enriched with EGM supplements.

Activities of different CYP isoenzymes (CYP1A2, CYP2B6 and CYP3A4), as analyzed by applying a drug cocktail and measuring isoenzyme specific products, were distinctly increased in mono-cultures using the two optimized co-culture media compared to mono-cultures using HCM-I/II. Co-culture with HUVEC did not result in a further increase of CYP activities.

The gene expression analysis of stage specific markers relative to undifferentiated hiPSC revealed a down-regulation of the pluripotency marker *POU5F1* in all experimental conditions. Expression of *AFP* was increased in all experimental groups compared to undifferentiated hiPSC. The highest values were observed in the co-cultures using HCM-I/II enriched with EGM supplements and in the corresponding mono-cultures. A similar result was observed for *ALB* gene expression. The gene expression of the epithelial marker *KRT18* was also increased, although to a lower extent than that of *AFP* and *ALB*, showing no differences between the different culture conditions. In contrast, the gene expression of *HNF4A* was distinctly higher in mono-cultures using the two co-culture media as compared to HCM-I/II. Again, addition of HUVEC did not show a further effect. As expected, the gene expression of the endothelial marker *PECAMI* was distinctly higher in both co-cultures as compared to hiPSC mono-cultures, although lower than in HUVEC mono-cultures analyzed as a positive control for the endothelial cell marker.

To complement the results from gene expression, some of these markers were additionally analyzed on the protein expression level using immunofluorescence analysis. Immunoreactivity for the pluripotency marker *POU5F1* was observed only in undifferentiated hiPSC, whereas all HLC cultures were devoid of this marker. The epithelial marker *KRT18* was observed in all HLC cultures although to a varying extent: Cells in HCM-I/II mono-cultures were to around 80% positive for *KRT18*, whereas in the other experimental groups 40% to 60% of the cells

expressed this marker, resulting in a heterogeneous appearance. The hepatocyte marker HNF4A was also detected in all HLC cultures with the HCM-I/II mono-cultures showing almost two thirds of positive cells, whereas all other HLC cultures with or without HUVEC contained one third or less HNF4A positive cells. The presence of HUVEC was confirmed by positive staining of the endothelial cell marker PECAM1 in both co-culture conditions, while mono-cultures were negative for this marker.

In summary, the results show that the positive effect of the media adapted for co-culture purposes outweighed the effect of the HUVEC co-culture itself.

DISCUSSION

The generation of hepatocytes from hiPSC holds great potential for the development of *in vitro* models for pharmacological investigations and for potential clinical use in cell-based liver therapy approaches. To date, the phenotype of hiPSC-derived HLC is still immature when compared to their *in vivo* counterparts, the PHH [8]. Therefore, the potential of different 3D culture systems to improve the hepatic maturation of HLC was investigated in the present thesis. The detailed comparison of hepatic differentiation of hiPSC in static 2D cultures and perfused 3D bioreactors by Freyer *et al.* (2016) revealed differences with respect to glucose metabolism, which was significantly lower in 3D bioreactors as compared with 2D cultures. In addition, the cell population in 3D bioreactors was more heterogeneous than that in 2D cultures as indicated by gene and protein expression analysis of pluripotency and differentiation markers. These results could be attributed to gradient formation of nutrients and growth factors in 3D cell aggregates leading to a lower metabolic activity and a diverging differentiation of cells growing in the center of the cell aggregates. This assumption is supported by pictures of immunohistochemical staining showing a tissue-like organization of the cells including structures similar to bile-ducts and pronounced cell-cell contacts in the form of tight junctions. The 3D cell aggregates could also have a protective effect against cell damage caused by activin A applied for DE differentiation, which can cause apoptosis [17]. This would explain the significantly lower LDH release in 3D bioreactors compared to 2D cultures during the first 3 days of differentiation.

The functionality of hiPSC-derived HLC was assessed by analyzing the secretion of hepatic proteins such as albumin, urea production and activity of CYP isoenzymes (Freyer *et al.*, 2016; Meier *et al.*, 2017). Secretion of the albumin precursor protein AFP was observed in both studies in all culture systems and was in both cases highest in 2D cultures. In contrast, secretion of the

mature hepatocyte marker ALB was higher in 3D bioreactors than in 2D cultures (Freyer *et al.*, 2016) or could not even be detected in other culture systems than the 3D bioreactors (Meier *et al.*, 2017). In humans, AFP expression only occurs during liver embryogenesis, in fetal liver cells, and hepatocellular carcinomas [18], while ALB is produced by mature hepatocytes in the adult liver. Thus, the findings of AFP and ALB secretion indicate a higher maturation grade of HLC in 3D bioreactors than in 2D cultures or 3D spheroids. Urea production was measured as a further functional marker of mature hepatocytes and was observed in all culture systems with the 3D bioreactors showing the lowest but also most stable urea production rates in both studies (Freyer *et al.*, 2016; Meier *et al.*, 2017). For potential pharmacological applications the activity of drug-metabolizing enzymes is of particular interest. Hence, activities of different pharmacological relevant CYP isoenzymes were detected by measuring their ability to convert different drugs into isoenzyme specific products. Activities of CYP1A2 and CYP3A4 were observed in both studies, whereas CYP2B6 activity was detected only in the study by Freyer *et al.* (2016) and here only in 3D bioreactors but not in 2D cultures.

Differences in the differentiation outcome between the two studies can be attributed to several factors one of them being the varying differentiation protocols. The hepatoblast differentiation was achieved either by the application of DMSO (Meier *et al.*, 2017) or by addition of HGF (Freyer *et al.*, 2016). DMSO supports hepatocyte differentiation after DE induction [4] and down-regulates pluripotency genes [19] potentially by affecting histone acetylation [20] resulting in an altered gene transcription. HGF plays an important role in liver development [21] and supports HLC differentiation in a concentration dependent manner [3]. Another difference between the two differentiation protocols is the duration of the maturation phase with OSM, which took either 4 days (Freyer *et al.*, 2016) or 9 days (Meier *et al.*, 2017). The short duration of OSM application in the study of Freyer *et al.* (2016) could be the reason for the still high AFP secretion at the end of differentiation, which was not yet down-regulated as was the case for the study by Meier *et al.* (2017). In addition, albumin and urea secretion were still increasing at the end of the differentiation (Freyer *et al.*, 2016). Hence, a prolongation of the differentiation stage with OSM could lead to further maturation of the cells.

Furthermore the differentiation outcome could be influenced by differences in differentiation characteristics between the applied hiPSC lines. It was shown that HLC derived from different hiPSC lines displayed an inter-individual metabolic diversity [22], which is also characteristic for PHH obtained from different donors. Besides the used cell line, another factor of variation are the applied assays used to evaluate the differentiation outcome. For example, the different magnitudes for AFP secretion could be due to different ways of measuring AFP in the

supernatant either using a clinical chemistry analyzer (Freyer *et al.*, 2016) or an ELISA (Meier *et al.*, 2017). Thus, a direct comparison of data from different studies can be difficult, even if the experiments were performed in the same lab.

Despite certain differences between the studies of Freyer *et al.* (2016) and Meier *et al.* (2017) the overall outcome of both studies clearly shows that the use of perfused 3D bioreactors provides an instrument to enhance the hepatic maturation of HLC with respect to protein secretion, liver tissue formation and activities of drug-metabolizing enzymes. However, the functionality of HLC generated in the bioreactor system still remains low compared to PHH.

Hence, in the next step the effect of co-culturing hiPSC-derived DE cells with non-parenchymal cells during hepatic differentiation was investigated (Freyer *et al.*, 2017). An important precondition to a functional co-culture system is the use of a culture medium, which provides suitable conditions for hiPSC differentiation as well as support of the co-cultured cell type. For this reason DE cells were differentiated in static 2D cultures in the presence or absence of HUVEC comparing two different media mixtures having been adapted for co-culture purposes. The results were compared to hepatic differentiation in hiPSC mono-cultures using the HCM-I/II medium as a control.

The analysis of stage-specific marker expression and CYP activities revealed that both co-culture media improved the hepatic maturation of the HLC as compared to the HCM-I/II control cultures, regardless whether HUVEC were present or not. The favorable effects of the co-culture media on the differentiation outcome might be attributed to some of the factors contained in those media. The basic fibroblast growth factor (bFGF) contained in both co-culture media has been shown to support hepatoblast differentiation [23] and to induce gene expression of *HNF4A* [24]. In addition the test media contained an increased concentration of glucocorticoids compared to the HCM-I/II control medium, which induce expression of CYP2B, CYP2C and CYP3A in humans [25]. The fact that HUVEC did not further improve the hepatic maturation of HLC might be due to the chosen culture model and conditions. A larger growth area for HUVEC could be provided by creating a separate compartment from hiPSC using Transwells or different extracellular matrices. By this way, direct contact would be prevented while permitting the exchange of soluble factors. Optimization of the proportion of HUVEC in the co-cultures would be another option for achieving a significant influence of the cells. Furthermore, the addition of further cell types, apart from HUVEC, might be favorable, in accordance to reports on co-culture with HUVEC during hepatic differentiation of hiPSC in combination with either mesenchymal stem cells [11] or adipose derived stem cells [26] in 3D cultures.

In conclusion, the results of the studies emphasize the potential of the bioreactor technology to support the hepatic maturation of hiPSC-derived HLC whereas the effect of a co-culture with non-parenchymal cells investigated in 2D cultures was so far outweighed by the effect of the optimized co-culture media.

Hence, the next logical step to combine the three studies of the present thesis would be the investigation of HUVEC-hiPSC co-cultures during hepatic differentiation in the 3D bioreactors. This could be combined, e.g. with studies on different cell densities and ratios, and integration of further cell types in 3D co-culture models.

REFERENCES

1. Thomson JA, Itskovitz-Eldor J, Shapiro SS, Waknitz MA, Swiergiel JJ, Marshall VS, Jones JM. Embryonic stem cell lines derived from human blastocysts. *Science*, 1998; 282:1145-7.
2. Takahashi K, Tanabe K, Ohnuki M, Narita M, Ichisaka T, Tomoda K, Yamanaka S. Induction of pluripotent stem cells from adult human fibroblasts by defined factors. *Cell*, 2007; 131:861-872.
3. Hay DC, Zhao D, Ross A, Mandalam R, Lebkowski J, Cui W. Direct differentiation of human embryonic stem cells to hepatocyte-like cells exhibiting functional activities. *Cloning Stem Cells*, 2007; 9:51-62.
4. Hay DC, Zhao D, Fletcher J, Hewitt ZA, McLean D, Urruticoechea-Uriguen A, Black JR, Elcombe C, Ross JA, Wolf R, Cui W. Efficient differentiation of hepatocytes from human embryonic stem cells exhibiting markers recapitulating liver development in vivo. *Stem Cells*, 2008; 26: 894-902.
5. Hay DC, Fletcher J, Payne C, Terrace JD, Gallagher RC, Snoeys J, Black JR, Wojtacha D, Samuel K, Hannoun Z, Pryde A, Filippi C, Currie IS, Forbes SJ, Ross JA, Newsome PN, Iredale JP. Highly efficient differentiation of hESCs to functional hepatic endoderm requires Activin A and Wnt3a signaling. *Proc Natl Acad Sci U S A*, 2008; 105: 12301-12306.
6. Szkolnicka D, Farnworth SL, Lucendo-Villarin B, Hay DC. Deriving functional hepatocytes from pluripotent stem cells. *Curr Protoc Stem Cell Biol*, 2014; 30:1G.5.1-12.
7. Yi F, Liu GH, Izpisua Belmonte JC. Human induced pluripotent stem cells derived hepatocytes: Rising promise for disease modeling, drug development and cell therapy. *Protein Cell*, 2012; 4:246–250.

8. Baxter M, Withey S, Harrison S, Segeritz CP, Zhang F, Atkinson-Dell R, Rowe C, Gerrard DT, Sison-Young R, Jenkins R, Henry J, Berry AA, Mohamet L, Best M, Fenwick SW, Malik H, Kitteringham NR, Goldring CE, Piper Hanley K, Vallier L, Hanley NA. Phenotypic and functional analyses show stem cell-derived hepatocyte-like cells better mimic fetal rather than adult hepatocytes. *J Hepatol*, 2015; 62:581–9.
9. Lauschke VM, Hendriks DF, Bell CC, Andersson TB, Ingelman-Sundberg M. Novel 3D culture systems for studies of human liver function and assessments of the hepatotoxicity of drugs and drug candidates. *Chem Res Toxicol*, 2016; 29:1936-1955.
10. Zeilinger K, Schreiter T, Darnell M, Söderdahl T, Lübberstedt M, Dillner B, Knobloch D, Nüssler AK, Gerlach JC, Andersson TB. Scaling down of a clinical three-dimensional perfusion multicompartiment hollow fiber liver bioreactor developed for extracorporeal liver support to an analytical scale device useful for hepatic pharmacological in vitro studies. *Tissue Eng Part C Methods*, 2011; 17:549-56.
11. Takebe T, Sekine K, Enomura M, Koike H, Kimura M, Ogaeri T, Zhang RR, Ueno Y, Zheng YW, Koike N, Aoyama S, Adachi Y, Taniguchi H. Vascularized and functional human liver from an iPSC-derived organ bud transplant. *Nature*, 2013; 499:481–484.
12. Matsumoto K, Yoshitomi H, Rossant J, Zaret KS. Liver organogenesis promoted by endothelial cells prior to vascular function. *Science*, 2001; 294:559–563.
13. Yu J, Hu K, Smuga-Otto K, Tian S, Stewart R, Slukvin II, Thomson JA. Human induced pluripotent stem cells free of vector and transgene sequences. *Science*, 2009; 324:797–801.
14. van de Bunt M, Lako M, Barrett A, Gloyn AL, Hansson M, McCarthy MI, Beer NL, Honoré C. Insights into islet development and biology through characterization of a human iPSC-derived endocrine pancreas model. *Islets*, 2016; 8:83-95.
15. Pfeiffer E, Kegel V, Zeilinger K, Hengstler JG, Nüssler AK, Seehofer D, Damm G. Featured Article: Isolation, characterization, and cultivation of human hepatocytes and non-parenchymal liver cells. *Exp Biol Med (Maywood)*, 2015; 240:645-656.
16. Knöspel F, Freyer N, Stecklum M, Gerlach JC, Zeilinger K. Periodic harvesting of embryonic stem cells from a hollow-fiber membrane based four-compartment bioreactor. *Biotechnol Prog*, 2016; 32:141–151.
17. Chen YG, Wang Q, Lin SL, Chang CD, Chuang J, Ying SY. Activin signaling and its role in regulation of cell proliferation, apoptosis, and carcinogenesis. *Exp Biol Med (Maywood)*, 2006; 231:534–544.

18. Terentiev AA, Moldogazieva NT. Alpha-fetoprotein: a renaissance. *Tumour Biol*, 2013; 34:2075–2091.
19. Czysz K, Minger S, Thomas N. DMSO efficiently down regulates pluripotency genes in human embryonic stem cells during definitive endoderm derivation and increases the proficiency of hepatic differentiation. *PLoS One*, 2015; 10:e0117689.
20. Leiter JM, Helliger W, Puschendorf B. Increase in histone acetylation and transitions in histone variants during Friend cell differentiation. *Exp Cell Res*, 1984; 155:222–231.
21. Schmidt C, Bladt F, Goedecke S, Brinkmann V, Zschiesche W, Sharpe M, Gherardi E, Birchmeier C. Scatter factor/hepatocyte growth factor is essential for liver development. *Nature*, 1995; 373:699–702.
22. Asplund A, Pradip A, van Giezen M, Aspegren A, Choukair H, Rehnström M, Jacobsson S, Ghosheh N, El Hajjam D, Holmgren S, Larsson S, Benecke J, Butron M, Wigander A, Noaksson K, Sartipy P, Björquist P, Edsbacke J, Küppers-Munther B. One standardized differentiation procedure robustly generates homogenous hepatocyte cultures displaying metabolic diversity from a large panel of human pluripotent stem cells. *Stem Cell Rev*, 2016; 12:90-104.
23. Ameri J, Ståhlberg A, Pedersen J, Johansson JK, Johannesson MM, Artner I, Semb H. FGF2 specifies hESC-derived definitive endoderm into foregut/midgut cell lineages in a concentration-dependent manner. *Stem Cells*, 2010; 28:45–56.
24. DeLaForest A, Nagaoka M, Si-Tayeb K, Noto FK, Konopka G, Battle MA, Duncan SA. HNF4A is essential for specification of hepatic progenitors from human pluripotent stem cells. *Development*, 2011; 138:4143–4153.
25. Pascussi JM, Gerbal-Chaloin S, Drocourt L, Maurel P, Vilarem MJ. The expression of CYP2B6, CYP2C9 and CYP3A4 genes: A tangle of networks of nuclear and steroid receptors. *Biochim Biophys Acta*, 2003; 1619:243–253.
26. Ma X, Qu X, Zhu W, Li YS, Yuan S, Zhang H, Liu J, Wang P, Lai CS, Zanella F, Feng GS, Sheikh F, Chien S, Chen S. Deterministically patterned biomimetic human iPSC-derived hepatic model via rapid 3D bioprinting. *Proc. Natl. Acad. Sci. USA*, 2016; 113:2206–2211.

EIDESSTATTLICHE VERSICHERUNG

„Ich, Nora Freyer, versichere an Eides statt durch meine eigenhändige Unterschrift, dass ich die vorgelegte Dissertation mit dem Thema: „Optimizing culture conditions for hepatic differentiation of human induced pluripotent stem cells: from 3D culture systems to co-cultures“ selbstständig und ohne nicht offengelegte Hilfe Dritter verfasst und keine anderen als die angegebenen Quellen und Hilfsmittel genutzt habe.

Alle Stellen, die wörtlich oder dem Sinne nach auf Publikationen oder Vorträgen anderer Autoren beruhen, sind als solche in korrekter Zitierung (siehe „Uniform Requirements for Manuscripts (URM)“ des ICMJE -www.icmje.org) kenntlich gemacht. Die Abschnitte zu Methodik (insbesondere praktische Arbeiten, Laborbestimmungen, statistische Aufarbeitung) und Resultaten (insbesondere Abbildungen, Graphiken und Tabellen) entsprechen den URM (s.o) und werden von mir verantwortet.

Meine Anteile an den ausgewählten Publikationen entsprechen denen, die in der untenstehenden gemeinsamen Erklärung mit dem/der Betreuer/in, angegeben sind. Sämtliche Publikationen, die aus dieser Dissertation hervorgegangen sind und bei denen ich Autor bin, entsprechen den URM (s.o) und werden von mir verantwortet.

Die Bedeutung dieser eidesstattlichen Versicherung und die strafrechtlichen Folgen einer unwahren eidesstattlichen Versicherung (§156,161 des Strafgesetzbuches) sind mir bekannt und bewusst.“

Datum

Unterschrift

ANTEILSERKLÄRUNG AN DEN ERFOLGTEN PUBLIKATIONEN

Nora Freyer hatte folgenden Anteil an den folgenden Publikationen:

Publikation 1: **Nora Freyer**, Fanny Knöspel, Nadja Strahl, Leila Amini, Petra Schrade, Sebastian Bachmann, Georg Damm, Daniel Seehofer, Frank Jacobs, Mario Monshouwer, Katrin Zeilinger. Hepatic differentiation of human induced pluripotent stem cells in a perfused three-dimensional multicompartment bioreactor. Biores Open Access, 2016, 5(1):235-48.

Beitrag im Einzelnen:

- Planung, Koordination und Durchführung der hepatischen Differenzierung
- Auswertung der Daten
- Literaturrecherche
- Schreiben des Artikels

Publikation 2: Florian Meier, **Nora Freyer**, Joanna Brzeszczynska, Fanny Knöspel, Lyle Armstrong, Majlinda Lako, Selina Greuel, Georg Damm, Eva Ludwig-Schwellinger, Ulrich Deschl, James A. Ross, Mario Beilmann, Katrin Zeilinger. Hepatic differentiation of human iPSC in different 3D models: a comparative study. Int J of Mol Med, 2017, 40(6):1759-1771.

Beitrag im Einzelnen:

- Studiendesign gemeinsam mit Florian Meier und Joanna Brzeszczynska, Planung sowie Durchführung der hepatischen Differenzierung im 3D-Bioreaktor
- Datenauswertung für Protein- und Harnstoffsekretion und CYP-Aktivitäten
- Schreiben des Artikels gemeinsam mit Florian Meier

Publikation 3: **Nora Freyer**, Selina Greuel, Fanny Knöspel, Nadja Strahl, Leila Amini, Frank Jacobs, Mario Monshouwer, Katrin Zeilinger. Effects of co-culture media on hepatic differentiation of hiPSC with or without HUVEC co-culture. Int J Mol Sci, 2017, 18(8). pii: E1724.

Beitrag im Einzelnen:

- Studiendesign, Durchführung der Ko-Kultur-Versuche mit hiPSC und HUVEC während der hepatischen Differenzierung
- Datenauswertung für die hepatische Differenzierung von hiPSC mit und ohne HUVEC
- Schreiben des Artikels gemeinsam mit Selina Greuel

Unterschrift, Datum und Stempel des betreuenden Hochschullehrers/der betreuenden Hochschullehrerin

Unterschrift des Doktoranden/der Doktorandin

Hepatic Differentiation of Human Induced Pluripotent Stem Cells in a Perfused Three-Dimensional Multicompartment Bioreactor

Nora Freyer,¹ Fanny Knöspel,¹ Nadja Strahl,¹ Leila Amini,¹ Petra Schrade,² Sebastian Bachmann,² Georg Damm,^{3,4} Daniel Seehofer,^{3,4} Frank Jacobs,⁵ Mario Monshouwer,⁵ and Katrin Zeilinger^{1,*}

Abstract

The hepatic differentiation of human induced pluripotent stem cells (hiPSC) holds great potential for application in regenerative medicine, pharmacological drug screening, and toxicity testing. However, full maturation of hiPSC into functional hepatocytes has not yet been achieved. In this study, we investigated the potential of a dynamic three-dimensional (3D) hollow fiber membrane bioreactor technology to improve the hepatic differentiation of hiPSC in comparison to static two-dimensional (2D) cultures. A total of 100×10^6 hiPSC were seeded into each 3D bioreactor ($n = 3$). Differentiation into definitive endoderm (DE) was induced by adding activin A, Wnt3a, and sodium butyrate to the culture medium. For further maturation, hepatocyte growth factor and oncostatin M were added. The same differentiation protocol was applied to hiPSC maintained in 2D cultures. Secretion of alpha-fetoprotein (AFP), a marker for DE, was significantly ($p < 0.05$) higher in 2D cultures, while secretion of albumin, a typical characteristic for mature hepatocytes, was higher after hepatic differentiation of hiPSC in 3D bioreactors. Functional analysis of multiple cytochrome P450 (CYP) isoenzymes showed activity of CYP1A2, CYP2B6, and CYP3A4 in both groups, although at a lower level compared to primary human hepatocytes (PHH). CYP2B6 activities were significantly ($p < 0.05$) higher in 3D bioreactors compared with 2D cultures, which is in line with results from gene expression. Immunofluorescence staining showed that the majority of cells was positive for albumin, cytokeratin 18 (CK18), and hepatocyte nuclear factor 4-alpha (HNF4A) at the end of the differentiation process. In addition, cytokeratin 19 (CK19) staining revealed the formation of bile duct-like structures in 3D bioreactors similar to native liver tissue. The results indicate a better maturation of hiPSC in the 3D bioreactor system compared to 2D cultures and emphasize the potential of dynamic 3D culture systems in stem cell differentiation approaches for improved formation of differentiated tissue structures.

Keywords: stem cells; tissue engineering

Introduction

During drug development, only one out of nine compounds gets approved by the regulatory authorities, usually due to a lack of efficacy or toxic side effects.¹ Thus, models for assessment of drug toxicity, especially

hepatotoxicity, in the early phase of drug development are needed. Animal models, although indispensable in preclinical studies, are not sufficiently predictive for humans due to interspecies differences.² Primary human hepatocytes (PHH) have been widely accepted

¹Bioreactor Group, Berlin Brandenburg Center for Regenerative Therapies (BCRT), Charité—Universitätsmedizin Berlin, Berlin, Germany.

²Charité Centrum Grundlagenmedizin, Institut für Vegetative Anatomie, Charité—Universitätsmedizin Berlin, Berlin, Germany.

³Department of General-, Visceral- and Transplantation Surgery, Charité—Universitätsmedizin Berlin, Berlin, Germany.

⁴Department of Hepatobiliary Surgery and Visceral Transplantation, University of Leipzig, Leipzig, Germany.

⁵Janssen Research and Development, Beerse, Belgium.

Part of this work was previously presented at the following meeting: Freyer N, Strahl N, Knöspel F, Urbaniak T, Zeilinger K. Hepatic differentiation of hiPSC in a 3D multicompartment bioreactor, 30th Annual Meeting of the German Association of the Study of the Liver (GASL), 2014, 24 and 25th January, Tübingen, Germany, abstract published in *Gastroenterol* 52, p. 3.12.

*Address correspondence to: Dr. med. vet. Katrin Zeilinger, Bioreactor Group, Berlin Brandenburg Center for Regenerative Therapies (BCRT), Charité—Universitätsmedizin Berlin, Campus Virchow-Klinikum, Augustenburger Platz 1, Berlin 13353, Germany, E-mail: katrin.zeilinger@charite.de



as the gold standard for predictive *in vitro* studies on hepatic drug toxicity.³ However, PHH display a huge variation in cell function and enzyme activities because of interdonor variances,⁴ and the high demand of freshly isolated PHH is difficult to address due to the scarce availability of human liver tissue.

Human induced pluripotent stem cells (hiPSC) represent a promising cell source for the generation of human hepatocytes for studies on hepatic drug toxicity. Due to the unlimited self-renewing capacity of hiPSC, they provide the option for cell production in large amounts and at a constant quality. In addition, variances due to genetic polymorphism can be investigated by using different hiPSC lines representative of individual patient groups.⁵

Several protocols have been established to generate stem cell-derived hepatocytes from human pluripotent stem cells.^{6–9} These procedures mimic the embryonic development of the liver by adding different growth factors necessary for each developmental stage. The resulting hepatocyte-like cells (HLC) were successfully applied for *in vitro* studies on human drug exposure,^{10,11} hepatitis B and C infection,^{12,13} or malaria pathogenesis¹⁴ among others, and they have been shown to repopulate the livers of chimeric mice and rescue the disease phenotype in these animals.¹⁵ However, the HLC obtained with existing protocols still show an immature phenotype with reduced hepatic functionality when compared to PHH.^{16,17}

To overcome these drawbacks, improved culture models are demanded, which address the needs of the cells in their natural environment. Several studies have shown that three-dimensional (3D) culture of PHH in natural or synthetic scaffolds supports cell–cell contacts, cell polarization, and preservation of liver functions such as cytochrome P450 (CYP) activities, albumin production, and glycogen synthesis.^{18–20} To improve oxygenation and medium exchange in hepatocyte cultures, various perfused 3D culture systems have been developed.^{21–23}

In the 3D multicompartiment bioreactor used in this study, the cells are maintained in a perfused 3D environment allowing for physiological signal exchange and autocrine or paracrine stimulation, close to the natural situation in the organ. We have previously shown that this 3D bioreactor system supports stable culture of PHH under serum-free conditions^{24,25} and is suitable for differentiation of human embryonic stem cells (hESC).^{26,27}

Thus, we hypothesize that the usage of the 3D bioreactor system could improve the hepatic maturation and

liver-specific functionality of hiPSC-derived hepatocytes compared with conventional two-dimensional (2D) cultures. The functionality of the cells upon differentiation in 2D cultures or 3D bioreactors was evaluated by measurement of typical hepatocyte products (albumin, urea) and CYP activities. Cultures were further characterized by means of immunohistochemical investigations, transmission electron microscopy (TEM), and analysis of liver-specific mRNA expression. Data from hiPSC-derived differentiated cells were compared to those from freshly isolated or 2D cultured PHH.

Materials and Methods

Bioreactor technology

The 3D multicompartiment bioreactor consists of three independent, but interwoven hollow fiber capillary systems that serve for counter-current medium perfusion (two medium compartments). Cells are supplied with oxygen by direct membrane oxygenation through integrated gas capillaries (gas compartment), which are perfused with an air/CO₂ mixture. Cells are cultured in the extracapillary space (cell compartment). The analytical scale bioreactors used in this study have a cell compartment volume of 2 mL. A detailed description of the technology is provided elsewhere.²⁸

Bioreactors are operated in a perfusion device with two modular pump units, one for medium recirculation and one for medium feed. The bioreactor incubation chamber is heated by two heating units located inside the chamber, each consisting of a heating cartridge and a fan. A platinum measuring resistor monitors the temperature inside the chamber and software is used to set and maintain the desired temperature. Gas flow rates and gas compositions are regulated using electronically operated gas valves for air, CO₂, and the resulting gas mixture (Vögtlin Instruments). Bioreactors, tubing systems, and perfusion devices were manufactured by Stem Cell Systems.

Hepatic differentiation of hiPSC in 3D bioreactors or 2D cultures

The hiPSC line DF6-9-9T²⁹ (WiCell Research Institute) was cultured under feeder-free conditions on Nunclon™ six-well cell culture plates (ThermoScientific Nunc™) coated with 8.68 μg/cm² Matrigel (growth factor reduced). Cells were expanded with the mTeSR™1 medium (StemCell Technologies) with 0.05 mg/mL gentamicin (Merck). Afterward, a total of 100 × 10⁶ hiPSC were seeded into a precoated bioreactor (8.68 μg/cm²; Matrigel) and cultured over a total of 20 days.



Bioreactors were maintained at 37°C, the medium recirculation rate was 10 mL/min, and the feed rate was 1 mL/h. Based on daily measurements of the pH, glucose, and lactate values, CO₂ and medium perfusion rates were adjusted, if necessary, to maintain a stable pH between 7.2 and 7.4 and sufficient glucose levels (>25 mg/dL).

After a proliferation phase of 3 days with mTeSRTM1, differentiation of the cells in 3D bioreactors was induced based on the protocols described by Hay et al.^{6,30,31} for 2D cultures. In the first step, differentiation into definitive endoderm (DE) was induced by perfusion with the Roswell Park Memorial Institute (RPMI) 1640 culture medium (Merck) supplemented with 100 ng/mL activin A (Peprotech), 50 ng/mL Wnt3a (R&D Systems), 1 μM sodium butyrate (Sigma-Aldrich), and 2% (v/v) B27 supplements without insulin (Life Technologies) for 3 days.

Subsequently, bioreactors were perfused over 13 days with a hepatocyte culture medium consisting of basal medium and single quotes (Lonza) and 10 ng/mL hepatocyte growth factor (HGF; Peprotech) to induce differentiation of DE-cells to hepatoblasts. For further maturation to HLC, 10 ng/mL oncostatin M (Peprotech) was added during the last 4 days of differentiation.

2D cultures were performed in parallel with 3D bioreactor cultures for control, applying the same differentiation protocol with daily medium exchange.

Metabolic parameters

The metabolic activity of the cells was assessed by daily measurement of glucose and lactate concentrations with a blood gas analyzer (ABL 700; Radiometer). Potential cell damage was detected by analyzing the release of lactate dehydrogenase (LDH) using an automated clinical chemistry analyzer (Cobas[®] 8000; Roche Diagnostics) as well as the production of urea and the albumin precursor protein alpha-fetoprotein (AFP). Albumin secretion, as a marker for mature hepatocytes, was detected using an ELISA Quantitation kit and tetramethylbenzidine (TMB) substrate (both from Bethyl Laboratories) according to the manufacturer's instructions.

Culture of PHH

The PHH were isolated from macroscopically healthy tissue that remained from resected human liver of patients with primary or secondary liver tumors or benign local liver diseases. Informed consent of the patients for the use of tissue for research purposes was obtained according to the ethical guidelines of the Charité—Universitätsmedizin Berlin. Part of the tissue sample was fixed in formaldehyde for immunofluorescence staining. Cell isolation was performed according to Pfeiffer et al.³²

Hepatocytes were seeded at a density of 2.0 × 10⁵ cells/cm² in six-well plates (BD Sciences) coated with rat tail collagen. Cells were cultivated using Heparmed Vito 143 supplemented with 10% fetal calf serum (PAA), 0.8 mg/mL insulin, 5 mg/L transferrin, 0.003 mg/L glucagon, 100 U/mL penicillin, and 100 μg/mL streptomycin (all Merck).

Measurement of cytochrome P450 (CYP) isoenzyme activities

Activities of the pharmacologically relevant CYP isoenzymes CYP1A2, CYP2B6, CYP2C9, and CYP3A4 were measured in (1) undifferentiated hiPSC, (2) HLC differentiated in 2D cultures or (3) 3D bioreactors, and (4) PHH cultures (24 h after seeding) serving as control. The cells were incubated with a cocktail containing phenacetin (Sigma) as a substrate for CYP1A2, bupropion (Toronto Research Chemicals) as a substrate for CYP2B6, diclofenac as a substrate for CYP2C9, and midazolam as a substrate for CYP3A4/5 (both from Sigma-Aldrich). Samples were taken at 1, 2, 4, and 6 h subsequent to substrate application. An overview of the used substrates, their final concentrations, and the corresponding CYP isoenzymes is provided in Table 1.

Formed metabolites (acetaminophen, 6-OH-bupropion, 4-OH-diclofenac, 1-OH-midazolam) were quantified by liquid chromatography tandem-mass spectrometry. Deuterated 1-OH-midazolam was added as an internal standard. Separation was carried out using an Acquity UPLC C18 column and eluted fractions were directly passed through a Xevo TQ-S tandem mass

Table 1. CYP Isoenzymes Tested and Their Corresponding Substrates with Resulting Products and Applied Concentrations

Enzyme	Substrate	Product	Final concentration [μM]	Transition reactions for analysis of probe products
CYP1A2	Phenacetin	Acetaminophen	100	152 → 110
CYP2B6	Bupropion	6-Hydroxybupropion	500	256 → 238
CYP2C9	Diclofenac	4'-Hydroxydiclofenac	25	312 → 266
CYP3A4/5	Midazolam	1'-Hydroxymidazolam	10	342 → 324



Table 2. Applied Biosystems TaqMan Gene Expression Assays[®]

Gene symbol	Gene name	Assay ID
<i>POU5F1</i>	POU domain, class 5, transcription factor 1	HS00999632_g1
<i>NANOG</i>	Nanog homeobox	HS02387400_g1
<i>SOX7</i>	SRY-box 7	HS00846731_s1
<i>SOX17</i>	SRY-box 17	HS00751752_s1
<i>AFP</i>	Alpha fetoprotein	HS00173490_m1
<i>ALB</i>	Albumin	HS00910225_m1
<i>CYP1A2</i>	Cytochrome P450 family 1 subfamily A member 2	HS00167927_m1
<i>CYP2B6</i>	Cytochrome P450 family 2 subfamily B member 6	HS03044634_m1
<i>CYP2C9</i>	Cytochrome P450 family 3 subfamily A member 4	HS00426397_m1
<i>CYP3A4</i>	Cytochrome P450 family 3 subfamily A member 4	HS00604506_m1
<i>GATA2</i>	GATA binding protein 2	HS00231119_m1
<i>NEFL</i>	Neurofilament, light polypeptide	HS00196245_m1
<i>GAPDH</i>	Glyceraldehyde-3-phosphate dehydrogenase	HS03929097_g1

spectrometer (both from Waters Corp.). Acquired data were processed with Thermo Xcaliber 20 software (Thermo Scientific).

Gene expression analysis

RNA was isolated from undifferentiated hiPSC, from HLC differentiated in 2D cultures or 3D bioreactors, and from freshly isolated PHH serving as reference cells. RNA isolation and subsequent cDNA synthesis were performed as described elsewhere.³³ Each cDNA template was mixed with polymerase chain reaction (PCR) Master mix (Applied Biosystems) and human-specific primers and probes (TaqMan Gene Expression Assay system; Life Technologies; Table 2). Quantitative real-time PCR (qRT-PCR) was performed using a Real time cycler (Mastercycler ep Realplex 2; Eppendorf). The expression of specific genes was normalized to that of the house-

keeping gene glyceraldehyde-3-phosphate dehydrogenase (GAPDH) and fold changes of expression levels were calculated with the $\Delta\Delta C_t$ method.³⁴

Immunofluorescence studies

Immunofluorescence staining was performed with antibodies listed in Table 3 as described elsewhere³³ with following changes for 3D and tissue sections. The hollow fiber bed was excised *en-bloc*, fixed with 4% formaldehyde solution (Herbeta Arzneimittel), dehydrated, paraffinized, and cut into slides of 2.5 μm thickness. Subsequently, the slides were deparaffinized, rehydrated, and subjected to antigen retrieval in a citrate buffer (pH 6.0) in a pressure cooker for 15 min. The same procedure was applied to native human liver tissue serving as a positive control. Nuclei in native human liver tissue were stained with bisBenzimide H 33342 trihydrochloride (Sigma).

Ki-67 positive cells were quantified in undifferentiated hiPSC, 2D cultured DE cells, and HLC from 2D cultures or 3D bioreactors with the open source image processing program ImageJ using at least 10 randomly chosen visual fields for each group.

Transmission electron microscopy

For TEM, part of the 3D bioreactor cell compartment was fixed with 2.5% glutaraldehyde in 0.1 M sodium cacodylate buffer (both from Serva) over night, followed by postfixing in 1% OsO_4 (Science Services) with 0.8% potassium ferrocyanide (Merck) in 0.1 M sodium cacodylate buffer for 1.5 h. Subsequently, samples were progressively dehydrated in ethanol and then embedded in Epon (Serva). Ultrathin sections were stained with uranyl acetate and Reynold's lead citrate

Table 3. Antibodies Used for Immunofluorescence Staining

	Protein symbol	Species	Manufacturer	Cat.-No.	Final conc. [$\mu\text{g/mL}$]
Primary antibody					
Alpha fetoprotein	AFP	mouse	Santa Cruz	Sc-8399	2
Albumin	ALB	mouse	Sigma	A6684	67
Cytokeratin 18	CK18	mouse	Santa Cruz	Sc-6259	2
Cytokeratin 19	CK19	rabbit	Santa Cruz	Sc-25724	2
Cytochrome P450 1A2	CYP1A2	mouse	Santa Cruz	Sc-53614	2
Cytochrome P450 2B6	CYP2B6	rabbit	Santa Cruz	Sc-67224	2
Hepatocyte nuclear factor 4 alpha	HNF4A	rabbit	Santa Cruz	Sc-8987	2
Marker of proliferation Ki-67	MKI67	mouse	BD Biosciences	556003	10
Multidrug resistance-associated protein 2	MRP2	rabbit	Sigma	M8316	9
POU domain, class 5, transcription factor 1	OCT3	rabbit	Santa Cruz	Sc-9081	2
Stage-specific embryonic antigen 4	SSEA4	mouse	R&D Systems	MAB1435	10
Tight junction protein 1	TJP1	mouse	LSBio	LS B2228	30
Secondary antibody					
Alexa Fluor [®] 488 anti-mouse		goat	Life Technologies	A-11029	2
Alexa Fluor 594 anti-rabbit		goat	Life Technologies	A-11037	2

Final concentrations are given in $\mu\text{g/mL}$.



(Merck) and microphotographs were taken using an electron microscope EM 906 (Carl Zeiss).

Statistical evaluation

Experiments were performed in triplicates, unless stated otherwise, and results are presented as mean \pm standard error of the mean.

The area under curve (AUC) was calculated for time courses of biochemical parameters and differences between culture systems were detected with a subsequent two-tailed Student's *t*-test. CYP activities of undifferentiated hiPSC were compared with those of HLC from 2D cultures or 3D bioreactors by one-way analysis of variance (ANOVA) followed by Bonferroni's multiple comparison test. Differences in gene expression between both culture systems were detected by applying an unpaired, two-tailed Student's *t*-test. PHH were compared with all other groups by one-way ANOVA followed by Dunnett's multiple comparison test. Differences were judged as significant if the *p*-value was <0.05 .

Results

Metabolic activity and integrity of HLC in 2D cultures or 3D bioreactors

In both culture systems, the metabolic activity of the cells during hepatic differentiation, assessed by glucose consumption and lactate production, showed an increase over time (Fig. 1A, B). Average glucose consumption rates were significantly higher ($p \leq 0.05$) in 2D cultures than in 3D bioreactors (Fig. 1A). The time course of lactate production reflected that of glucose consumption (Fig. 1B). LDH release, indicating cell injury, was significantly higher ($p \leq 0.01$) in 2D cultures than in 3D bioreactors during the first 3 days of differentiation, but decreased from day 3 on to basal levels. In contrast, LDH release in 3D bioreactors remained on a basal level over the whole culture period (Fig. 1C).

Secretion of stage-specific proteins and metabolites

The synthesis of liver-specific proteins and the activity of the urea cycle were evaluated during hepatic differentiation. The endoderm-specific marker AFP showed an increase during the hepatoblast differentiation stage, starting on day 7 in 2D cultures and on day 9 in 3D bioreactors, but the increase was significantly higher ($p \leq 0.05$) in 2D cultures (Fig. 1D). Albumin also showed an increase during the hepatoblast differentiation phase beginning on day 12 of differentiation in 2D cultures and 3D bioreactors. However, maximum values achieved were thrice higher in 3D bioreactors than in 2D cultures (Fig. 1E), although the difference was not significant.

Values of urea secretion showed a constant increase in 3D bioreactors until day 17 to the threefold of secretion rates detected on day 1 of culture. A fluctuating time course was observed in 2D cultures with peaks at the beginning of culture and between day 9 and 13 (Fig. 1F). Values approximated those of 3D bioreactors during the final days of differentiation.

Functional analysis of different cytochrome P450 (CYP) isoenzymes

To investigate the CYP activity, the ability of the HLC to metabolize various substrates into their isoenzyme-specific products was analyzed and compared with CYP activities of undifferentiated hiPSC and those of PHH cultures determined 24 h after seeding.

CYP1A2 showed a higher activity in 3D bioreactors than in 2D cultures, while it was lower compared with undifferentiated hiPSC or PHH (Fig. 2A). A significant CYP2B6-dependent conversion of bupropion to 6-OH-bupropion was observed in 3D bioreactors compared to 2D cultures ($p \leq 0.05$ Fig. 2B). In contrast, CYP3A4 showed higher activities in undifferentiated hiPSC and in 2D cultures than in 3D bioreactors, although the differences were not significant (Fig. 2C). The isoenzyme CYP2C9 activity was detected neither in differentiated nor in undifferentiated hiPSC (data not shown). All enzyme activities investigated were significantly higher in PHH than in the HLC generated from hiPSC in 2D or 3D cultures (Fig. 2A–C).

Gene expression of pluripotency factors, and endodermal and hepatic markers

The expression of 12 stage-specific genes was comparatively analyzed by qRT-PCR in 2D or 3D cultures of HLC and in freshly isolated PHH (Fig. 3). Expression levels were plotted relative to those of undifferentiated hiPSC (d0) to investigate the hepatic maturation state of the cells.

The expression of the pluripotency markers *POU5F1* and *NANOG* decreased in both culture systems compared to undifferentiated hiPSC, but the decrease was significantly higher in 2D cultures ($p \leq 0.05$, Fig. 3A, B). PHH showed *POU5F1* levels similar to HLC in 2D cultures, while *NANOG* expression was similar to those in 3D bioreactors (Fig. 3A, B).

To exclude differentiation into nonendodermal cells, markers for mesoderm (*GATA2*) and endoderm (neurofilament, *NEFL*) were analyzed as well. The analysis revealed a >100 -fold increase for *GATA2* in 3D bioreactors, which is significantly higher than in 2D cultures showing an ~ 20 -fold increase (Fig. 3C). The expression



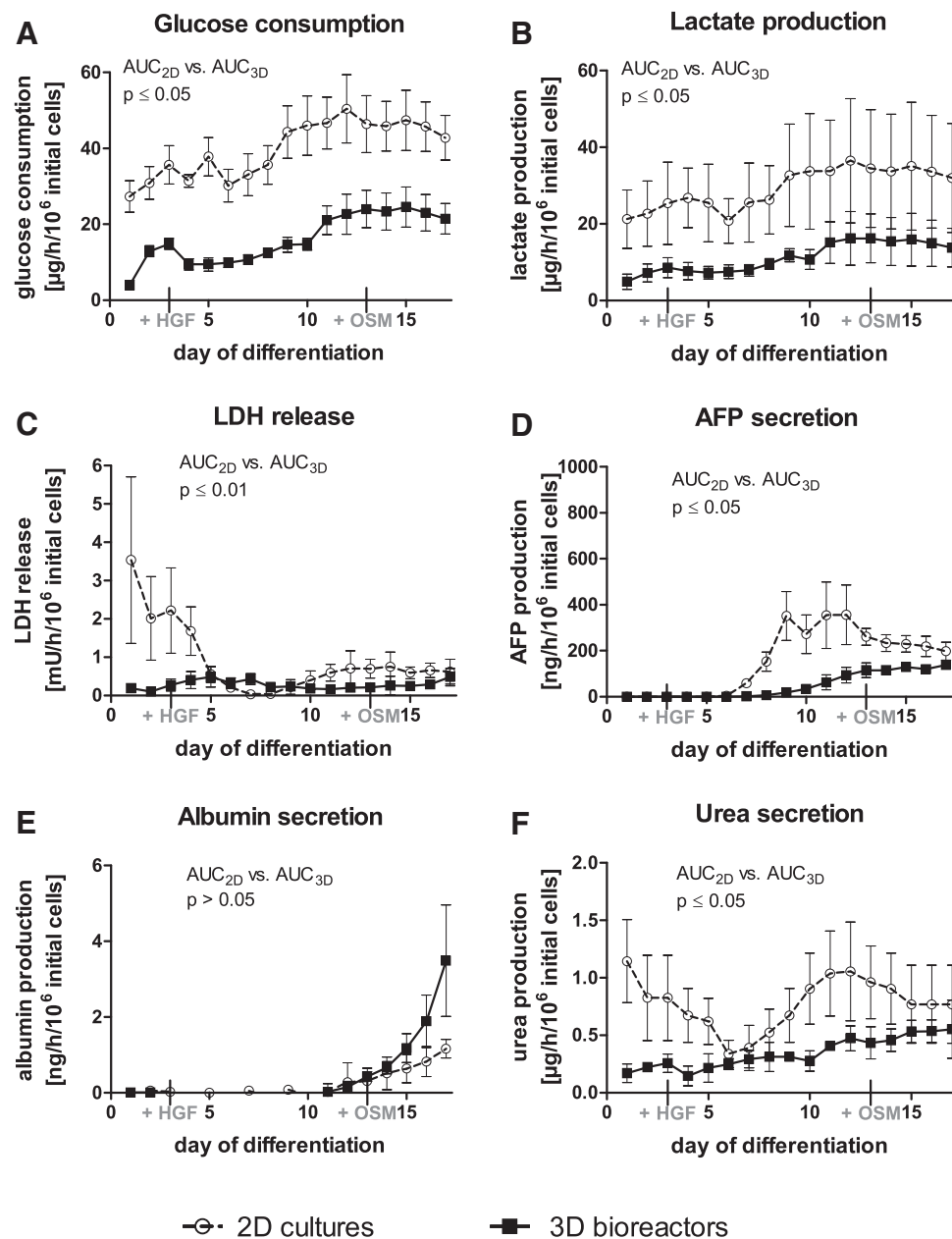


FIG. 1. Metabolic activity of hiPSC during hepatic differentiation in 2D cultures (dotted line) or in 3D bioreactor cultures (black line). (A) Glucose consumption, (B) lactate production, (C) release of LDH, (D) secretion of AFP, (E) albumin production, and (F) urea secretion. Values were normalized to 1×10^6 inoculated cells. AUC was calculated and differences were detected with the unpaired, two-tailed Student's *t*-test (3D bioreactors: $n=3$, 2D cultures: $n=4$, mean \pm SEM). AFP, alpha-fetoprotein; AUC, area under curve; 2D, two dimensional; 3D, three dimensional; hiPSC, human induced pluripotent stem cells; LDH, lactate dehydrogenase; SEM, standard error of the mean.



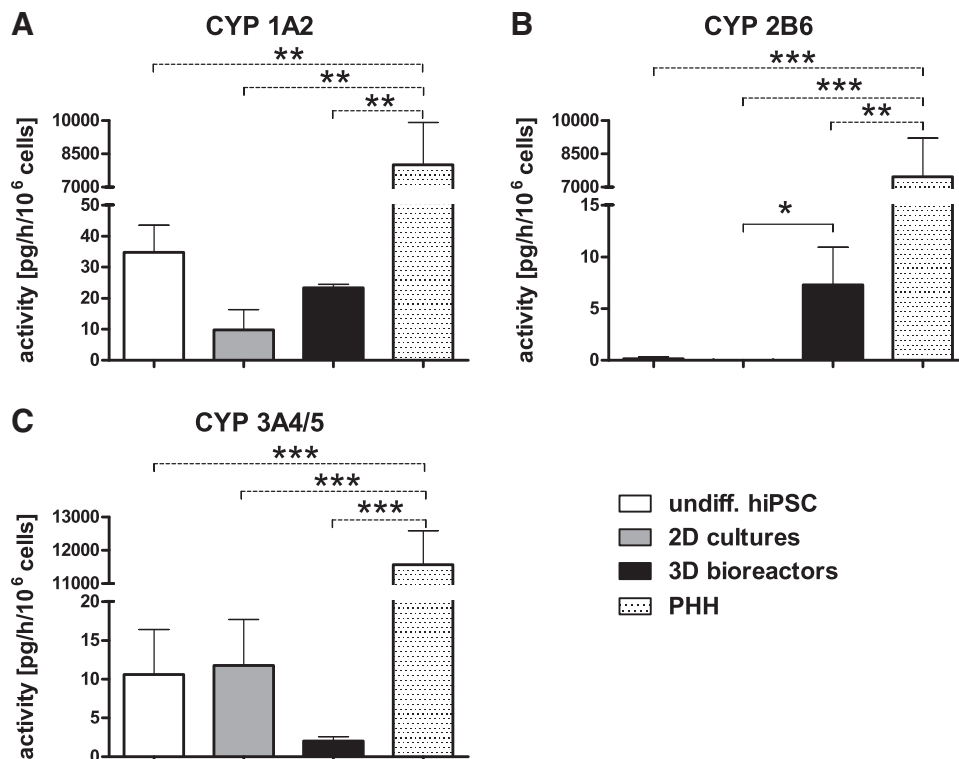


FIG. 2. Activities of different cytochrome P450 (CYP) isoenzymes in undifferentiated hiPSC (white), in hiPSC after hepatic differentiation in 2D cultures (gray) or 3D bioreactors (black), or in PHH (dotted). CYP activities were determined by measuring the conversion rates of selected substrates into isoenzyme-specific products. **(A)** Formation of acetaminophen from phenacetin by CYP1A2, **(B)** formation of 6-OH-bupropion from bupropion by CYP2B6, and **(C)** formation of 1-OH-midazolam from midazolam by CYP3A4/5. Differences in metabolic activity between undifferentiated hiPSC, 2D cultures and 3D bioreactors, were calculated using one-way ANOVA with Bonferroni's multiple comparison test (solid line). In addition, differences between PHH to all other groups were calculated using one-way ANOVA with Dunnett's multiple comparison test (dotted line). (3D bioreactors: $n=3$, 2D cultures and undifferentiated hiPSC: $n=4$, PHH: $n=5$; mean \pm SEM), * $p \leq 0.05$, ** $p \leq 0.01$, *** $p \leq 0.001$. ANOVA, analysis of variance; PHH, primary human hepatocytes.

of *NEFL* did not change significantly in comparison to undifferentiated hiPSC (Fig. 3D). PHH showed only scarce expression of *NEFL* and *GATA2* (Fig. 3C, D).

In contrast, most markers for endoderm and mature hepatocytes increased in both culture systems. *AFP* showed a >60,000-fold increased expression in both 2D cultures and 3D bioreactors, relative to undifferentiated hiPSC (Fig. 3E), and the expression of *SOX17* (Fig. 3F), another endodermal marker, showed a 20-fold increase, while PHH showed no relevant expression of those markers. Since *AFP* and *SOX17* are markers for both, definitive and extraembryonic endoderm, *SOX7* (Fig. 3G) was analyzed as a specific marker for extraembryonic endoderm. The expression of *SOX7*

was increased in both culture systems and was similar to that detected in PHH.

Among the markers investigated for mature hepatocytes, the highest increase was detected for albumin (*ALB*), which was increased in both groups by >2,000-fold, with 3D bioreactors showing twice the expression compared to 2D cultures (Fig. 3H).

In contrast, the expression of *CYP1A2* was decreased compared with undifferentiated hiPSC both in 2D cultures and 3D bioreactors (Fig. 3I), which is in line with the results from activity measurements (Fig. 2A). A decrease of mRNA expression was also detected for *CYP2B6*, but the expression was still significantly higher in 3D bioreactors ($p \leq 0.05$, Fig. 3J) and is in accordance to



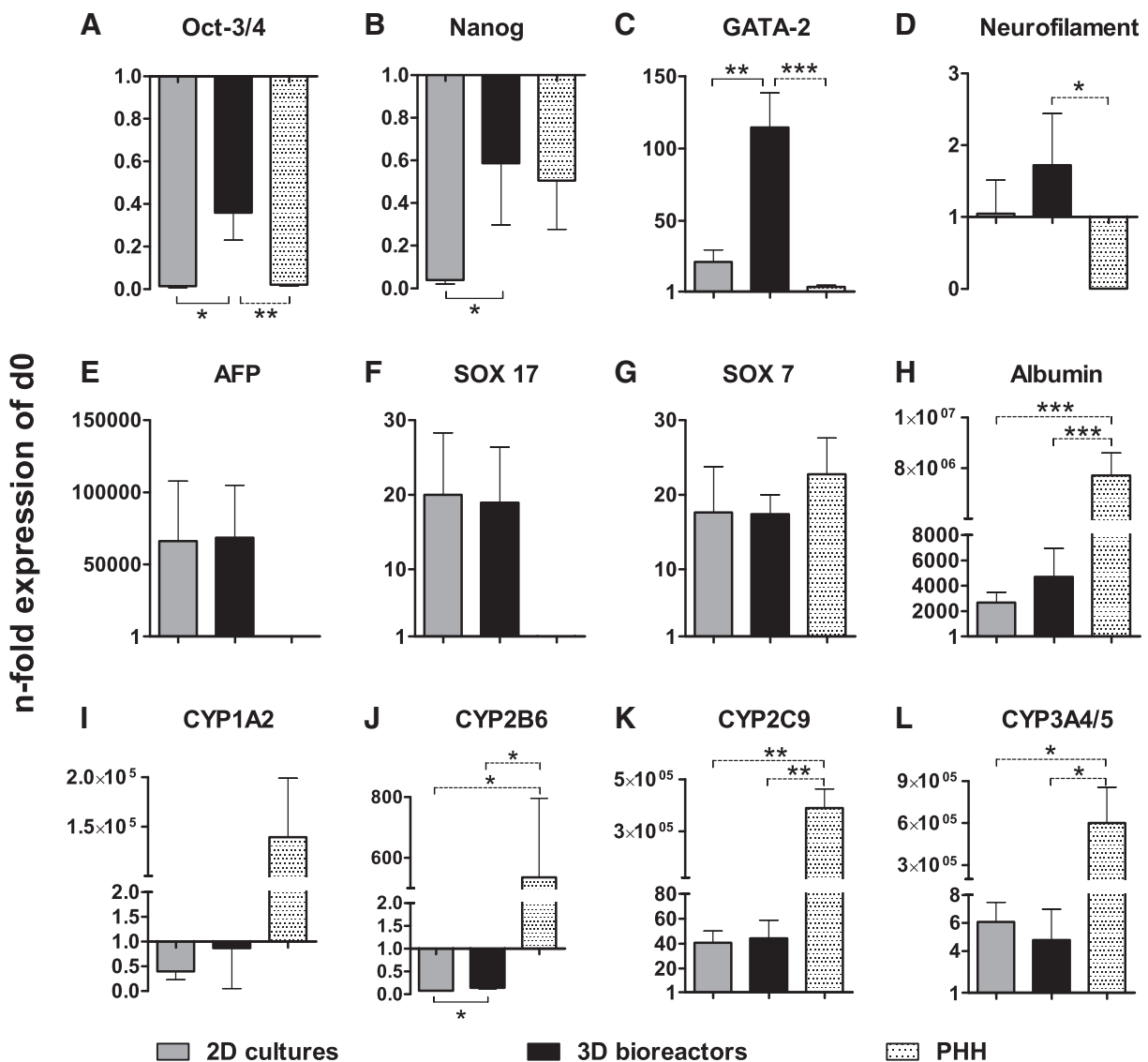


FIG. 3. Gene expression of pluripotency markers (A) Oct-3/4 and (B) Nanog, mesodermal marker (C) GATA-2, ectodermal marker (D) neurofilament, endodermal markers (E) AFP and (F) SOX 17, extra-embryonic marker (G) SOX 7 and hepatic markers (H) albumin, (I) CYP1A2, (J) CYP2B6, (K) CYP2C9 and (L) CYP3A4/5 in hiPSC after hepatic differentiation in 2D cultures or 3D bioreactors, and in PHH relative to undifferentiated hiPSC (d0). Samples for mRNA expression analysis were taken after hepatic differentiation of hiPSC in 2D cultures (black) or 3D bioreactors (gray). For mRNA expression analysis of PHH (dotted), freshly isolated cells were used. Fold changes relative to undifferentiated hiPSC were calculated with normalization to GAPDH expression by the $\Delta\Delta C_t$ method. Differences in gene expression between 2D cultures and 3D bioreactors were calculated using the unpaired, two-tailed Student's *t*-test (solid line). In addition, differences between PHH and all other groups were calculated by means of one-way ANOVA with Dunnett's multiple comparison test (dotted line) (3D bioreactors: $n=3$, 2D cultures and undifferentiated hiPSC: $n=4$, PHH: $n=3$; mean \pm SEM), * $p \leq 0.05$, ** $p \leq 0.01$, *** $p \leq 0.001$.



the findings from activity measurements (Fig. 2B). Expression of *CYP2C9* and *CYP3A4/5* was increased by around 40- or five-fold, respectively, compared with undifferentiated cells showing no significant differences between 2D cultures and 3D bioreactors (Fig. 3K, L). All markers for mature hepatocytes showed a distinctly lower expression in HLC than in PHH, irrespective of the culture system.

Immunohistochemical characterization of hiPSC-derived differentiated cells

To determine the amount of proliferating cells before, during, and after the hepatic differentiation of hiPSC, an immunofluorescence staining with the proliferation marker Ki-67 was performed. In cultures of undifferentiated hiPSC, almost all cells ($97.7\% \pm 1.6\%$) were positive for Ki-67 (Fig. 4A1). In 2D cultured DE cells,

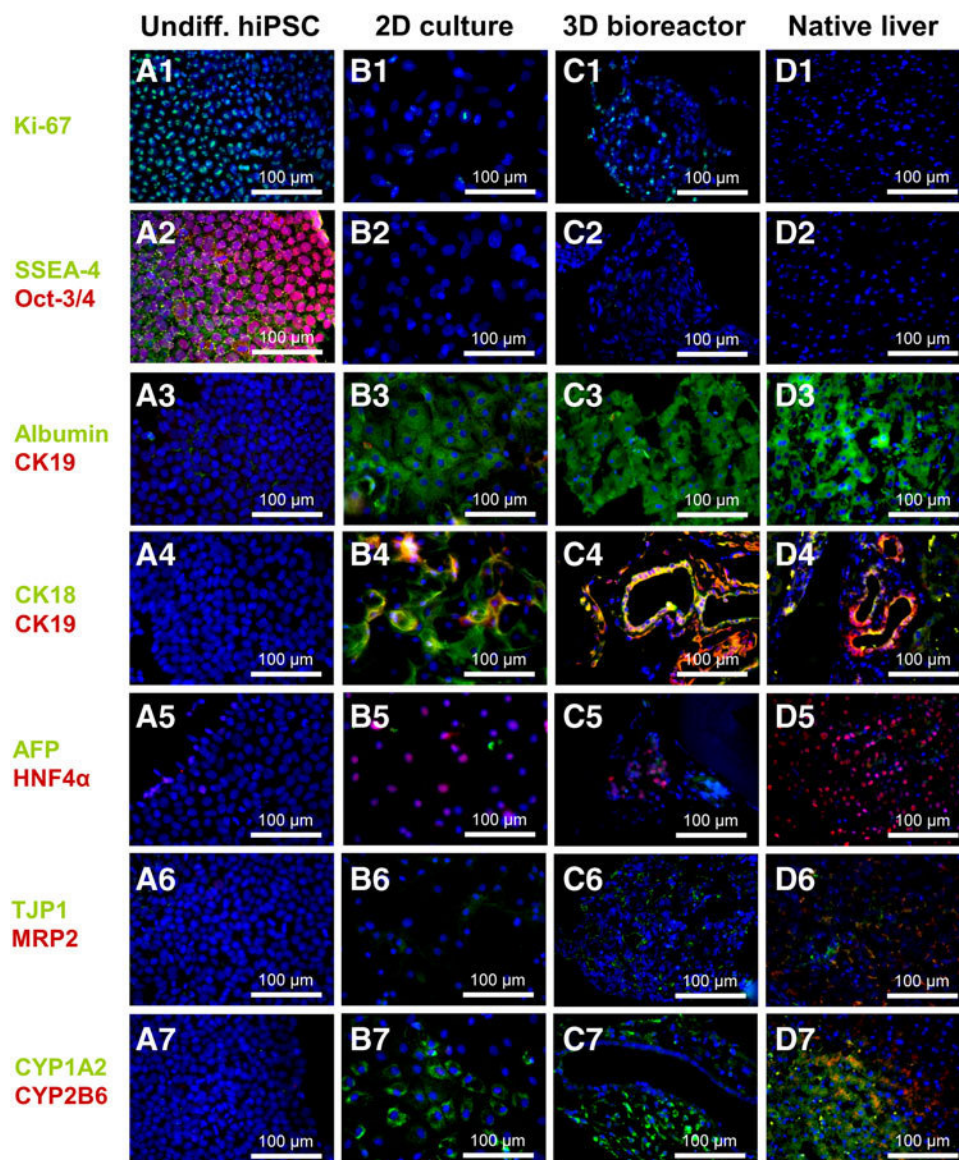


FIG. 4. Immunofluorescence analysis of hiPSC before and after hepatic differentiation in 2D cultures or 3D bioreactors compared with native human liver tissue. Samples from cultures or liver tissue were stained with **(A1–D1)** Ki-67, **(A2–D2)** SSEA-4 and Oct-3/4, **(A3–D3)** albumin and CK19, **(A4–D4)** CK18 and CK19, **(A5–D5)** AFP and HNF4 α , **(A6–D6)** TJP1 and MRP2, and with **(A7–D7)** CYP1A2 and CYP2B6. Nuclei were counterstained with DAPI (blue) or with bisBenzimide H 33342 trihydrochloride in native human liver tissue (blue). CK19, cytokeratin 19.



approximately two thirds of the cells ($63.6\% \pm 12.6\%$) were proliferating (picture not shown). After hepatic differentiation, around one third of the cells were still proliferating in 2D cultures ($32.6\% \pm 20.4\%$, Fig. 4B1) and 3D bioreactors ($30.3\% \pm 18.7\%$, Fig. 4C1). In the native human liver, no Ki-67-positive cells could be detected (Fig. 4D1).

The pluripotency markers SSEA4 and OCT3 were expressed in the majority of undifferentiated hiPSC (Fig. 4A2), but could not be detected in hiPSC-derived HLC in 2D cultures (Fig. 4B2) or 3D bioreactors (Fig. 4C2), or in native human liver tissue (Fig. 4D2). Regarding the expression of hepatocyte-specific markers, the majority of cells was positive for albumin in 2D cultures as well as 3D bioreactors (Fig. 4B3, C3), similar to native human liver tissue (Fig. 4D3).

Cytokeratin 19 (CK19), characteristic for biliary cells, was only detected in a few sparsely distributed cells in 2D cultures (Fig. 4B4), whereas in 3D bioreactors, ring-shaped cell arrangements lined with cells positive for CK18 and CK19 were observed, indicating formation of bile duct-like tubular structures (Fig. 4C4) resembling those occurring in native human liver tissue (Fig. 4D4). Staining for hepatocyte nuclear factor 4-alpha (HNF4A) showed a few positive cells, which were negative for AFP in both 2D cultures and 3D bioreactors (Fig. 4B5, C5). This is in contrast to native human liver tissue where almost all cells showed immunoreactivity for HNF4A (Fig. 4D5).

Staining of tight junction protein (TJP1) and the transporter multidrug resistance-associated protein 2 (MRP2) revealed no immunoreactivity in 2D cultures (Fig. 4B6), while in 3D bioreactors (Fig. 4C6), abundant cells were positive for TJP1 as indicated by thin borders between the cells. In the native liver tissue, most of the cells were double positive for MRP2 and TJP1 (Fig. 4D6).

Immunofluorescence analysis of CYP isoenzymes showed that most of the cells in 2D cultures and 3D bioreactors were positive for CYP1A2, but negative for CYP2B6 (Fig. 4B7, C7), which is in line with the functional analysis showing higher activities for CYP1A2. In 3D bioreactors, the inner ring of tubular-like structures lacked CYP1A2 immunoreactivity indicating a zonation of the cells. In native human liver tissue, cells were positive for both CYP isoenzymes (Fig. 4D7). The undifferentiated hiPSC were negative for all liver-specific markers (Fig. 4A3–A7).

Ultrastructural characteristics of hiPSC-derived differentiated cells

Ultrastructural studies of hiPSC-derived cells after hepatic differentiation in 3D bioreactors showed a hetero-

geneous cell population with some similarities to native liver tissue. Cells displaying a high nucleus to cytoplasm ratio indicate the presence of still immature cells (Fig. 5A). In other areas, cells showed microvilli at their apical side with abundant cell–cell contacts consisting of tight junctions and desmosomes indicating cell polarization typical for hepatocytes (Fig. 5B, C). The majority of cells contained numerous mitochondria, which is also a typical feature of hepatocytes due to their high metabolic activity. Distinct interdigitations between neighboring cells and rough endoplasmic reticulum in the cytoplasm were observed in addition to well-developed Golgi apparatuses (Fig. 5D).

Discussion

Hepatocytes derived from hiPSC represent a promising cell source for pharmacological toxicity testing. Although numerous protocols for the hepatic differentiation of hiPSC exist and are continuously refined, the obtained cells still show a fetal phenotype,^{16,17} and the maturation state of the obtained cells needs to be further improved. In this study, we investigated the potency of a dynamic 3D bioreactor technology to promote the hepatic maturation of hiPSC-derived hepatocytes when compared to conventional 2D cultures. The differentiation outcome of hiPSC cultured in 2D cultures or 3D bioreactors was analyzed by means of metabolic, phenotypical, and functional parameters.

To allow a direct comparison of the two culture systems, the results for secreted metabolites and proteins as well as for CYP activities were normalized to the initial cell number. Potential proliferation activities of HLC in 2D cultures or 3D bioreactors were quantified by means of Ki-67 staining. The protein Ki-67 is expressed during all active phases of the cell cycle (G1, S, G2, mitosis), but is absent in resting cells (G0).³⁵ The quantitative analysis of the Ki-67 staining revealed that at the end of hepatic differentiation, there was still mitotic activity. However, since the amount of proliferating cells with $\sim 30\%$ was comparable in 2D cultures and 3D bioreactors, it can be concluded that the observed differences in metabolite/protein secretion and CYP activities are not associated with differences in cell growth.

Glucose consumption rates and lactate production rates as indicators for energy metabolism were doubled in 2D cultures compared to 3D bioreactors. This could be caused by the formation of 3D cell aggregates within the bioreactor leading to a gradient and a differential metabolic activity of cells growing either on the surface or in the center of the aggregates. It has been reported that



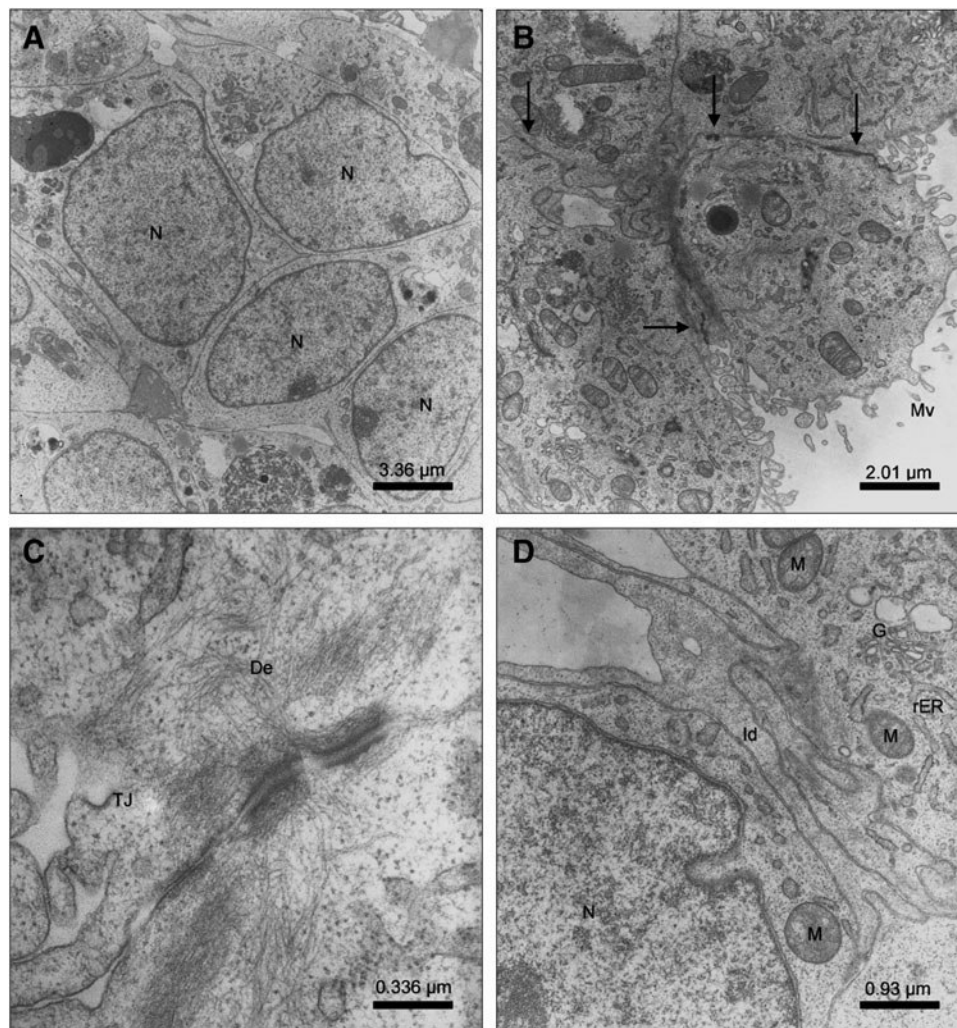


FIG. 5. Ultrastructural characteristics of hiPSC after hepatic differentiation in 3D bioreactors. **(A)** Cells with a high nucleus:cytoplasm ratio indicating immature cells (N). **(B)** Cells with distinct microvilli (Mv) and abundant cell-cell contacts (arrows) between neighboring cells. **(C)** Tight junction (TJ) and desmosome (De) between two neighboring cells. **(D)** Interdigitations (Id) between two cells with mitochondria (M), rough endoplasmic reticulum (rER), and Golgi apparatus (G).

concentration gradients influence cell differentiation and tissue formation.^{36,37} Thus, formation of gradients could also be a reason for the heterogeneous cell population observed in 3D bioreactors as indicated by immunohistochemical analyses and increased *GATA2* mRNA expression.

In the described hollow fiber bioreactor, the aggregate size is controlled by the distance between the capillaries. In other bioreactor technologies such as stirred tank vessels, the aggregate size is influenced by the impeller design³⁸ and the stirring velocity,³⁹ but stirring can cause shear stress and cell damage.⁴⁰ Another bioreactor technology with minimized shear stress is the

rotating-wall vessel, which consists of a horizontally rotating cylindrical culture vessel with a coaxial tubular oxygenator avoiding nutrient compartmentalization and barrier formation.⁴¹

Furthermore, a significantly lower LDH release was detected in 3D bioreactors compared with 2D cultures. One possible reason could be a protective effect of 3D cell aggregates against damage caused by the applied activin A, which can induce apoptosis.⁴² However, LDH is released during both necrosis and apoptosis⁴³ and therefore does not allow distinguishing between necrosis and apoptosis. An apoptosis assay would be



needed to clarify whether the observed LDH release is due to apoptosis processes.

AFP expression and secretion were detected in HLC in both 2D cultures and 3D bioreactors, with significantly higher secretion rates in 2D cultures. In contrast, albumin secretion showed a distinctly higher increase in 3D cultures than in 2D cultures. *In vivo* AFP is only expressed during liver embryogenesis, in fetal liver cells, and hepatocellular carcinomas,⁴⁴ while albumin is produced by differentiated hepatocytes in the adult liver. Thus, the findings of *AFP* and *ALB* expression indicate a higher maturation grade of HLC in 3D bioreactors than in 2D cultures.

Expression of *AFP* in HLC in association with expression of markers for mature hepatocytes such as *ALB* and various *CYP* isoenzymes has been described in several studies.^{7,45,46} Gieseck et al.⁴⁷ also observed lower AFP secretion rates and higher albumin secretion rates in 3D clump cultures compared to 2D cultures, which emphasizes the value of 3D culture systems to promote hepatic maturation of hiPSC. Since albumin secretion was still increasing at the end of hepatic differentiation, a further maturation could be achieved by prolongation of the differentiation period.

This finding is supported by the observed increase of urea secretion in 3D bioreactors. Urea is the major end product of protein nitrogen metabolism and is synthesized by the urea cycle in the liver from ammonia. Hence, urea secretion is an important functional marker for mature hepatocytes. To further validate results from urea secretion, the expression of enzymes from the urea cycle such as carbamoyl phosphate synthetase I or transcarbamylase could be analyzed.

In addition to *AFP* and *SOX17* as markers for both, definitive and extraembryonic endoderm, *SOX7* was analyzed as a specific marker for extraembryonic endoderm. The gene expression of *SOX7* was similar in HLC in 2D cultures, in 3D bioreactors, and in PHH, indicating that the hiPSC-derived HLC did not contain significant amounts of extraembryonic cells, which confirms the hepatic origin of *AFP* and also of *SOX17* in this study. According to the Human Protein Atlas, the *SOX7* expression is strongest in the placenta, but a weak expression is also found in the human liver.⁴⁸

The ability to metabolize drugs through specific *CYP* isoenzymes is crucial for potential application of hiPSC-derived HLC in pharmacological studies. Functional activities of *CYP1A2* and *CYP3A4* were detected in both 2D cultures and 3D bioreactors, while the *CYP2B6* activity was observed only in 3D bioreactors. However, all *CYP* isoenzyme activities were significantly lower in HLC than in

PHH. Data from other studies also showed a lower expression and activity of *CYPs* in differentiated hiPSC compared to PHH.^{5,49} However, since different experimental conditions were used in those studies, a direct comparison of *CYP* activities from different publications is difficult.

Measurements of mRNA expression levels revealed that the pluripotency markers *POU5F1* and *NANOG* were stronger downregulated in 2D cultures than in 3D bioreactors. This could be explained by the formation of an activin A gradient within the 3D cell aggregates. Activin A recapitulates the nodal signaling pathway *in vitro*, which stimulates DE derivation from pluripotent stem cells.⁵⁰ In lower concentrations, activin A is used to maintain pluripotency of hiPSC⁵¹ and hESC.⁵² This could imply that DE formation is decreased in the center of the cell aggregates and other factors such as dimethylsulfoxide (DMSO) might be required to block the effect of activin A on the pluripotency.⁵³

On the other hand, the formation of gradients of activin A and other factors might also promote 3D tissue formation from HLC by reflecting the physiological situation in the liver lobule, which is characterized by an oxygen gradient between the periportal and the perivenous area. This is supported by immunohistochemical and TEM pictures showing tissue-like organization of the cells within 3D bioreactors, including bile duct-like structures characterized by CK18/CK19 double staining. Miki et al.²⁶ also observed the formation of bile duct-like structures after hepatic differentiation of hESC in the 3D bioreactor. Bile ducts are lined with cholangiocytes, which, like the hepatocytes, originate from the bipotent hepatoblasts.⁵⁴

Current protocols for direct differentiation of pluripotent stem cells to cholangiocytes and their *in vitro* generation from hepatoblasts are to some extent similar to protocols used for hepatocyte differentiation since they use factors such as epidermal growth factor, insulin, and hydrocortisone.^{55,56} De Assuncao et al.⁵⁵ observed that cholangiocyte markers already became apparent during the hepatic progenitor phase, which would explain the appearance of cells positive for CK19 in this study.

In addition, abundant tight junctions were detected by immunohistochemical staining and ultrastructural analysis using TEM. The presence of tight junctions is a prerequisite for the formation of bile canaliculi as a characteristic feature of differentiated hepatocytes. In contrast to tight junction protein, the transporter protein MRP2, which is expressed in the canalicular (apical) membrane area of the hepatocyte and contributes to biliary transport, was negative both in 2D cultures and 3D bioreactor cultures, indicating incomplete cell polarization.



The detailed comparison of hiPSC-derived HLC with PHH showed that further improvement of HLC maturation is needed. This could be achieved by combining other promising differentiation strategies with the 3D bioreactor culture: for example, differentiation into the mesodermal direction during DE differentiation, detected by *GATA2* expression in the 3D bioreactor, could be excluded by adding specific inhibitors⁵⁷ and cocultivation with primitive endothelial cells or mesenchymal stem cells could recapitulate the *in vivo* organogenesis even more closely in the 3D culture.¹⁵ In addition, Kim et al.⁴⁶ could show that repeated stimulation of HLC with xenobiotics could improve their metabolizing activity.

A further strategy is based on the usage of an hiPSC line, which is derived from primary hepatoblasts as already shown for mouse iPSC.⁵⁸ This could also improve the hepatic differentiation since recent studies suggest that iPSC retain a residual donor cell memory, which may impact their capacity to differentiate into the cell type of origin.⁵⁹

Conclusion

In conclusion, the hepatic maturation of hiPSC-derived HLC was improved in 3D bioreactors compared with 2D cultures in terms of albumin secretion, CYP2B6 activity, and formation of tissue-like structures with cell-cell contacts. However, some aspects of hepatic functionality were still insufficient, for example, *AFP* was still expressed, and the activity of CYP2C9 and expression of the biliary transporter MRP2 could not be detected. The 3D bioreactor could be used to investigate approaches to improve the maturation of hiPSC-derived hepatocytes and generate fully differentiated hepatocytes from hiPSC in a physiological-like 3D environment in the future.

Acknowledgments

The research leading to these results has received support from the Innovative Medicines Initiative Joint Undertaking under grant agreement no. 115439, resources of which are composed of financial contribution from the European Union's Seventh Framework Programme (FP7/2007-2013) and EFPIA companies' in kind contribution. This article reflects only the author's views and neither the IMI JU, EFPIA, nor the European Commission is liable for any use that may be made of the information contained therein.

Author Disclosure Statement

No competing financial interests exist.

References

1. Kola I, Landis J. Can the pharmaceutical industry reduce attrition rates? *Nat Rev Drug Discov.* 2004;3:711–715.
2. Lewis DF, Ioannides C, Parke DV. Cytochromes P450 and species differences in xenobiotic metabolism and activation of carcinogen. *Environ Health Perspect.* 1998;106:633–641.
3. Giri S, Bader A. Improved preclinical safety assessment using micro-BAL devices: the potential impact on human discovery and drug attrition. *Drug Discov Today.* 2011;16:382–397.
4. Ingelman-Sundberg M. Pharmacogenetics of cytochrome P450 and its applications in drug therapy: the past, present and future. *Trends Pharmacol Sci.* 2004;25:193–200.
5. Takayama K, Morisaki Y, Kuno S, et al. Prediction of interindividual differences in hepatic functions and drug sensitivity by using human iPSC-derived hepatocytes. *Proc Natl Acad Sci U S A.* 2014;111:16772–16777.
6. Hay DC, Zhao D, Ross A, et al. Direct differentiation of human embryonic stem cells to hepatocyte-like cells exhibiting functional activities. *Cloning Stem Cells.* 2007;9:51–62.
7. Sullivan GJ, Hay DC, Park IH, et al. Generation of functional human hepatic endoderm from human induced pluripotent stem cells. *Hepatology.* 2010;51:329–335.
8. Hannan NR, Segeritz CP, Touboul T, et al. Production of hepatocyte-like cells from human pluripotent stem cells. *Nat Protoc.* 2013;8:430–437.
9. Szkolnicka D, Farnworth SL, Lucendo-Villarin B, et al. Deriving functional hepatocytes from pluripotent stem cells. *Curr Protoc Stem Cell Biol.* 2014;30:1G.5.1–12.
10. Medine CN, Lucendo-Villarin B, Storck C, et al. Developing high-fidelity hepatotoxicity models from pluripotent stem cells. *Stem Cells Transl Med.* 2013;2:505–509.
11. Sjogren AK, Liljevald M, Glinghammar B, et al. Critical differences in toxicity mechanisms in induced pluripotent stem cell-derived hepatocytes, hepatic cell lines and primary hepatocytes. *Arch Toxicol.* 2014;88:1427–1437.
12. Schwartz RE, Trehan K, Andrus L, et al. Modeling hepatitis C virus infection using human induced pluripotent stem cells. *Proc Natl Acad Sci U S A.* 2012;109:2544–2548.
13. Shlomai A, Schwartz RE, Ramanan V, et al. Modeling host interactions with hepatitis B virus using primary and induced pluripotent stem cell-derived hepatocellular systems. *Proc Natl Acad Sci U S A.* 2014;111:12193–12198.
14. Ng S, Schwartz RE, March S, et al. Human iPSC-derived hepatocyte-like cells support Plasmodium liver-stage infection in vitro. *Stem Cell Reports.* 2015;4:348–359.
15. Takebe T, Sekine K, Enomura M, et al. Vascularized and functional human liver from an iPSC-derived organ bud transplant. *Nature.* 2013;499:481–484.
16. Baxter M, Withey S, Harrison S, et al. Phenotypic and functional analyses show stem cell-derived hepatocyte-like cells better mimic fetal rather than adult hepatocytes. *J Hepatol.* 2015;62:581–589.
17. Godoy P, Schmidt-Heck W, Natarajan K, et al. Gene networks and transcription factor motifs defining the differentiation of stem cells into hepatocyte-like cells. *J Hepatol.* 2015;63:934–942.
18. Kern A, Bader A, Pichlmayr R, et al. Drug metabolism in hepatocyte sandwich cultures of rats and humans. *Biochem pharmacol.* 1997;54:761–772.
19. Tuschl G, Hrach J, Walter Y, et al. Serum-free collagen sandwich cultures of adult rat hepatocytes maintain liver-like properties long term: a valuable model for in vitro toxicity and drug-drug interaction studies. *Chem Biol Interact.* 2009;181:124–137.
20. Schyschka L, Sánchez JJM, Wang Z, et al. Hepatic 3D cultures but not 2D cultures preserve specific transporter activity for acetaminophen-induced hepatotoxicity. *Arch Toxicol.* 2013;87:1581–1593.
21. Powers MJ, Janigian DM, Wack KE, et al. Functional behavior of primary rat liver cells in a three-dimensional perfused microarray bioreactor. *Tissue Eng.* 2002;8:499–513.
22. Mazzei D, Guazzardi S. A low shear stress modular bioreactor for connected cell culture under high flow rates. *Biotechnol Bioeng.* 2010;106:127–137.
23. Tilles AW, Baskaran H, Roy P, et al. Effects of oxygenation and flow on the viability and function of rat hepatocytes cocultured in a microchannel flat-plate bioreactor. *Biotechnol Bioeng.* 2015;73:379–389.
24. Hoffmann SA, Müller-Vieira U, Biemel K, et al. Analysis of drug metabolism activities in a miniaturized liver cell bioreactor for use in pharmacological studies. *Biotechnol Bioeng.* 2012;109:3172–3181.
25. Lübberstedt M, Müller-Vieira U, Biemel KM, et al. Serum-free culture of primary human hepatocytes in a miniaturized hollow-fibre membrane



- bioreactor for pharmacological in vitro studies. *J Tissue Eng Regen Med*. 2015;9:1017–1026.
26. Miki T, Ring A, Gerlach J. Hepatic differentiation of human embryonic stem cells is promoted by three-dimensional dynamic perfusion culture conditions. *Tissue Eng Part C Methods*. 2011;17:557–568.
 27. Stachelscheid H, Wulf-Goldenberg A, Eckert K, et al. Teratoma formation of human embryonic stem cells in three-dimensional perfusion culture bioreactors. *J Tissue Eng Regen Med*. 2013;7:729–741.
 28. Zeilinger K, Schreiter T, Darnell M, et al. Scaling down of a clinical 3D perfusion multi-compartment hollow fiber liver bioreactor developed for extracorporeal liver support to an analytical scale device useful for hepatic pharmacological in vitro studies. *Tissue Eng Part C Methods*. 2011;17:549–556.
 29. Yu J, Hu K, Smuga-Otto K, et al. Human induced pluripotent stem cells free of vector and transgene sequences. *Science*. 2009;324:797–801.
 30. Hay DC, Zhao D, Fletcher J, et al. Efficient differentiation of hepatocytes from human embryonic stem cells exhibiting markers recapitulating liver development in vivo. *Stem Cells*. 2008;26:894–902.
 31. Hay DC, Fletcher J, Payne C, et al. Highly efficient differentiation of hESCs to functional hepatic endoderm requires Activin A and Wnt3a signaling. *Proc Natl Acad Sci U S A*. 2008;105:12301–12306.
 32. Pfeiffer E, Kegel V, Zeilinger K, et al. Featured article: isolation, characterization, and cultivation of human hepatocytes and non-parenchymal liver cells. *Exp Biol Med (Maywood)*. 2015;240:645–656.
 33. Knöspel F, Freyer N, Stecklum M, et al. Periodic harvesting of embryonic stem cells from a hollow-fiber membrane based four-compartment bioreactor. *Biotechnol Prog*. 2016;32:141–151.
 34. Livak KJ, Schmittgen TD. Analysis of relative gene expression data using real-time quantitative PCR and the 2(-Delta Delta C(T)) Method. *Methods*. 2001;25:402–408.
 35. Scholzen T, Gerdes J. The Ki-67 protein: from the known and the unknown. *J Cell Physiol*. 2000;182:311–322.
 36. Singh M, Berkland C, Detamore MS. Strategies and applications for incorporating physical and chemical signal gradients in tissue engineering. *Tissue Eng Part B Rev*. 2008;14:341–366.
 37. Uzel SG, Amadi OC, Pearl TM, et al. Simultaneous or sequential orthogonal gradient formation in a 3D cell culture microfluidic platform. *Small*. 2016;12:612–622.
 38. Olmer R, Lange A, Selzer S, et al. Suspension culture of human pluripotent stem cells in controlled, stirred bioreactors. *Tissue Eng Part C Methods*. 2012;18:772–784.
 39. Storm MP, Orchard CB, Bone HK, et al. Three-dimensional culture systems for the expansion of pluripotent embryonic stem cells. *Biotechnol Bioeng*. 2010;107:683–695.
 40. Kinney MA, Sargent CY, McDevitt TC. The multiparametric effects of hydrodynamic environments on stem cell culture. *Tissue Eng Part B Rev*. 2011;17:249–262.
 41. Hammond TG, Hammond JM. Optimized suspension culture: the rotating-wall vessel. *Am J Physiol Renal Physiol* 2001;281:F12–F25.
 42. Chen YG, Wang Q, Lin SL, et al. Activin signaling and its role in regulation of cell proliferation, apoptosis, and carcinogenesis. *Exp Biol Med (Maywood)*. 2006;231:534–544.
 43. Denecker G, Vercaemmen D, Steemans M, et al. Death receptor-induced apoptotic and necrotic cell death: differential role of caspases and mitochondria. *Cell Death Differ*. 2001;8:829–840.
 44. Terentiev AA, Moldogazieva NT. Alpha-fetoprotein: a renaissance. *Tumour Biol*. 2013;34:2075–2091.
 45. Cameron K, Tan R, Schmidt-Heck W, et al. Recombinant laminins drive the differentiation and self-organization of hESC-derived hepatocytes. *Stem Cell Reports*. 2015;5:1250–1262.
 46. Kim JH, Jang YJ, An SY, et al. Enhanced metabolizing activity of human ES cell-derived hepatocytes using a 3D culture system with repeated exposures to xenobiotics. *Toxicol Sci*. 2015;147:190–206.
 47. Gieseck RL 3rd, Hannan NR, Bort R, et al. Maturation of induced pluripotent stem cell derived hepatocytes by 3D-culture. *PLoS One*. 2014;9:e86372.
 48. Uhlén M, Fagerberg L, Hallström BM, et al. Tissue-based map of the human proteome. *Science*. 2015;347:1260419.
 49. Ek M, Söderdahl T, Küppers-Munther B, et al. Expression of drug metabolizing enzymes in hepatocyte-like cells derived from human embryonic stem cells. *Biochem Pharmacol*. 2007;74:496–503.
 50. D'Amour KA, Agulnick AD, Eliazar S, et al. Efficient differentiation of human embryonic stem cells to definitive endoderm. *Nat Biotechnol*. 2005;23:1534–1541.
 51. Tomizawa M, Shinozaki F, Sugiyama T, et al. Activin A is essential for feeder-free culture of human induced pluripotent stem cells. *J Cell Biochem*. 2013;114:584–588.
 52. Beattie GM, Lopez AD, Bucay N, et al. Activin A maintains pluripotency of human embryonic stem cells in the absence of feeder layers. *Stem Cells*. 2005;23:489–495.
 53. Czysk K, Minger S, Thomas N. DMSO efficiently down regulates pluripotency genes in human embryonic stem cells during definitive endoderm derivation and increases the proficiency of hepatic differentiation. *PLoS One*. 2015;10:e0117689.
 54. Zhang Y, Bai XF, Huang CX. Hepatic stem cells: existence and origin. *World J Gastroenterol*. 2003;9:201–204.
 55. De Assuncao TM, Sun Y, Jalan-Sakrkar N, et al. Development and characterization of human-induced pluripotent stem cell-derived cholangiocytes. *Lab Invest*. 2015;95:684–696.
 56. Dianat N, Dubois-Pot-Schneider H, Steichen C, et al. Generation of functional cholangiocyte-like cells from human pluripotent stem cells and HepaRG cells. *Hepatology*. 2014;60:700–714.
 57. Loh KM, Ang LT, Zhang J, et al. Efficient endoderm induction from human pluripotent stem cells by logically directing signals controlling lineage bifurcations. *Cell Stem Cell*. 2014;14:237–252.
 58. Lee SB, Seo D, Choi D, et al. Contribution of hepatic lineage stage-specific donor memory to the differential potential of induced mouse pluripotent stem cells. *Stem Cells*. 2012;30:997–1007.
 59. Vaskova EA, Stekleneva AE, Medvedev SP, et al. "Epigenetic memory" phenomenon in induced pluripotent stem cells. *Acta Naturae*. 2013;5:15–21.

Cite this article as: Freyer N, Knöspel F, Strahl N, Amini L, Schrade P, Bachmann S, Damm G, Seehofer D, Jacobs F, Monshouwer M, Zeilinger K (2016) Hepatic differentiation of human induced pluripotent stem cells in a perfused three-dimensional multicompartment bioreactor. *BioResearch Open Access* 5:1, 235–248, DOI: 10.1089/biores.2016.0027.

Abbreviations Used

ANOVA = analysis of variance
AUC = area under curve
DE = definitive endoderm
hESC = human embryonic stem cells
HGF = hepatocyte growth factor
hiPSC = human induced pluripotent stem cells
HLC = hepatocyte-like cells
LDH = lactate dehydrogenase
PHH = primary human hepatocytes
TEM = transmission electron microscopy

Publish in BioResearch Open Access



- Broad coverage of biomedical research
- Immediate, unrestricted online access
- Rigorous peer review
- Compliance with open access mandates
- Authors retain copyright
- Highly indexed
- Targeted email marketing

liebertpub.com/biores



Hepatic differentiation of human iPSCs in different 3D models: A comparative study

FLORIAN MEIER^{1*}, NORA FREYER^{2*}, JOANNA BRZESZCZYNSKA³, FANNY KNÖSPEL², LYLE ARMSTRONG⁴, MAJLINDA LAKO⁴, SELINA GREUEL², GEORG DAMM^{5,6}, EVA LUDWIG-SCHWELLINGER⁷, ULRICH DESCHL¹, JAMES A. ROSS³, MARIO BEILMANN^{1*} and KATRIN ZEILINGER^{2*}

¹Boehringer Ingelheim Pharma GmbH and Co.KG, Nonclinical Drug Safety Germany, D-88397 Biberach an der Riss; ²Bioreactor Group, Berlin Brandenburg Center for Regenerative Therapies (BCRT), Charité-Universitätsmedizin Berlin, Campus Virchow-Klinikum, D-13353 Berlin, Germany; ³Tissue Injury and Repair Group, Chancellor's Building, Edinburgh Medical School, University of Edinburgh, EH164SB Edinburgh; ⁴Institute of Genetic Medicine, University of Newcastle upon Tyne, NE13BZ Newcastle upon Tyne, UK; ⁵Department of Hepatobiliary Surgery and Visceral Transplantation, University of Leipzig, D-04103 Leipzig; ⁶Department of General, Visceral and Transplantation Surgery, Charité Universitätsmedizin Berlin, D-13353 Berlin; ⁷Boehringer Ingelheim Pharma GmbH and Co.KG, Drug Metabolism and Pharmacokinetics Germany, D-88397 Biberach an der Riss, Germany

Received April 28, 2017; Accepted September 8, 2017

DOI: 10.3892/ijmm.2017.3190

Abstract. Human induced pluripotent stem cells (hiPSCs) are a promising source from which to derive distinct somatic cell types for *in vitro* or clinical use. Existing protocols for hepatic differentiation of hiPSCs are primarily based on 2D cultivation of the cells. In the present study, the authors investigated the generation of hiPSC-derived hepatocyte-like cells using two different 3D culture systems: A 3D scaffold-free microspheroid culture system and a 3D hollow-fiber perfusion bioreactor. The differentiation outcome in these 3D systems was compared with that in conventional 2D cultures, using primary human hepatocytes as a control. The evaluation was made based on specific mRNA expression, protein secretion, antigen expression and metabolic activity. The expression of α -fetoprotein was lower, while cytochrome P450 1A2 or 3A4 activities were higher in the 3D culture systems as compared with the 2D differentiation system. Cells differentiated in the 3D bioreactor showed an increased expression of albumin and hepatocyte nuclear factor 4 α , as well as secretion of α -1-antitrypsin as compared with the 2D differentiation system, suggesting a higher degree of maturation. In contrast, the 3D scaffold-free microspheroid culture provides an easy and robust method to

generate spheroids of a defined size for screening applications, while the bioreactor culture model provides an instrument for complex investigations under physiological-like conditions. In conclusion, the present study introduces two 3D culture systems for stem cell derived hepatic differentiation each demonstrating advantages for individual applications as well as benefits in comparison with 2D cultures.

Introduction

The liver represents the central organ for drug metabolism and also a main target organ for drug-associated toxicity. Therefore, the parenchymal cells of the liver, the hepatocytes, are of special interest for pharmacological and toxicological investigations.

Primary human hepatocytes (PHH) are considered to be the gold standard for such investigations, however their availability is limited and their metabolic activity varies, primarily due to the mostly unknown genetic backgrounds of the donors (1). Primary hepatocytes are also isolated from animals, such as rats, but they have a limited predictability due to cross-species differences in drug metabolism and sensitivity (2). Therefore, the development of *in vitro* culture models using easy accessible cells of human origin is gaining increasing scientific interest.

Pluripotent stem cells (PSC) constitute a promising cell source for the generation of hepatocytes, due to their capacity to differentiate into all cell types of the organism and their ability to replicate while maintaining pluripotency. The innovation of induced pluripotent stem cell (iPSC) technology opened up the possibility of deriving pluripotent cells from different donors (3,4) thereby circumventing the ethical concerns associated with the use of human embryonic stem cells. Thus, pluripotent cell lines with distinct genotypes can be generated,

Correspondence to: Dr Mario Beilmann, Boehringer Ingelheim Pharma GmbH and Co.KG, Nonclinical Drug Safety Germany, Birkendorfer Straße 65, D-88397 Biberach an der Riss, Germany
E-mail: mario.beilmann@boehringer-ingelheim.com

*Contributed equally

Key words: human induced pluripotent stem cells, hepatocyte-like cells, 3D culture, primary human hepatocytes, hepatic differentiation

which are of interest in relation to specific disease mechanisms, and to the development of drugs (5,6). These properties of PSC in combination with the increasing knowledge of the *in vivo* embryonic development of hepatocytes (7) have led to the establishment of several protocols for the *in vitro* differentiation of PSC into hepatocyte-like cells (HLCs) (8-10). Current protocols mimic the different stages of the *in vivo* development of hepatocytes by the sequential addition of specific growth factors, like activin A, Wnt3a, hepatocyte growth factor (HGF) and oncostatin M (OSM) (8,11). Small chemical molecules, such as dimethyl sulfoxide (DMSO), bromo-indirubin-3'-oxim and SB431542 (12) can be applied as well. The generated HLCs demonstrate some characteristics of hepatocytes, such as susceptibility to hepatitis C virus infection (13), secretion of hepatic proteins (14,15) and activity of metabolic enzymes (16,17). However, the drug metabolizing capabilities of HLCs obtained with current protocols are still below those of PHH (18). Recent findings suggested that HLCs resemble immature or fetal hepatocytes rather than adult hepatocytes (19,20).

In order to increase the functionality and the maintenance of HLCs, the use of extracellular matrices (21,22), transcription factor overexpression (23,24) or modified cultivation media (25) were suggested. Further approaches focus on complex culture systems to provide an organotypic environment that better approximates the *in vivo* situation. Cultivation of cells in a 3D environment facilitates the formation of physiological cell-cell-contacts, which have been demonstrated to be crucial for the preservation of a mature hepatic phenotype (26). Different 3D culture systems were investigated for hepatic differentiation of PSC, including scaffold-based technologies (27-29) or scaffold-free culture systems, which rely on the self-assembly of the cells (17,30). However, due to the lack of standardized methods to characterize the HLCs after hepatic differentiation, it is difficult to compare the results from different approaches and culture models.

In the present study, the authors investigated the hepatic differentiation of human iPSCs (hiPSCs) in two different 3D culture systems, a scaffold-free microspheroid culture system and a 3D hollow-fiber perfusion bioreactor (31). The differentiation outcome in these 3D systems was compared with that in conventional 2D cultures. All culture systems were treated with the same differentiation protocol, allowing a comparative analysis of the generated HLCs at mRNA, protein and metabolic level. In addition, data from hiPSC-derived differentiated cells were compared to those from PHH. Based on the results, promising approaches for the development of physiologically relevant *in vitro* liver models were identified.

Materials and methods

Culture of hiPSCs. The generation and characterization of the hiPSC line SB Adult3 clone 4 (AD3C4) is described by van de Bunt *et al.* (32). The hiPSC lines AD2C3, AD3C1 and AD4C1 were generated and characterized in the same way from fibroblasts 24245, 23447 and 23801 (Lonza CC-2511, tissue acquisition numbers are given; Lonza Group, Ltd., Basel, Switzerland), respectively. Cells were seeded on culture plates coated with growth-factor-reduced Matrigel (Corning Inc., Corning, NY, USA). For expansion, hiPSCs

were maintained at 37°C, 5% CO₂ using mTeSR™1 medium (Stemcell Technologies, Inc., Vancouver, BC, Canada) supplemented with 100,000 U/l penicillin and 100 mg/l streptomycin (Thermo Fisher Scientific, Inc., Waltham, MA, USA). The cells were passaged with 0.5 mM EDTA (Thermo Fisher Scientific, Inc.) every 3-5 days, after reaching a confluence of ~70%.

Hepatocyte-like cell differentiation in 2D cultures. Differentiation of hiPSCs in 2D monolayer cultures (Fig. 1A) was performed according to Szkolnicka *et al.* (11) with minor changes. In detail, hiPSCs were plated onto Matrigel-coated [1:20 diluted in Dulbecco's modified Eagle's medium (DMEM)/F12 medium] 24-well plates and differentiated into definitive endodermal (DE) cells using the STEMdiff™ Definitive Endoderm kit (Stemcell Technologies, Inc.) according to the manufacturer's instructions until day 5. From day 5 to 8 cultures were maintained in SR-DMSO-Medium [knockout DMEM supplemented with 20% knockout serum replacement medium, 0.5% GlutaMAX, 1% non-essential amino acids, 0.1 mM β-mercaptoethanol, DMSO (Sigma-Aldrich; Merck KGaA, Darmstadt, Germany) and 1% penicillin/streptomycin]. From day 9 on, hepatocyte maturation medium [HepatoZYME-SFM, 1% GlutaMAX, 1% penicillin/streptomycin, 10 μM hydrocortisone 21-hemisuccinate sodium salt (Sigma-Aldrich; Merck KGaA), 10 ng/ml human HGF and 20 ng/ml human OSM (both from PeproTech EC Ltd., London, UK)] was used and renewed every other day. All reagents were purchased from Thermo Fisher Scientific, Inc., if not stated otherwise.

Adaptations for differentiation using 3D microspheroids. For the 3D microspheroid differentiation (Fig. 1B), the first steps of differentiation were performed in conventional 2D cultures using 6-well plates as described above. On day 11 of the differentiation process, the cells were detached enzymatically with TrypLE™ (Thermo Fisher Scientific, Inc.) and plated onto low attachment 96-well plates. These were prepared by adding 50 μl of 60°C warm 1.5% agarose (Serva Electrophoresis GmbH, Heidelberg, Germany)-DMEM/F12 (Thermo Fisher Scientific, Inc.) solution into each well of the plate (33). Cells were seeded in these 96-well plates at a density of 10,000 cells/well in 150 μl of hepatocyte maturation medium. Every other day 100 μl of the medium were renewed. The method of spheroid formation was proven with additional hiPSC lines, showing the robust generation of one spheroid of constant size per well (Fig. 2).

Adaptations for differentiation using perfused 3D bioreactors. For hepatic differentiation under dynamic conditions, a hollow-fiber bioreactor technology was used (Fig. 1C). The bioreactor (StemCell Systems GmbH, Berlin, Germany) consists of independent yet interwoven hollow-fiber capillary systems, which serve for counter-current medium perfusion via two medium capillary systems and decentralized oxygenation via one gas capillary system. The cells are cultured in the extra-capillary space (cell compartment) (31). The cell compartment volume of the used bioreactors was 2 ml and they were integrated into a perfusion circuit (StemCell Systems GmbH) with a total volume of 20 ml. Electronic control of system functions was provided by a perfusion device (StemCell Systems GmbH) that contained two modular pump units, a heating unit and a gas-mixing unit.

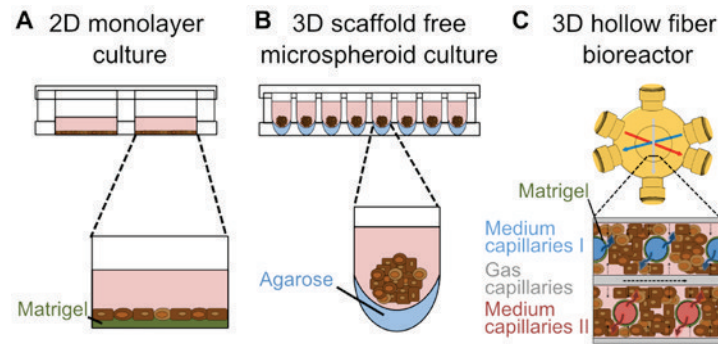


Figure 1. Cultivation systems used for hepatic differentiation of hiPSCs. (A) In the 2D monolayer culture, hiPSCs were differentiated on Matrigel coated 24-well plates. (B) In the 3D scaffold-free microspheroid culture cells were cultivated in 96-well plates. Within one well of the plate, one microspheroid was generated by self-aggregation of differentiating cells on top of a low attachment surface coated with agarose. (C) In the 3D hollow fiber bioreactor, hiPSCs were differentiated in the extra-capillary space of the bioreactor. The three capillary systems supply medium (blue and red) and oxygen (grey). The capillaries were coated with Matrigel on the extra-capillary-side to allow cell attachment. hiPSCs, human induced pluripotent stem cells.

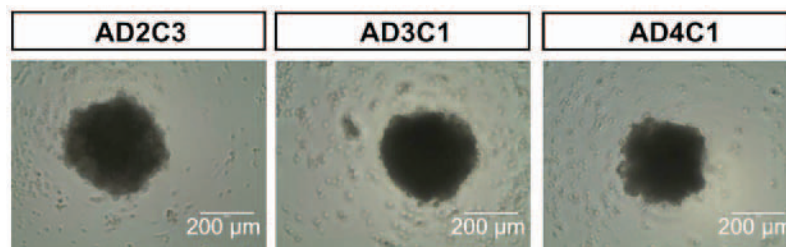


Figure 2. Microspheroids derived from three different human induced pluripotent stem cell lines at day 18.

Prior to cell inoculation the bioreactors were flushed with 3 mg Matrigel in 5 ml DMEM/F-12 medium and incubated at RT for 1 h. Afterwards, 1×10^8 hiPSCs were seeded into each bioreactor. Cultures were maintained at 37°C, the medium recirculation rate was 10 ml/min and the feed rate was 1 ml/h. A mixture of 95% air and 5% CO₂ was supplied at a flow rate of 20 ml/min. CO₂ perfusion rates were adjusted, if required, to maintain a stable pH between 7.2 and 7.4. After an adaptation phase of two days with mTeSR™1, differentiation of the cells was performed with the same media compositions as used for 2D cultures. After each differentiation step, the culture medium was rinsed out by flushing the perfusion circuit with 60 ml of the culture medium used in the next differentiation step.

Culture of primary human hepatocytes. PHH were isolated from macroscopically healthy tissue from resected human livers of patients with informed consent of the patients according to the ethical guidelines of the Charité Universitätsmedizin Berlin (Berlin, Germany). Cell isolation was performed according to Pfeiffer *et al* (34). Hepatocytes were seeded at a density of 2.0×10^5 cells/cm² in 24-well plates (BD Biosciences, Franklin Lakes, NJ, USA) coated with rat-tail collagen. Cells were cultivated using Heparmed Vito 143 supplemented with 0.8 mg/l insulin, 5 mg/l transferrin, 0.003 mg/l glucagon, 100,000 U/l penicillin and 100 mg/l streptomycin (all from Merck KGaA), and 10% FCS (GE Healthcare Life Sciences, Chalfont, UK). PHH were either used directly after isolation (PHH 0 h) or after 24 h of cultivation in 2D culture plates (PHH 24 h).

Glucose and lactate measurements. The metabolic activity of the cells was assessed by measuring glucose and lactate concen-

trations with a blood gas analyzer (ABL 700; Radiometer, Copenhagen, Denmark).

RNA isolation and reverse transcription-quantitative polymerase chain reaction (RT-qPCR). Total RNA was isolated using TRIzol™ (Thermo Fisher Scientific, Inc.), following the manufacturer's instructions. The High Capacity cDNA reverse transcription kit (Applied Biosystems; Thermo Fisher Scientific, Inc.) was used to convert 1 µg of RNA to cDNA following the manufacturer's instructions. The quantitative validation of the expression of selected genes was performed by RT-qPCR, as previously described (35). In detail, the Applied Biosystems StepOne real-time PCR system was applied using custom PrimerDesign primers (Primerdesign Ltd., Chandler's Ford, UK) and the SYBR-Green PCR master mix (cat. no. 4368577; Applied Biosystems; Thermo Fisher Scientific, Inc.), following the manufacturer's instructions. Primers are listed in Table I. Reactions were run in triplicate on a StepOne Plus instrument (Applied Biosystems; Thermo Fisher Scientific, Inc.). Running conditions were: 95°C for 10 min, followed by 40 cycles of 95°C for 15 sec and 60°C for 60 sec.

Data from RT-qPCR were normalized to multiple internal control genes (18S, EIF 2A4, β-actin and SDHA) with the geNorm algorithm as described by Vandesompele *et al* (36). Results are presented as fold-changes in gene expression relative to 2D cultures on day 18 calculated with the ΔΔCq method (37).

Enzyme-linked immunosorbent assay (ELISA). Cell culture supernatants were clarified by centrifugation and stored at -20°C until assayed. The secretion of α-fetoprotein (AFP),

Table I. Primer sequences for the custom real-time PCR (Primerdesign Ltd.).

Gene symbol	Gene name	Forward primer 5'→3' sequence	Reverse primer 3'→5' sequence	Amplicon size (bp)
<i>AFP</i>	α -fetoprotein	CAGTAATTCTAAGAGTTGCTAAAGGAT	CCTGGATGTAATTTCTGTAATTCTTCTT	117
<i>AHR</i>	Aryl hydrocarbon receptor	AATTTTGACCCTGGTTTTTGGATT	TGGTTTGGAAATAATTGTGAATAGCA	129
<i>ALB</i>	Albumin	TGACAAATCACTTCATACCCTTTTT	GCATTCATTTCTCTCAGGTTCTTG	118
<i>CXCR4</i>	C-X-C motif chemokine receptor 4	CCAAAGAAGGATATAATGAAGTCACT	GGGCTAAGGGCACAAGAGA	88
<i>CYP1A2</i>	Cytochrome P450 family 1 subfamily A member 2	GCCTTCATCCTGGAGACCTT	TCAGCGTTGTGTCCCTTGT	82
<i>CYP3A4</i>	Cytochrome P450 family 3 subfamily A member 4	ACCGTAAGTGGAGCCTGAAT	AAGTAATTTGAGGTCTCTGGTGT	90
<i>CYP3A7</i>	Cytochrome P450 family 3 subfamily A member 7	AGAGAGATAAGGAAGGAAAGTAGTGA	TGTGTACGGGTTCCATATAGATAGA	114
<i>HNF4A</i>	Hepatocyte nuclear factor 4 α	GACCTCTACTGCCTTGGACAA	GATGAAGTCGGGGGTTGGA	87
<i>NANOG</i>	Nanog homeobox	GCTGTGTGTAATGATAGATT	GAGGTTTCAGGATGTTGGAGAG	85
<i>SOX9</i>	SRY-box 9	GGACCAGTACCCGCACTTG	AATCCGGGTGGTCTTCTTG	143
<i>SOX17</i>	SRY-box 17	GTAGAAGGGGATGTCCAAGTAAT	TGTGAAGATTAAGGTAACTGAATGT	144

albumin (ALB) and α -1-antitrypsin (A1AT) was quantified with an ELISA, using the antibodies provided in Table II and the protocol as described by Liu *et al.* (38). ELISA plates were read at 490 nm with a reference wavelength of 630 nm using a MRX II plate reader (Dynex Technologies, Chantilly, VA, USA) and the concentration of the appropriate protein in each sample was calculated from standard curves using MRX II Endpoint software 2.02 (Dynex Technologies).

Urea analysis. Cell culture supernatants were clarified by centrifugation and stored at -20°C until assayed. Urea was measured in the cell culture supernatant without any additional treatment, using the QuantiChrom™ Urea assay kit (DIUR-500; BioAssay Systems, Hayward, CA, USA) according to the manufacturer's instructions.

Immunofluorescence analysis. The 2D cultures were fixed in 4% paraformaldehyde (PFA; Electron Microscopy Science, Hatfield, PA, USA) in phosphate-buffered saline (PBS) at room temperature for 10 min. Primary and secondary antibodies were applied in PBS with 0.5% Triton X-100 and 1% BSA (both from Sigma-Aldrich; Merck KGaA) and incubated at 4°C overnight or at room temperature for 1.5 h, respectively. All primary and secondary antibodies are provided in Table III.

Finally, a nuclear counter stain was performed with 0.8 μ g/ml Hoechst 33342 (Thermo Fisher Scientific, Inc.) in PBS at room temperature for 30 min. The quantification of immunoreactive cells was performed with the Cellomics Array Scan V^{Ti} and Cellomics Scan and View Software (version 6.3.1) (both from Thermo Fisher Scientific, Inc.).

The microspheroids were collected in a 1.5 ml reaction tube and fixed in 4% PFA (Electron Microscopy Science) in PBS at 4°C overnight. An ~60°C warm 2% agarose solution in PBS was prepared, added to the microspheroids and centrifuged at 20,000 x g for 1 sec. The resulting agarose plug was dehydrated in a tissue processor (Tissue-Tek VIP; Sakura Finetek Europe B.V., Flemingweg, The Netherlands), paraffinized and cut into slides of 4.0 μ m thickness.

For immunohistochemical staining of the bioreactor cultures the hollow-fiber bed was excised en bloc, fixed with 4% formaldehyde solution (Herbeta Arzneimittel Detlef Karlowski e.K., Berlin, Germany) at room temperature for 1 h, dehydrated, paraffinized and cut into slides of 4.0 μ m thickness.

Paraffin sections were rehydrated and boiled in 10 mM citrate buffer (pH 6.0) for 12 min. Pre-blocking was performed with PBS containing 0.5% Triton X-100 and 1% BSA at room temperature for 1 h. Antibody staining was performed as described above. The primary and secondary antibodies used are

Table II. Antibodies used for analysis of hepatic export proteins using ELISA.

Species and antigen name	Type	Target	Provider, catalog no.	Dilution
Rabbit anti-albumin (capture antibody)	Polyclonal	Anti-human	Agilent Technologies, Inc., A0001	1:1,000
Mouse anti-albumin antibody (intermediate antibody)	Monoclonal	Anti-human	Sigma-Aldrich, A6684	1:1,000
Rabbit anti-IgGs, HRP conjugated (detection antibody)	Polyclonal	Anti-mouse	Agilent Technologies, Inc., P0260	1:1,000
Rabbit anti-AFP (capture antibody)	Polyclonal	Anti-human	Agilent Technologies, Inc., A0008	1:2,000
Rabbit anti-AFP, HRP conjugated (detection antibody)	Polyclonal	Anti-human	Agilent Technologies, Inc., P0128	1:2,500
Sheep anti-A1AT, HRP conjugated (detection antibody)	Polyclonal	Anti-human	Abcam, ab 8768	1:1,500

Agilent Technologies, Inc.; Sigma-Aldrich; Merck KGaA; Abcam, Cambridge, UK. ELISA, enzyme-linked immunosorbent assay; AFP, α -fetoprotein.

Table III. Primary and secondary antibodies used for immunofluorescence analysis.

Species and antigen name	Type	Target	Provider, catalog no.	Dilution
Mouse anti- α -fetoprotein	Monoclonal	Anti-human	Thermo Fisher Scientific, Inc., 180003	1:1,000
Mouse anti-cytokeratin 18	Monoclonal	Anti-human	Santa Cruz Biotechnology, Inc., sc-6259	1:100
Rabbit anti-albumin	Polyclonal	Anti-human	Dako Cytomation, A0001	1:2,000
Rabbit anti-hepatocyte nuclear factor 4 α	Polyclonal	Anti-human	Santa Cruz, sc-8987	1:100
A488 goat anti-mouse	Polyclonal	Anti-mouse	Thermo Fisher Scientific, Inc., A11029	1:500
A594 goat anti-rabbit	Polyclonal	Anti-rabbit	Thermo Fisher Scientific, Inc., A11037	1:500

Thermo Fisher Scientific, Inc.; Santa Cruz Biotechnology, Inc., Dallas, TX, USA.

Table IV. Applied substrates and their corresponding CYP isoenzymes with resulting products and applied concentrations.

Substrate	Corresponding CYP isoenzyme	Provider	Final concentration	Solutions for elution	Recorded transitions
Midazolam	CYP3A4/5	Roche Diagnostics GmbH	25 μ M	Double distilled water containing 0.1% formic acid and acetonitrile containing 0.1% formic acid	1'-Hydroxymidazolam 342.1-324.0 m/z
Phenacetin	CYP1A2	Sigma-Aldrich	200 μ M	Double distilled water containing 0.1% formic acid and methanol containing 0.1% formic acid	Paracetamol 152.1-110.1 m/z
Bupropion	CYP2B6	Sigma-Aldrich	75 μ M	Double distilled water containing 0.1% formic acid and methanol containing 0.1% formic acid	Hydroxybupropion 256.1-238.1 m/z

Roche Diagnostics GmbH, Basel, Switzerland; Sigma-Aldrich; Merck KGaA.

detailed in Table III. Finally, the cells were embedded in Roti-Mount FluorCare DAPI (Carl Roth GmbH + Co. KG, Karlsruhe, Germany). The quantification of marker positive cells was performed with the Opera Phenix and the Harmony software (version 4.1) (both from PerkinElmer, Inc., Waltham, MA, USA).

Cytochrome P450 (CYP) analysis. CYP iso-enzyme activities were analyzed based on assays established in previous studies (39,40). A substrate mix containing midazolam, phenacetin and bupropion was prepared in the respective culture medium without pretreatment for induction. Details of the

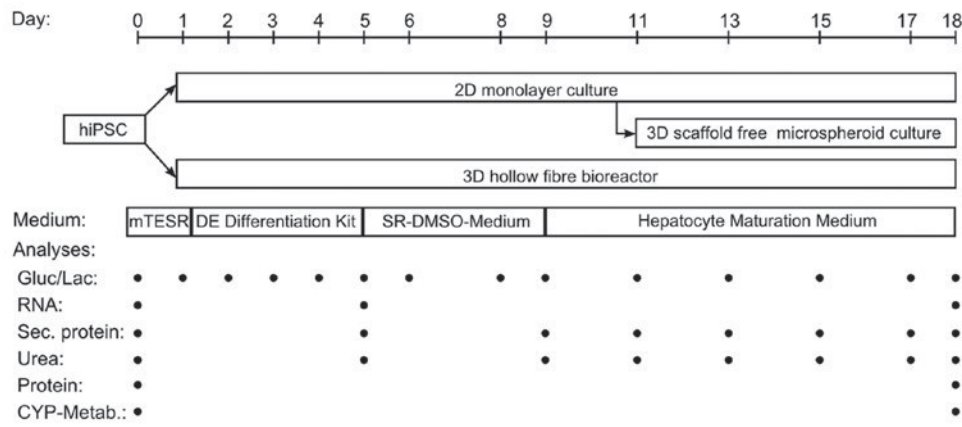


Figure 3. Comparative analyses of three cultivation systems for hepatic differentiation of hiPSCs. The cells were differentiated into HLCs by the use of a 2D monolayer culture, a 3D scaffold-free microspheroid culture and a 3D hollow fibre bioreactor. For all systems identical differentiation media were used as indicated. Analyses of glucose consumption/lactate production (Gluc/Lac), mRNA expression (RNA), secretion of proteins (sec. protein), urea production (Urea), intracellular protein expression (protein) and metabolism of substrates by cytochrome P450 isoenzymes (CYP-Metab.) were performed at the indicated days. hiPSCs, human induced pluripotent stem cells; HLCs, hepatocyte-like cells.

used substrates, their final concentrations and information on the LC-MS analysis are provided in Table IV. A medium blank was used for normalization. In 2D cultures, the assay was performed on four wells of a 24-well plate and the supernatants were pooled per time-point. In microspheroids, the assay was performed in 8 wells of a 96-well plate by collecting ~10 microspheroids/well. Supernatants of the wells were pooled per time-point. For the bioreactors, 1 ml of a 20-fold concentrated substrate mix was applied to the bioreactor system. For all culture systems, samples were taken after 0, 1, 2 and 6 h.

The supernatants were diluted with quench solution (20% methanol or acetonitrile with 0.1% formic acid) containing the stable isotope-labeled metabolite as an internal standard. LC-MS analysis was performed using the following equipment: HTS-xt PAL autosampler (CTC Analytics AG, Zwingen, Switzerland), 1290 infinity G4220A binary pump and degasser (Agilent Technologies, Inc., Santa Clara, CA, USA), MistraSwitch column oven (Maylab Analytical Instruments GmbH, Vienna, Austria) and a YMC C18 Triart, 30x2 mm, 1.9 μ m (YMC Europe GmbH, Dinslaken, Germany) column. All ion chromatograms were recorded on a 6500 Triple Quad (QqQ) LC-MS/MS-system hybrid mass spectrometer (AB Sciex Pte, Concord, ON, Canada) equipped with an Iondrive™ Turbo V ion source operated in the positive electrospray ionization mode. Integration of chromatograms as well as determination of peak areas was performed by Analyst software version 1.6.2 (Applied Biosystems/MDS Sciex).

DNA isolation. RLT buffer (Qiagen GmbH, Hilden, Germany) was added to a defined number of wells, number of microspheroids or volume of the cell compartment of bioreactors. The DNA was isolated from the cell extracts by use of the QIAamp DNA micro kit (Qiagen GmbH) according to the manufacturer's protocol.

Statistical analysis. Data evaluation and graphical illustration were performed with GraphPad Prism 5.0 and 7.0 (GraphPad Software, Inc., San Diego, CA, USA). Experiments were performed in triplicate, unless stated otherwise, and results are presented as median \pm interquartile range. Data for energy

metabolism and secretion of proteins were normalized to the initial cell number and area under curve (AUC) was calculated. Data for CYP activities were normalized against the DNA content at day 18. Differences between the different culture systems or to PHH were detected applying the Mann-Whitney test or the unpaired, two-tailed t-test.

Results

Differentiation of hiPSCs to HLCs. The hiPSC line AD3C4 was selected from different previously tested hiPSC lines generated within the StemBANCC consortium. The comparative study of a 2D cell culture differentiation system (Fig. 1A) with a 3D scaffold-free microspheroid system (Fig. 1B) and a perfused 3D hollow-fiber bioreactor (Fig. 1C) was performed using three independent batches of AD3C4 hiPSCs at the same passage number. To compare the different culture systems, mRNA levels and secretion of stage specific markers as well as immunohistochemical staining and CYP activity were analyzed (Fig. 3).

Energy metabolism. In order to evaluate the energy metabolism during hepatic differentiation of hiPSCs, the glucose consumption rates and lactate production rates were determined at the time of medium exchange (2D culture, microspheroids) or daily (bioreactor). Glucose consumption and lactate production rates increased in 2D cultures and microspheroids during the first 6 days of differentiation. Following this, rates continuously declined in both culture systems during the whole differentiation period (Fig. 4A). The bioreactor cultures showed a slight increase of glucose consumption and lactate production rates during the first 2 days of differentiation and afterwards also a continuous but slight decrease until the end of hepatic differentiation. At the end of differentiation, these values were comparable to 2D cultures and microspheroids (Fig. 4A). The AUC for glucose consumption was significantly higher in 2D cultures and microspheroids compared with bioreactors ($p < 0.0001$). The time course of lactate production mirrored that of glucose consumption and the AUC for lactate production was also significantly higher

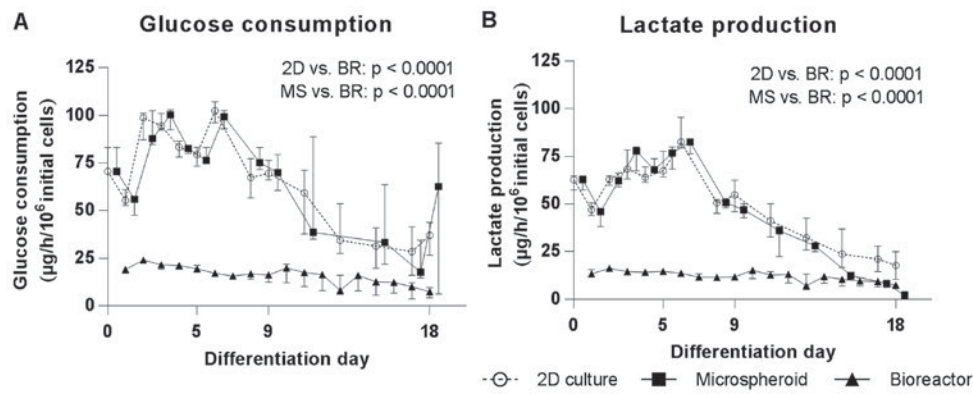


Figure 4. Energy metabolism of hiPSCs during hepatic differentiation in 2D cultures (2D, circles), MS (squares) or BR (triangles). (A) Glucose consumption and (B) lactate production are shown. Areas under curve were calculated for each dataset and differences between groups were determined with the unpaired, two-tailed t-test. P-values < 0.1 are given in the graphs (2D cultures: $n=6$; microspheroids and bioreactors: $n=3$, median of biological replicates \pm interquartile range). MS, microspheroids; BR, bioreactors; hiPSCs, human induced pluripotent stem cells.

in 2D cultures and microspheroids compared with bioreactors ($p < 0.0001$) (Fig. 4B)

Gene expression profiling of hiPSC-derived HLCs. To evaluate the maturation state of the HLCs obtained in the different culture systems compared to freshly isolated and cultured PHH, the mRNA expression of stage-specific genes was analyzed and calculated in relation to 2D differentiated HLCs at day 18. The expression of the pluripotency-associated homeobox gene *Nanog* (*NANOG*) was downregulated in HLC relative to undifferentiated hiPSCs, irrespective of the culture system (Fig. 5A). Within the HLC and PHH groups, the 2D differentiated HLCs expressed the highest amount of *NANOG*. The DE markers SRY-box 17 (*SOX17*) and C-X-C motif chemokine receptor 4 (*CXCR4*) peaked at day 5 in 2D cultures and showed subsequently a downregulation (Fig. 5B and C). The significantly higher expression of *AFP* in the HLCs compared to cultured PHH ($p < 0.0001$) demonstrated the immature properties of the *in vitro* generated cells. Within the *in vitro* generated cells, the 2D HLCs displayed a significantly higher expression of *AFP* compared to HLCs derived in the bioreactor ($p=0.0477$), and a higher, although not significant, expression than the microspheroids. There was also a significantly lower *AFP* expression in cultured PHH compared to freshly isolated PHH ($p=0.032$) (Fig. 5D). The cholangiocyte marker SRY-box 9 (*SOX9*) showed the highest expression in HLCs from 2D cultures and bioreactors (Fig. 5E). Microspheroids and cultured PHH expressed significantly lower amounts of *SOX9*. Expression of the hepatocyte marker *ALB* was highest in freshly isolated PHH and showed a significant drop after 24 h of cultivation ($p=0.0028$) (Fig. 5F). HLCs derived in the bioreactor expressed *ALB* at a higher amount compared to 2D HLCs and microspheroids indicating a higher degree of maturation in the bioreactor system. The expression of hepatocyte nuclear factor 4 α (*HNF4A*) was significantly higher in HLCs as compared to cultured PHH ($p \leq 0.0003$) (Fig. 5G). Among the HLCs, cells derived in the bioreactor expressed significantly more *HNF4A* than cells generated in 2D or in microspheroids ($p \leq 0.0059$). Furthermore, there was a significant drop of *HNF4A* expression in cultured PHH compared to freshly isolated PHH ($p \leq 0.0001$). Regarding the expression of metabolic enzymes, the *CYP3A4* expression presented a

significant decrease from freshly isolated PHH to cultured PHH and a further decrease from cultured PHH to all *in vitro* generated HLCs ($p \leq 0.0142$) (Fig. 5H). The highest *CYP3A7* expression among the HLCs could be detected in the bioreactor system. There was again a significant decrease of *CYP3A7* expression from freshly isolated PHH to PHH cultured over 24 h ($p < 0.0001$) (Fig. 5I). *CYP1A2* indicated only a marginal expression in HLCs in all culture systems. In contrast, freshly isolated PHH demonstrated a high expression, which however significantly decreased within 24 h of cultivation (Fig. 5J). The nuclear receptor aryl hydrocarbon receptor (*AHR*) was expressed in the *in vitro* systems at levels positioned between freshly isolated PHH (high expression) and cultivated PHH (low expression) (Fig. 5K). In conclusion, among the *in vitro* systems the bioreactor system showed the highest maturation stage on mRNA expression level, but was still lower as compared to freshly isolated PHH.

Secretion of hepatic proteins and metabolites by HLCs. The detection of secreted hepatic proteins allows an estimation of the differentiation status of the cells over time. The secretion of *AFP* increased in all culture systems from day 9 until day 13 and subsequently decreased until day 18 reaching basal levels (Fig. 6A). Secretion of *ALB* and *A1AT* could be detected only in the bioreactors from differentiation day 9 and 11 onwards, respectively (Fig. 6B and C). Urea production was significantly higher in the microspheroids than in 2D cultures ($p=0.0027$) or bioreactors ($p=0.0022$) and peaked at day 13 of differentiation (Fig. 6D). However, the strong production of urea decreased subsequently to a lower level as compared to the 2D cultures and bioreactors, which produced a constant level of urea from day 11 onwards (Fig. 6D). Compared to the 2D cultures, cells in the bioreactor produced significantly less urea ($p=0.0021$).

Immunohistochemical characterization of HLCs. Immunohistochemical analysis of liver-specific markers was performed to characterize the cell composition in the different culture systems at day 18 (Fig. 7A-C). The hepatocyte marker *HNF4A* was detectable in half of the cells in the 2D cultures, whereas this proportion was lower in the microspheroids and bioreactors (Fig. 7D-F and J). A shift from the nuclear

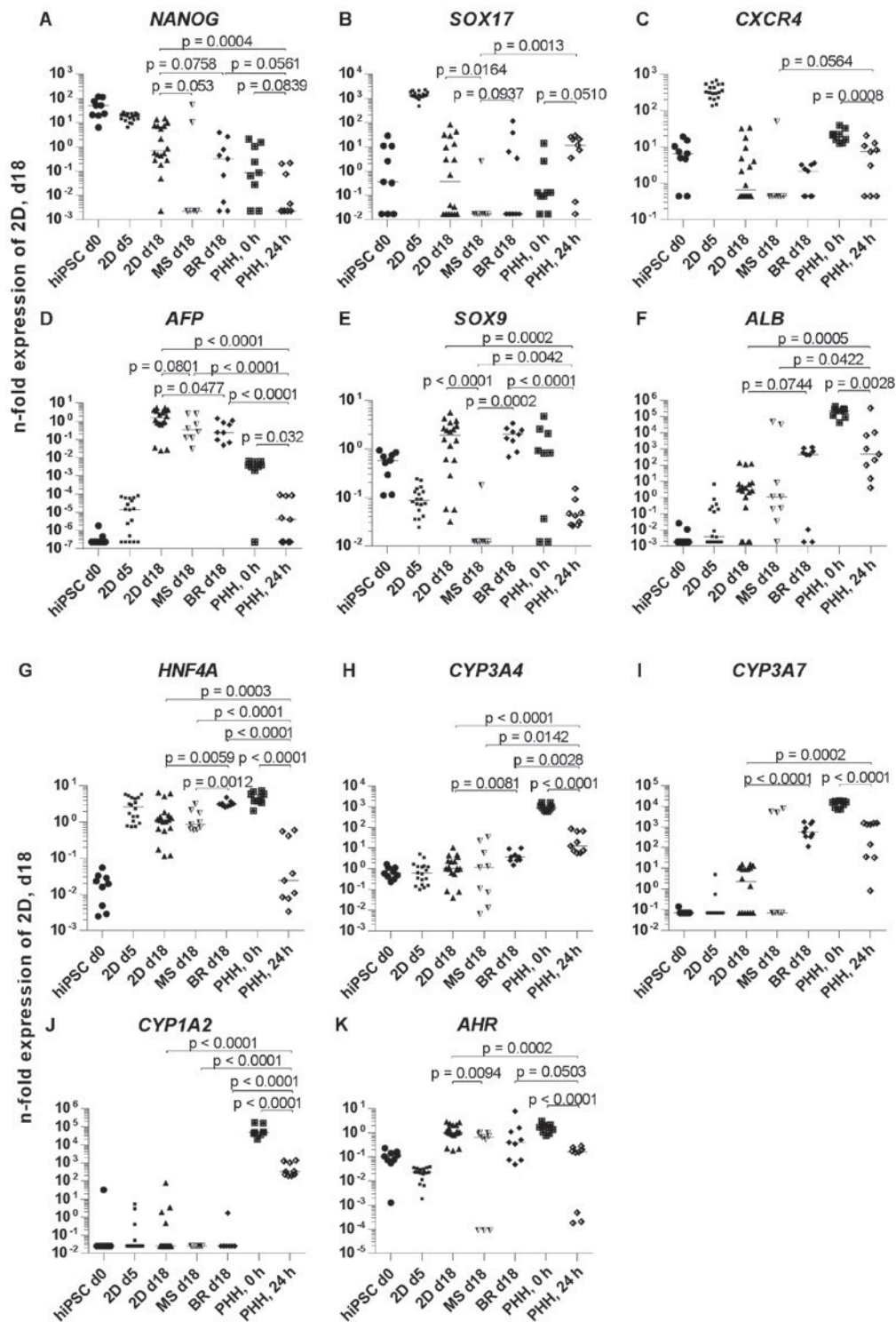


Figure 5. Gene expression of hiPSC derived hepatocyte-like cells in 2D cultures, microspheroids, bioreactors or in PHH. The mRNA expression of (A) *NANOG*, (B) *SOX17*, (C) *CXCR4*, (D) *AFP*, (E) *SOX9*, (F) *ALB*, (G) *HNF4A*, (H) *CYP3A4*, (I) *CYP3A7*, (J) *CYP1A2* and (K) *AHR* is shown. Samples for expression analysis were taken before (hiPSC day 0) and after hepatic differentiation of hiPSC in 2D cultures (2D day 18), microspheroids (MS day 18) or bioreactors (BR day 18). In addition, samples were taken after definitive endodermal differentiation in 2D cultures (2D day 5). Further, mRNA samples from freshly isolated (0 h) or 2D cultured PHH (24 h) were used for expression analyses. Differences in gene expression between groups were calculated using the Mann-Whitney test. Data from day 0 and 5 were not included in comparative statistics because the aim was to compare the different culture systems among each other and to the current 'gold-standard', the cultured PHH. $p < 0.1$ are given in the graphs [median and data points of 3 resp. 6 (for 2D cultures) independent experiments plus technical replicates (three per experiment) are shown]. hiPSC, human induced pluripotent stem cells; PHH, primary human hepatocytes; MS, microspheroids; BR, bioreactors; *NANOG*, Nanog homeobox; *SOX17*, SRY-box 17; *CXCR4*, C-X-C motif chemokine receptor 4; *AFP*, α -fetoprotein; *SOX9*, SRY-box 9; *ALB*, albumin; *HNF4A*, hepatocyte nuclear factor 4 α ; *CYP3A4*, cytochrome P450 family 3 subfamily A member 4; *CYP3A7*, cytochrome P450 family 3 subfamily A member 7; *CYP1A2*, cytochrome P450 family 1 subfamily A member 2; *AHR*, aryl hydrocarbon receptor; d, day.

staining to a diffuse cytoplasmic and weak nuclear staining was obvious, implying a possible downregulation of HNF4A.

In contrast, cytokeratin 18 (CK18) was detectable at similar levels in all culture systems (Fig. 7D-F and K). The fetal

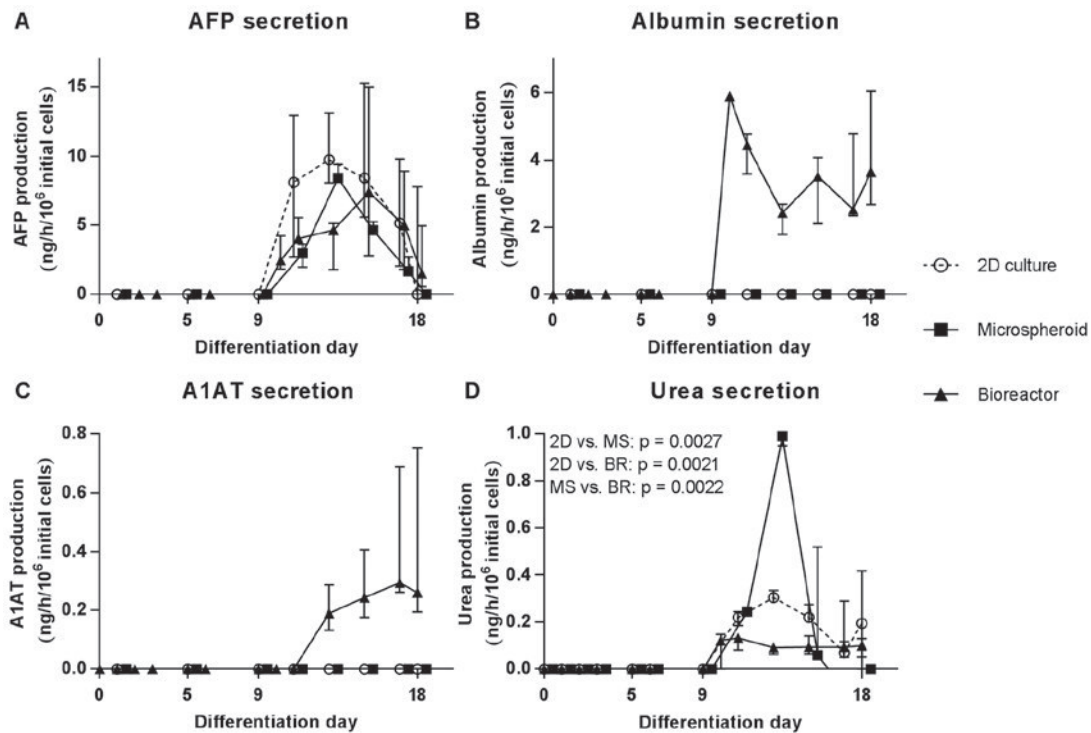


Figure 6. Secretion of specific proteins and metabolites by hiPSCs during hepatic differentiation in 2D cultures (2D, circles), MS (squares) or bioreactors (BR, triangles). (A) Secretion of AFP, (B) albumin (ALB), (C) A1AT and (D) urea is shown. Values are normalized to 10^6 initial cells on day 0 (2D cultures and bioreactors) or day 11 (microspheroids). Areas under curve were calculated for each dataset and differences between groups were determined with the unpaired, two-tailed t-test (2D cultures: n=6; microspheroids and bioreactors: n=3, median of biological replicates \pm interquartile range). MS, microspheroids; BR, bioreactors; AFT, α -fetoprotein; A1AT, α -1-antitrypsin; hiPSCs, human induced pluripotent stem cells.

hepatic marker AFP was present in three quarters of the cells in the 2D culture system, which was significantly higher compared to the microspheroids ($p < 0.0001$) and the bioreactors ($p = 0.0004$) (Fig. 7G-I and L). The number of ALB-positive cells was significantly higher in 2D cultures ($p = 0.0017$) and bioreactors ($p = 0.0476$) compared with microspheroids (Fig. 7G-I and M). Cells double-positive for AFP and ALB, which indicate a transition from fetal-like to mature hepatocytes, were present in all *in vitro* culture systems, with a significant lower amount in microspheroids compared to 2D cultures ($p = 0.0254$) (Fig. 7N). In addition, the immunohistochemical analysis revealed an irregular distribution of cells positive for HNF4A or ALB in 3D culture systems. Furthermore, the microspheroids showed a decrease in size with increasing culture time and holes could be detected within the spheroids and in the aggregates from the bioreactor at day 18.

CYP3A4 activity of HLCs in different culture systems. The basal capacity of CYP-dependent drug metabolism was examined in the HLC cultures by the application of substrates for CYP1A2 (phenacetin), CYP2B6 (bupropion) and CYP3A4/5 (midazolam). Activity of CYP2B6 could not be detected in HLCs irrespective of the cultivation system (data not shown). Data, normalized against the DNA content, measured at the day of the CYP analysis, showed a turnover of phenacetin in the linear range of the quantification method only for HLCs from the bioreactor and in PHH 2D-cultured for 24 h (Fig. 8A). In comparison to PHH the CYP1A2 activity of HLCs was ~ 5 times lower in the bioreactor and

not detectable in 2D cultures and 3D microspheroids, which is in line with the finding of marginal mRNA expression of *CYP1A2* (Fig. 5J). Activity of CYP3A4/5 was detectable in all HLC samples, but also in undifferentiated hiPSCs and PHH (Fig. 8B) which corresponds to the mRNA expression data (Fig. 5J). The CYP3A4/5 activity of PHH was significantly higher compared to all HLC culture systems ($p \leq 0.0007$). Cells obtained in the microspheroids had a slightly higher activity compared to the bioreactors and the 2D cultures. The lowest activity was detectable in the undifferentiated hiPSCs.

Discussion

Human iPS cells are of interest as a source for human hepatocytes including their possible use in pharmacological analyses and toxicity testing, ideally to gain sophisticated data *in vitro*. To date hiPSC-derived hepatocytes still show an immature phenotype and lack the functional range of their *in vivo* counterparts (19,20). In the present study, the propensity of two different 3D culture systems to enhance hepatic maturation of hiPSCs was investigated: i) Scaffold-free microspheroids based on the self-aggregation of pre-differentiated cells, and ii) a hollow-fiber bioreactor based on interwoven capillary systems, which form an adhesion scaffold for the cells residing in the extra-capillary space. The compared culture systems differ in their culture characteristics, for example in the bioreactor, cells are supplied with nutrients and oxygen via perfusion, and mass exchange is mainly influenced by perfusion rates and substance properties. In contrast, micro-

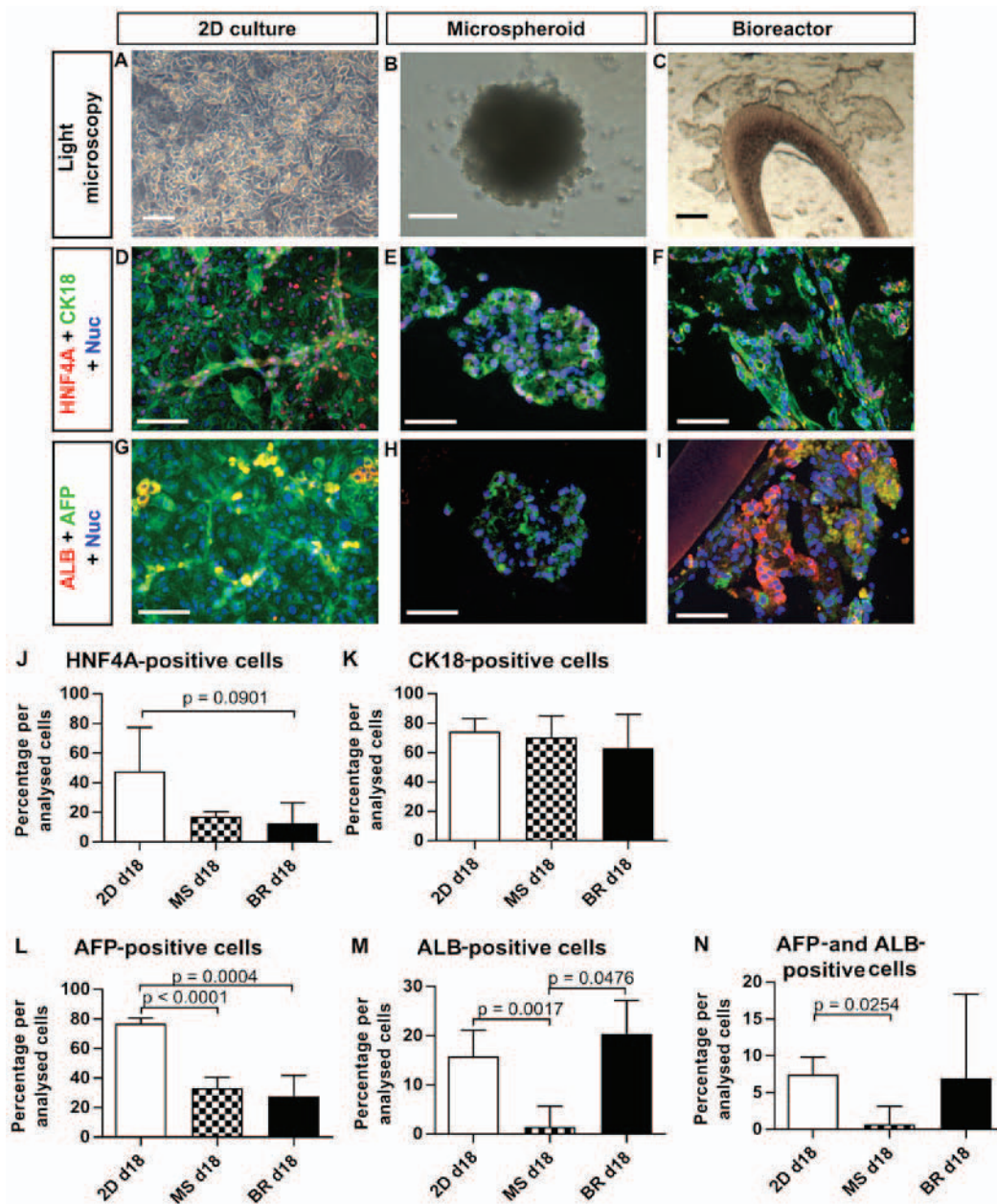


Figure 7. Expression of liver-specific immunohistochemical markers in human induced pluripotent stem cell-derived hepatocyte-like cells in 2D cultures (2D day 18), MS (day 18) or BR (day 18). (A-C) Bright-field images of the three culture systems at the day of analysis. (D-N) Expression of (D-F and J) HNF4A, (D-F and K) cytokeratin 18, (G-I, L and N) AFP and (G-I, M and N) ALB was determined by quantitative analysis of immunofluorescence pictures. Differences between groups were determined with the unpaired, two-tailed t-test (2D cultures: n=6; MS and BR: n=3, median of biological replicates \pm inter-quartile range). $p < 0.1$ are given in the graphs. Scale bars correspond to 100 μ m. d, day; MS, microspheroids; BR, bioreactors; HNF4A, hepatocyte nuclear factor 4 α ; CK18, cytokeratin 18; AFP, α -fetoprotein; ALB, albumin.

spheroids are maintained under static conditions and their size influences the supply of oxygen and nutrients to the center of the 3D cell aggregates. However, both 3D cultivation systems may support the formation of an *in vivo* like cell-cell interaction and microenvironment as already shown for PHH (41,42).

To evaluate the differentiation process and the maturation state of the obtained cells, metabolic parameters, secretion and expression of stage-specific markers, as well as CYP enzyme activities, were analyzed in comparison to 2D cultures, using freshly isolated or cultured PHH as controls.

Since the bioreactors and the microspheroids do not allow microscopic analysis on a cellular level of the cells during culture, alternative read outs were used to monitor the differ-

entiation process. Therefore, glucose consumption and lactate production were analyzed to evaluate the metabolic activity of hiPSCs in the different culture systems over time. The high rate of glucose consumption and lactate production at the beginning of differentiation in all systems is in consistency with the known glycolytic state of undifferentiated hiPSCs (43). With increasing length of culture, both rates decreased in all culture systems which could be explained either by a decreased cell proliferation or by a shift to oxidative phosphorylation as an energy source in association with cell differentiation (43).

The finding of cell differentiation is also supported by the observed downregulation of the pluripotency marker *NANOG*, a temporal peak of DE markers and an upregulation of hepatic

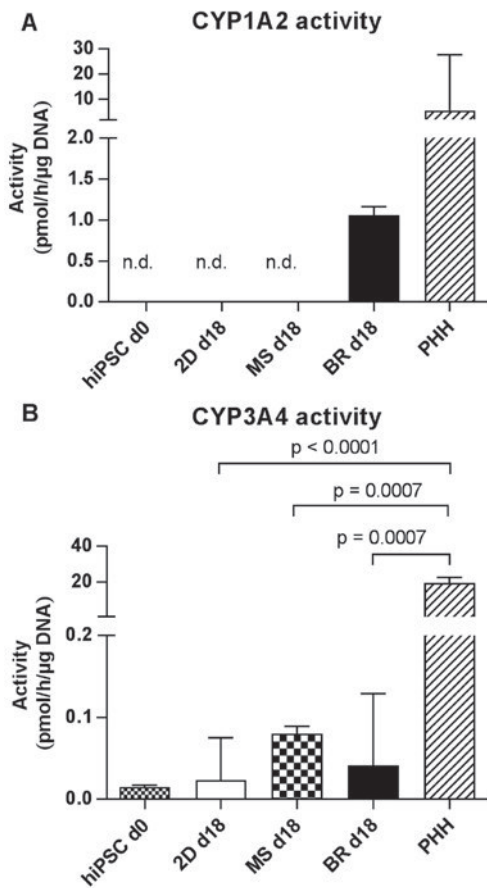


Figure 8. Activities of different cytochrome P450 (CYP) isoenzymes in hiPSC-derived hepatocyte-like cells in 2D cultures on day 18 (2D day 18), MS on day 18 (MS day 18), BR on day 18 (BR day 18), in undifferentiated hiPSCs on day 0 (hiPSC day 0) or in PHH 24 h after seeding. CYP activities were determined by measuring the formation of (A) acetaminophen from phenacetin via CYP1A2 and (B) the formation of 1-OH-midazolam from midazolam via CYP3A4/5. Differences in metabolic activity between undifferentiated hiPSCs, 2D cultures, microspheroids, bioreactors and PHH were calculated using the unpaired, two-tailed t-test (hiPSC day 0 cultures and 2D day 18 cultures: $n=6$; microspheroids day 18, bioreactors day 18 and adult PHH: $n=3$; median of biological replicates \pm interquartile range). $p < 0.1$ are given in the graphs. Values are normalized to the DNA content on day 18. n.d., not detected; d, day; hiPSCs, human induced pluripotent stem cells; PHH, primary human hepatocytes; MS, microspheroids; BR, bioreactors.

markers on mRNA level, although the extent of downregulation and upregulation varied between the compared culture systems. For example, the mRNA expression of the hepatic markers *ALB*, *CYP3A4* and *HNF4A* [important for the activation of CYP3A4 (44)] was significantly higher in bioreactors compared to 2D cultures, indicating a more mature state of the HLCs in the bioreactors. Moreover, expression of *SOX9*, which is weakly expressed in hepatoblasts and strongly in cholangiocytes (45) was observed in 2D cultures and bioreactors and was even higher than in freshly isolated PHH. This finding can be explained by the generation of cholangiocytes in these two differentiation systems in accordance to observations by Freyer *et al* (39) and Miki *et al* (46). Another explanation for the detected *SOX9* expression may be the presence of bipotent progenitors (hepatoblasts) in the differentiated cell populations. This assumption is supported by De Assuncao *et al* (47), who developed a protocol for cholangiocyte differentiation from hiPSCs and observed an increase in cholangiocyte

markers already during the hepatic progenitor phase. *AFP* expression was still significantly higher in HLCs than in PHH, although the 3D culture systems demonstrated a significant downregulation compared to the 2D culture. The downregulation of *AFP* expression during hepatic maturation has been challenging in hepatic differentiation protocols (17,22). The significant decrease of mRNA expression levels of hepatic markers such as *ALB*, *HNF4A* and *CYP3A4* in cultured PHH compared to freshly isolated PHH underlines again the importance of appropriate culture models to maintain the hepatic phenotype. Additionally, it demonstrates the difficulty to get standardized controls for hepatic differentiation approaches.

The finding of a more mature state of HLCs in bioreactors as compared with the other culture systems under investigation is supported by the detection of ALB and A1AT protein secretion solely in the culture perfusate of the bioreactors. However, it cannot be excluded that the absence of ALB and A1AT detection in the microspheroids and in 2D cultures is due to the low ratio of cell number to culture volume in 2D cultures (0.4×10^6 cells/ml) and in microspheroids (0.07×10^6 cells/ml) as compared with a ratio of 5×10^6 cells/ml in the bioreactors. Thus, the measured parameters are much more diluted in 2D cultures and in microspheroids than in the bioreactor system, and thus ALB and A1AT may be under the detection limit. This underlines another characteristic of the bioreactor system, which enables high-density culture of the differentiated cells. An exception to this observation was the high peak in urea secretion detected for microspheroids on day 13. This may be explained by the fact that the HLCs were subjected to cell stress during enzymatic detachment and cell reseeding for microspheroid formation on day 11. This is in line with findings from studies using PHH, which also showed a peak for urea secretion at the first day in culture together with a high enzyme release, which was attributed to cell stress during the preceding isolation procedure (40,48).

The results from protein secretion are in line with the analysis of the marker expression by immunohistochemistry showing the highest ratio of ALB to AFP positive cells in the bioreactors. In contrast, the amount of HNF4A positive cells was highest in 2D cultures whereas for CK18 positive cells no distinct differences between the culture systems could be detected. In addition, immunohistochemical analysis of the 3D cell aggregates in microspheroids and bioreactors revealed a heterogeneous cell population which may be a result of gradient formation of differentiation promoting factors since it has been reported that concentration gradients influence cell differentiation and tissue formation (49,50).

The basal metabolic activity of CYP1A2 and CYP3A4 of the *in vitro* generated cells was distinctly lower as compared to PHH. However, cells in the 3D systems displayed a higher CYP-functionality than 2D cultures, in line with previous studies showing increased CYP activities of PSC-derived hepatocytes in 3D models compared to 2D cultures (27,29,51). However, for pharmacological and toxicological applications of hiPSC-derived HLCs, a further increase of basal CYP activities would be desirable to approximate the functionality of PHH as the current gold standard for *in vitro* drug testing. The authors focused on basal CYP activities, since application for pharmacological and toxicological studies may require the opportunity to detect an induction by the test-compound, which may be masked by the routine use of an inducer (e.g. rifampin).

To further confirm the present results, both basal and induced levels of CYP-activities, should be measured in future studies to judge the metabolic capabilities of HLC derivatives. Beside the 3D cultivation, an extended culture duration may increase the activity of CYP enzymes as described by Gieseck *et al* (29). In addition, repeated exposure to xenobiotics, mimicking the process of *in vivo* drug metabolizing maturation during the first years of childhood (52), may be another approach to further increase CYP activity in future models (17).

Normalization of the results. The cells in the different culture systems may behave differently, thereby influencing the parameters used for normalization. Hence, to allow a detailed comparison of different culture systems the method of normalization needs to be considered carefully. Therefore, in the present study, the authors used two different methods for normalization. The initial cell number reflects the hiPSC number plated on 2D culture plates or injected into the bioreactor. In both systems the hiPSCs were subsequently cultured for one or two days in mTeSR™1 medium, leading to the proliferation of the hiPSCs and therefore to an unknown cell number at the start of differentiation. In addition, the cells still proliferated within the early differentiation phase as indicated by glucose consumption and lactate production. In contrast, for the microspheroid system the cell number reflects the number of differentiated cells at the start of the spheroid formation at day 11. At this differentiation stage, the cells have a low proliferation rate or have ceased to proliferate. Therefore, the values of energy metabolism and protein secretion obtained for the 2D cultures and bioreactors are probably overestimated, whereas for the microspheroid culture the values may represent more closely what is really expressed per cell. For the analysis of the CYP activities, which was performed only on day 18 of differentiation, the authors determined the DNA content at day 18 and used these values for normalization of CYP activities. This method is more accurate for day 18, but it does not reflect the cell number at the beginning of culture and during the differentiation. In conclusion, both methods have their valid reasons for being used.

To conclude, the HLCs generated in the described culture systems still demonstrate an immature hepatic phenotype when compared to PHH and there have been recent expert workshops (53), which attempt to move the field forward. However, the 3D systems, particularly the bioreactor, seem to increase the developmental state of the cells as compared with 2D cultures, which may be due to the more physiological environment in complex 3D culture systems. It can be concluded that the choice of the culture system for HLCs depends primarily on the intended application: The bioreactor system provides an *in vitro* instrument for complex analyses, e.g., studies on the physiology and pathophysiology of cell differentiation, or on complex effects of xenobiotics. In contrast, microspheroids, due to their easy and cost-efficient handling, could be used for investigation of a higher number of drug candidates where a certain culture complexity is desired. Thus, both culture systems open the perspective for the development of improved *in vitro* hepatocyte models.

Acknowledgements

The study leading to these results has received support from the Innovative Medicines Initiative Joint Undertaking under

(grant no. 115439), resources of which are composed of financial contribution from the European Union's Seventh Framework Programme (FP7/2007-2013) and EFPIA companies. This publication reflects only the author's views and neither the IMI JU nor EFPIA nor the European Commission are liable for any use that may be made of the information contained therein. L. Armstrong and M. Lako were additionally funded by European Research Council (grant no. 614620) and BBSRC UK (grant no. BB/I020209/1).

References

1. Lauschke VM and Ingelman-Sundberg M: The importance of patient-specific factors for hepatic drug response and toxicity. *Int J Mol Sci* 17: 1714, 2016.
2. Mueller SO, Guillouzo A, Hewitt PG and Richert L: Drug biokinetic and toxicity assessments in rat and human primary hepatocytes and HepaRG cells within the EU-funded Predict-IV project. *Toxicol In Vitro* 30: 19-26, 2015.
3. Takahashi K and Yamanaka S: Induction of pluripotent stem cells from mouse embryonic and adult fibroblast cultures by defined factors. *Cell* 126: 663-676, 2006.
4. Takahashi K, Tanabe K, Ohnuki M, Narita M, Ichisaka T, Tomoda K and Yamanaka S: Induction of pluripotent stem cells from adult human fibroblasts by defined factors. *Cell* 131: 861-872, 2007.
5. Rashid ST, Corbinea S, Hannan N, Marciniak SJ, Miranda E, Alexander G, Huang-Doran I, Griffin J, Ahrlund-Richter L, Skepper J, *et al*: Modeling inherited metabolic disorders of the liver using human induced pluripotent stem cells. *J Clin Invest* 120: 3127-3136, 2010.
6. Tafaleng EN, Chakraborty S, Han B, Hale P, Wu W, Soto-Gutierrez A, Feghali-Bostwick CA, Wilson AA, Kotton DN, Nagaya M, *et al*: Induced pluripotent stem cells model personalized variations in liver disease resulting from α 1-antitrypsin deficiency. *Hepatology* 62: 147-157, 2015.
7. Si-Tayeb K, Lemaigre FP and Duncan SA: Organogenesis and development of the liver. *Dev Cell* 18: 175-189, 2010.
8. Hay DC, Fletcher J, Payne C, Terrace JD, Gallagher RC, Snoeys J, Black JR, Wojtacha D, Samuel K, Hannoun Z, *et al*: Highly efficient differentiation of hESCs to functional hepatic endoderm requires ActivinA and Wnt3a signaling. *Proc Natl Acad Sci USA* 105: 12301-12306, 2008.
9. Hannan NRF, Segeritz CP, Touboul T and Vallier L: Production of hepatocyte-like cells from human pluripotent stem cells. *Nat Protoc* 8: 430-437, 2013.
10. Czysz K, Minger S and Thomas N: DMSO efficiently down regulates pluripotency genes in human embryonic stem cells during definitive endoderm derivation and increases the efficiency of hepatic differentiation. *PLoS One* 10: e0117689, 2015.
11. Szkolnicka D, Farnworth SL, Lucendo-Villarin B and Hay DC: Deriving functional hepatocytes from pluripotent stem cells. *Curr Protoc Stem Cell Biol* 30: 1G.5.1-12, 2014.
12. Tasnim F, Phan D, Toh YC and Yu H: Cost-effective differentiation of hepatocyte-like cells from human pluripotent stem cells using small molecules. *Biomaterials* 70: 115-125, 2015.
13. Schwartz RE, Trehan K, Andrus L, Sheahan TP, Ploss A, Duncan SA, Rice CM and Bhatia SN: Modeling hepatitis C virus infection using human induced pluripotent stem cells. *Proc Natl Acad Sci USA* 109: 2544-2548, 2012.
14. Bukong TN, Lo T, Szabo G and Dolganiuc A: Novel developmental biology-based protocol of embryonic stem cell differentiation to morphologically sound and functional yet immature hepatocytes. *Liver Int* 32: 732-741, 2012.
15. Siller R, Greenhough S, Naumovska E and Sullivan GJ: Small-molecule-driven hepatocyte differentiation of human pluripotent stem cells. *Stem Cell Reports* 4: 939-952, 2015.
16. Asplund A, Pradip A, van Giezen M, Aspegren A, Choukair H, Rehnström M, Jacobsson S, Ghosheh N, El Hajjam D, Holmgren S, *et al*: One standardized differentiation procedure robustly generates homogenous hepatocyte cultures displaying metabolic diversity from a large panel of human pluripotent stem cells. *Stem Cell Rev* 12: 90-104, 2016.
17. Kim JH, Jang YJ, An SY, Son J, Lee J, Lee G, Park JY, Park HJ, Hwang DY, Kim JH, *et al*: Enhanced metabolizing activity of human ES cell-derived hepatocytes using a 3D culture system with repeated exposures to xenobiotics. *Toxicol Sci* 147: 190-206, 2015.

18. Park H-J, Choi Y-J, Kim JW, Chun HS, Im I, Yoon S, Han YM, Song CW and Kim H: Differences in the epigenetic regulation of cytochrome P450 genes between human embryonic stem cell-derived hepatocytes and primary hepatocytes. *PLoS One* 10: e0132992, 2015.
19. Baxter M, Withey S, Harrison S, Segeritz CP, Zhang F, Atkinson-Dell R, Rowe C, Gerrard DT, Sison-Young R, Jenkins R, *et al*: Phenotypic and functional analyses show stem cell-derived hepatocyte-like cells better mimic fetal rather than adult hepatocytes. *J Hepatol* 62: 581-589, 2015.
20. Godoy P, Schmidt-Heck W, Natarajan K, Lucendo-Villarin B, Szkolnicka D, Asplund A, Björquist P, Widera A, Stöber R, Campos G, *et al*: Gene networks and transcription factor motifs defining the differentiation of stem cells into hepatocyte-like cells. *J Hepatol* 63: 934-942, 2015.
21. Kondo Y, Iwao T, Nakamura K, Sasaki T, Takahashi S, Kamada N, Matsubara T, Gonzalez FJ, Akutsu H, Miyagawa Y, *et al*: An efficient method for differentiation of human induced pluripotent stem cells into hepatocyte-like cells retaining drug metabolizing activity. *Drug Metab Pharmacokinet* 29: 237-243, 2014.
22. Cameron K, Tan R, Schmidt-Heck W, Campos G, Lyall MJ, Wang Y, Lucendo-Villarin B, Szkolnicka D, Bates N, Kimber SJ, *et al*: Recombinant laminins drive the differentiation and self-organization of hESC-derived hepatocytes. *Stem Cell Reports* 5: 1250-1262, 2015.
23. Takayama K, Inamura M, Kawabata K, Katayama K, Higuchi M, Tashiro K, Nonaka A, Sakurai F, Hayakawa T, Furue MK, *et al*: Efficient generation of functional hepatocytes from human embryonic stem cells and induced pluripotent stem cells by HNF4 α transduction. *Mol Ther* 20: 127-137, 2012.
24. Watanabe H, Takayama K, Inamura M, Tachibana M, Mimura N, Katayama K, Tashiro K, Nagamoto Y, Sakurai F, Kawabata K, *et al*: HHEX promotes hepatic-lineage specification through the negative regulation of *comesodermin*. *PLoS One* 9: e90791, 2014.
25. Tomizawa M, Shinozaki F, Motoyoshi Y, Sugiyama T, Yamamoto S and Ishige N: Transcription factors and medium suitable for initiating the differentiation of human induced pluripotent stem cells to the hepatocyte lineage. *J Cell Biochem* 117: 2001-2009, 2016.
26. Vinken M, Papeleu P, Snykers S, De Rop E, Henkens T, Chipman JK, Rogiers V and Vanhaecke T: Involvement of cell junctions in hepatocyte culture functionality. *Crit Rev Toxicol* 36: 299-318, 2006.
27. Ramasamy TS, Yu JS, Selden C, Hodgson H and Cui W: Application of three-dimensional culture conditions to human embryonic stem cell-derived definitive endoderm cells enhances hepatocyte differentiation and functionality. *Tissue Eng Part A* 19: 360-367, 2013.
28. Sivertsson L, Synnergren J, Jensen J, Björquist P and Ingelman-Sundberg M: Hepatic differentiation and maturation of human embryonic stem cells cultured in a perfused three-dimensional bioreactor. *Stem Cells Dev* 22: 581-594, 2013.
29. Gieseck RL III, Hannan NR, Bort R, Hanley NA, Drake RA, Cameron GW, Wynn TA and Vallier L: Maturation of induced pluripotent stem cell derived hepatocytes by 3D-culture. *PLoS One* 9: e86372, 2014.
30. Takebe T, Sekine K, Enomura M, Koike H, Kimura M, Ogaeri T, Zhang RR, Ueno Y, Zheng YW, Koike N, *et al*: Vascularized and functional human liver from an iPSC-derived organ bud transplant. *Nature* 499: 481-484, 2013.
31. Zeilinger K, Schreiter T, Darnell M, Söderdahl T, Lübberstedt M, Dillner B, Knobloch D, Nüssler AK, Gerlach JC and Andersson TB: Scaling down of a clinical three-dimensional perfusion multicompartment hollow fiber liver bioreactor developed for extracorporeal liver support to an analytical scale device useful for hepatic pharmacological in vitro studies. *Tissue Eng Part C Methods* 17: 549-556, 2011.
32. van de Bunt M, Lako M, Barrett A, Gloyn AL, Hansson M, McCarthy MI, Beer NL and Honoré C: Insights into islet development and biology through characterization of a human iPSC-derived endocrine pancreas model. *Islets* 8: 83-95, 2016.
33. Friedrich J, Seidel C, Ebner R and Kunz-Schughart LA: Spheroid-based drug screen: Considerations and practical approach. *Nat Protoc* 4: 309-324, 2009.
34. Pfeiffer E, Kegel V, Zeilinger K, Hengstler JG, Nüssler AK, Seehofer D and Damm G: Featured article: Isolation, characterization, and cultivation of human hepatocytes and non-parenchymal liver cells. *Exp Biol Med* (Maywood) 240: 645-656, 2015.
35. Brzeszczyńska J, Johns N, Schilb A, Degen S, Degen M, Langen R, Schols A, Glass DJ, Roubenoff R, Greig CA, *et al*: Loss of oxidative defense and potential blockade of satellite cell maturation in the skeletal muscle of patients with cancer but not in the healthy elderly. *Aging* (Albany NY) 8: 1690-1702, 2016.
36. Vandesompele J, De Preter K, Pattyn F, Poppe B, Van Roy N, De Paepe A and Speleman F: Accurate normalization of real-time quantitative RT-PCR data by geometric averaging of multiple internal control genes. *Genome Biol* 3: RESEARCH0034, 2002.
37. Livak KJ and Schmittgen TD: Analysis of relative gene expression data using real-time quantitative PCR and the 2(-Delta Delta C(T)) method. *Methods* 25: 402-408, 2001.
38. Liu J, Brzeszczyńska J, Samuel K, Black J, Palakkan A, Anderson RA, Gallagher R and Ross JA: Efficient episomal reprogramming of blood mononuclear cells and differentiation to hepatocytes with functional drug metabolism. *Exp Cell Res* 338: 203-213, 2015.
39. Freyer N, Knöspel F, Strahl N, Amini L, Schrade P, Bachmann S, Damm G, Seehofer D, Jacobs F, Monshouwer M, *et al*: Hepatic differentiation of human induced pluripotent stem cells in a perfused three-dimensional multicompartment bioreactor. *Biores Open Access* 5: 235-248, 2016.
40. Hoffmann SA, Müller-Vieira U, Biemel K, Knobloch D, Heydel S, Lübberstedt M, Nüssler AK, Andersson TB, Gerlach JC and Zeilinger K: Analysis of drug metabolism activities in a miniaturized liver cell bioreactor for use in pharmacological studies. *Biotechnol Bioeng* 109: 3172-3181, 2012.
41. Schyschka L, Sánchez JJ, Wang Z, Burkhardt B, Müller-Vieira U, Zeilinger K, Bachmann A, Nadalin S, Damm G and Nüssler AK: Hepatic 3D cultures but not 2D cultures preserve specific transporter activity for acetaminophen-induced hepatotoxicity. *Arch Toxicol* 87: 1581-1593, 2013.
42. Rennert K, Steinborn S, Gröger M, Ungerböck B, Jank AM, Ehgartner J, Nietzsche S, Dinger J, Kiehltopf M, Funke H, *et al*: A microfluidically perfused three dimensional human liver model. *Biomaterials* 71: 119-131, 2015.
43. Varum S, Rodrigues AS, Moura MB, Momcilovic O, Easley CA IV, Ramalho-Santos J, Van Houten B and Schatten G: Energy metabolism in human pluripotent stem cells and their differentiated counterparts. *PLoS One* 6: e20914, 2011.
44. Tirona RG, Lee W, Leake BF, Lan LB, Cline CB, Lamba V, Parviz F, Duncan SA, Inoue Y, Gonzalez FJ, *et al*: The orphan nuclear receptor HNF4 α determines PXR- and CAR-mediated xenobiotic induction of CYP3A4. *Nat Med* 9: 220-224, 2003.
45. Uhlén M, Fagerberg L, Hallström BM, Lindskog C, Oksvold P, Mardinoglu A, Sivertsson Å, Kampf C, Sjöstedt E, Asplund A, *et al*: Proteomics. Tissue-based map of the human proteome. *Science* 347: 1260419, 2015.
46. Miki T, Ring A and Gerlach J: Hepatic differentiation of human embryonic stem cells is promoted by three-dimensional dynamic perfusion culture conditions. *Tissue Eng Part C Methods* 17: 557-568, 2011.
47. De Assuncao TM, Sun Y, Jalan-Sakrikar N, Drinane MC, Huang BQ, Li Y, Davila JI, Wang R, O'Hara SP, Lomber GA, *et al*: Development and characterization of human-induced pluripotent stem cell-derived cholangiocytes. *Lab Invest* 95: 684-696, 2015.
48. Knöspel F, Jacobs F, Freyer N, Damm G, De Bondt A, van den Wyngaert I, Snoeys J, Monshouwer M, Richter M, Strahl N, *et al*: In vitro model for hepatotoxicity studies based on primary human hepatocyte cultivation in a perfused 3D bioreactor system. *Int J Mol Sci* 17: 584, 2016.
49. Singh M, Berkland C and Detamore MS: Strategies and applications for incorporating physical and chemical signal gradients in tissue engineering. *Tissue Eng Part B Rev* 14: 341-366, 2008.
50. Uzel SG, Amadi OC, Pearl TM, Lee RT, So PT and Kamm RD: Simultaneous or sequential orthogonal gradient formation in a 3D cell culture microfluidic platform. *Small* 12: 612-622, 2016.
51. Takayama K, Kawabata K, Nagamoto Y, Kishimoto K, Tashiro K, Sakurai F, Tachibana M, Kanda K, Hayakawa T, Furue MK, *et al*: 3D spheroid culture of hESC/hiPSC-derived hepatocyte-like cells for drug toxicity testing. *Biomaterials* 34: 1781-1789, 2013.
52. Ginsberg G, Hattis D, Sonawane B, Russ A, Banati P, Kozlak M, Smolenski S and Goble R: Evaluation of child/adult pharmacokinetic differences from a database derived from the therapeutic drug literature. *Toxicol Sci* 66: 185-200, 2002.
53. Goldring C, Antoine DJ, Bonner F, Crozier J, Denning C, Fontana RJ, Hanley NA, Hay DC, Ingelman-Sundberg M, Juhila S, *et al*: Stem cell-derived models to improve mechanistic understanding and prediction of human drug-induced liver injury. *Hepatology* 65: 710-721, 2017.





Article

Effects of Co-Culture Media on Hepatic Differentiation of hiPSC with or without HUVEC Co-Culture

Nora Freyer ^{1,*}, Selina Greuel ¹, Fanny Knöspel ¹, Nadja Strahl ¹, Leila Amini ¹, Frank Jacobs ², Mario Monshouwer ² and Katrin Zeilinger ¹

¹ Berlin-Brandenburg Center for Regenerative Therapies (BCRT), Charité—Universitätsmedizin Berlin, Campus Virchow-Klinikum, 13353 Berlin, Germany; selina.greuel@charite.de (S.G.); fanny.knoespel@gmx.de (F.K.); nadja.strahl@outlook.com (N.S.); leila.amini@charite.de (L.A.); katrin.zeilinger@charite.de (K.Z.)

² Janssen Research and Development, 2340 Beerse, Belgium; fjacobs1@its.jnj.com (F.J.); mmonshou@its.jnj.com (M.M.)

* Correspondence: nora.freyer@charite.de; Tel.: +49-30-450-559147

Received: 3 July 2017; Accepted: 2 August 2017; Published: 7 August 2017

Abstract: The derivation of hepatocytes from human induced pluripotent stem cells (hiPSC) is of great interest for applications in pharmacological research. However, full maturation of hiPSC-derived hepatocytes has not yet been achieved in vitro. To improve hepatic differentiation, co-cultivation of hiPSC with human umbilical vein endothelial cells (HUVEC) during hepatic differentiation was investigated in this study. In the first step, different culture media variations based on hepatocyte culture medium (HCM) were tested in HUVEC mono-cultures to establish a suitable culture medium for co-culture experiments. Based on the results, two media variants were selected to differentiate hiPSC-derived definitive endodermal (DE) cells into mature hepatocytes with or without HUVEC addition. DE cells differentiated in mono-cultures in the presence of those media variants showed a significant increase ($p < 0.05$) in secretion of α -fetoprotein and in activities of cytochrome P450 (CYP) isoenzymes CYP2B6 and CYP3A4 as compared with cells differentiated in unmodified HCM used as control. Co-cultivation with HUVEC did not further improve the differentiation outcome. Thus, it can be concluded that the effect of the used medium outweighed the effect of HUVEC co-culture, emphasizing the importance of the culture medium composition for hiPSC differentiation.

Keywords: human induced pluripotent stem cells (hiPSC); hepatic differentiation; human umbilical vein endothelial cells (HUVEC); co-culture

1. Introduction

Human induced pluripotent stem cells (hiPSC) hold great promise for application in cell therapies [1], but also in disease research [1,2] and drug toxicity testing with in vitro models [3]. In pharmacological research, there is a particular need for hepatic cells due to the central role of the liver in drug metabolism and toxicity [4,5]. Previous in vitro studies on hepatic drug toxicity using hepatocyte-like cells (HLC) differentiated from hiPSC showed promising results [6,7]. Despite these encouraging outcomes, the efficiency of the differentiation process of hiPSC towards functional HLC for further use, including hepatotoxicity assessment, remains low [8]. Several research groups managed to generate hiPSC-derived HLC with 60% [9] up to 80–85% [10] of differentiated cells being characterized by the expression of several hepatic markers, including albumin. However, hiPSC-derived HLC showed only 10% of the urea and albumin production capacity compared with primary human hepatocytes [9] and cytochrome P450 (CYP) isoenzyme activities of the generated HLC

were almost 30-fold lower than those of primary human hepatocytes [9]. Baxter et al. characterized human embryonic stem-cell derived HLC as being similar to fetal rather than to adult hepatocytes in terms of their metabolic profile [11]. Therefore, further improvement of the differentiation and maturation process is needed to generate fully functional HLC for clinical or in vitro use.

Current protocols for differentiation of hiPSC towards HLC mostly use a variation of a three-step differentiation protocol including differentiation into definitive endoderm (DE) cells, generation of hepatoblasts and further maturation into HLC [12]. DE differentiation is generally induced by the use of activin A [13,14] and Wnt3a [13,15]. Differentiation into hepatoblasts is supported by the addition of fibroblast growth factors (FGF) and bone morphogenetic proteins (BMP) [16,17] and hepatocyte maturation is induced by using hepatocyte growth factor (HGF) as well as oncostatin M (OSM) [18]. In addition to the optimization of the differentiation media and supplements, overexpression of hepatic transcription factors such as hepatocyte nuclear factor 4 α (HNF4A) [19] and manipulation of miRNA expression [20,21] were investigated aiming to improve hepatic maturation of hiPSC. Further support of the maturation of gained HLC was achieved by transferring the differentiation process to a 3D-culture system [6,22,23].

A promising approach to enhance the differentiation outcome and hepatic functionality of hiPSC-derived HLC can be seen in applying co-cultures with non-parenchymal liver cells. Matsumoto et al. observed that endothelial cells are essential for early organ development prior to the formation of a functioning local vasculature [24]. Takebe and colleagues recapitulated the early liver development by cultivating hiPSC-derived endodermal cells with human umbilical vein endothelial cells (HUVEC) and human mesenchymal stem cells. The observed expression profiles in the resulting hiPSC-liver buds were closer to native human liver tissue than hiPSC-derived HLC differentiated without HUVEC co-culture [25]. Since the cell behavior within such co-cultures relies on specific media compositions, special attention has to be given to the co-culture medium used to provide suitable conditions for all included cell types.

Within the scope to develop a co-culture model consisting of hiPSC-derived DE cells and HUVEC, a two-step approach was applied as shown in Figure 1. First, culture media used for endothelial cells or hepatocytes as well as mixtures thereof were tested in HUVEC mono-cultures. Based on the results, two of those media were selected to differentiate hiPSC-derived DE cells into mature hepatocytes in the presence or absence of HUVEC. Hepatic differentiation of hiPSC in mono- or co-cultures was assessed by measuring the protein and gene expression of stage-specific markers as well as the functionality of pharmacological relevant CYP isoenzymes.

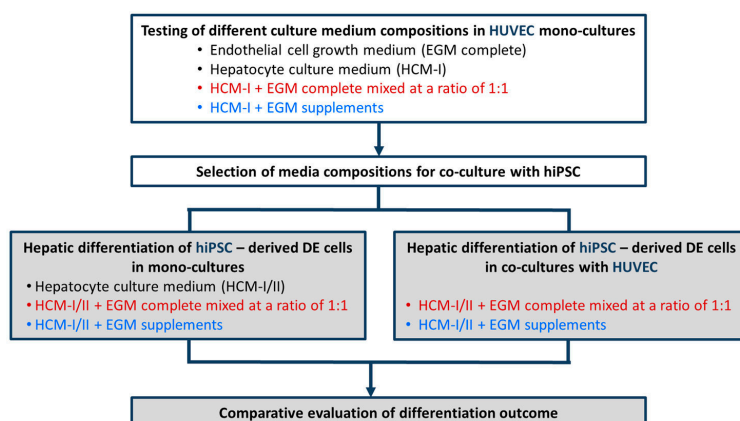


Figure 1. Schematic outline of experimental procedures for media testing in mono-cultures of human umbilical vein endothelial cells (HUVEC, white boxes) and for hepatic differentiation of hiPSC-derived definitive endodermal (DE) cells with or without HUVEC (grey boxes). Different mixtures of hepatocyte culture medium (HCM) and endothelial cell growth medium (EGM) were tested. Colors used for the different media compositions correspond to those used in the graphs.

2. Results

As a prerequisite for co-culture, a culture medium permitting endothelial cell maintenance during differentiation of hiPSC-derived DE cells towards the hepatic fate had to be determined. Therefore, HUVEC were cultured in the presence of 100% endothelial cell growth medium, consisting of basal medium and supplements (EGM complete), 100% hepatocyte culture medium (HCM-I), HCM-I and EGM complete mixed at a ratio of 1:1 (HCM-I + EGM complete) or HCM-I enriched with endothelial cell growth supplements (HCM-I + EGM supplements).

2.1. Effect of Culture Media Variations on Mono-Cultures of Human Umbilical Vein Endothelial Cells (HUVEC)

The use of pure HCM-I for HUVEC cultivation resulted in rapid cell disintegration and detachment and was therefore not further evaluated (data not shown). The results from HUVEC cultures treated with HCM-I + EGM complete, with HCM-I + EGM supplements or with EGM complete as control are shown in Figure 2. The curve progressions displaying glucose consumption rates of HUVEC cultivated in EGM complete or HCM-I + EGM complete were similar, showing an increase until day 4 and a slight decrease until day 6 followed by a slow, but stable increase until day 14 (Figure 2A). Values were only marginally lower in HCM-I + EGM complete than in EGM complete. In contrast, HUVEC grown in HCM-I + EGM supplements showed considerably lower glucose consumption rates over the whole culture period (Figure 2A). Values of lactate production mirrored those of glucose consumption (Figure 2B). Release of lactate dehydrogenase (LDH) as a marker for cell damage was detected at basal levels of maximally 3 U/L for all conditions (data not shown). Gene expression analysis of the endothelial cell markers platelet and endothelial cell adhesion molecule 1 (*PECAM1*) and von Willebrand factor (*VWF*) revealed a 3- to 3.5-fold increase in *PECAM1* gene expression and a 4-fold increase in *VWF* gene expression when using EGM complete or HCM-I + EGM complete (Figure 2C,D). In contrast, the expression levels of both, *PECAM1* and *VWF*, remained stable in HUVEC cultured in HCM-I + EGM supplements throughout the culture period of 14 days.

In accordance to the results of glucose and lactate measurement, cultures grown in EGM complete showed the highest cell density (Figure 3A), followed by those cultured in HCM-I + EGM complete (Figure 3B). Cultivation in HCM-I + EGM supplements resulted in a distinctly lower cell density as compared with the other media investigated (Figure 3C). Immunocytochemical staining of endothelial and hepatocyte markers was performed in HUVEC mono-cultures to evaluate the influence of the tested media on protein expression (Figure 3). Relative percentages of stained cells are provided in Table S1. In all conditions, the two endothelial cell markers *PECAM1* and *VWF* could clearly be observed, whereas the two hepatocyte markers *HNF4A* and cytokeratin 18 (*KRT18*) were not detectable (Figure 3D–I). However, the proportion of cells expressing endothelial cell markers differed between the conditions. Almost all cells ($91 \pm 6\%$) cultured in EGM complete were positive for *PECAM1* (Figure 3D), whereas only around 70% of the cells cultured in HCM-I + EGM complete or in HCM-I + EGM supplements showed *PECAM1* immunoreactivity (Figure 3E,F). Immunoreactivity for *VWF* was observed in approximately 80% of the cells when grown in EGM complete or in HCM-I + EGM complete (Figure 3G,H), while only $62 \pm 12\%$ of the cells cultured in HCM-I + EGM supplements appeared positive for this marker (Figure 3I).

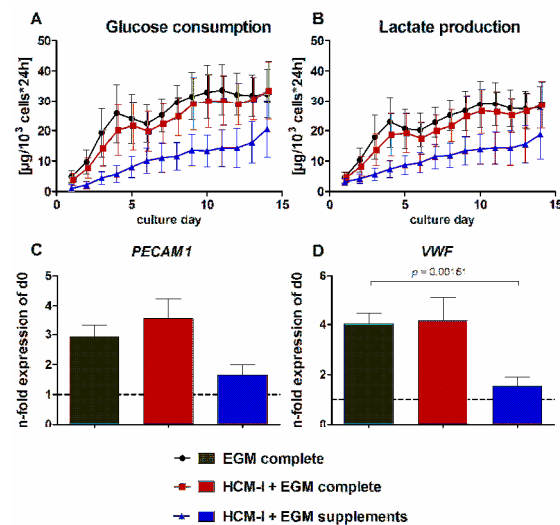


Figure 2. Effect of different media compositions on mono-cultures of human umbilical vein endothelial cells (HUVEC). The cells were cultured over 14 days in endothelial cell growth medium, consisting of basal medium and supplements (EGM complete), in a 1:1 mixture of hepatocyte culture medium and EGM complete (HCM-I + EGM complete) or in HCM enriched with endothelial cell growth supplements (HCM-I + EGM supplements). The graphs show time-courses of glucose consumption (A) and lactate production (B) as well as gene expression analyses of the endothelial cell markers platelet endothelial cell adhesion molecule 1 (*PECAM1*) (C) and von Willebrand factor (*VWF*) (D). Fold changes of mRNA expression were calculated relative to HUVEC before starting the experiments (d0) with normalization to glyceraldehyde-3-phosphate dehydrogenase (*GAPDH*) expression by the $\Delta\Delta C_t$ method. The area under the curve was calculated for time-courses of biochemical parameters and differences between groups were detected using the unpaired, two-tailed Student's *t*-test; for glucose consumption and lactate production $n = 6$, gene expression analysis $n = 3$, mean \pm standard error of the mean.

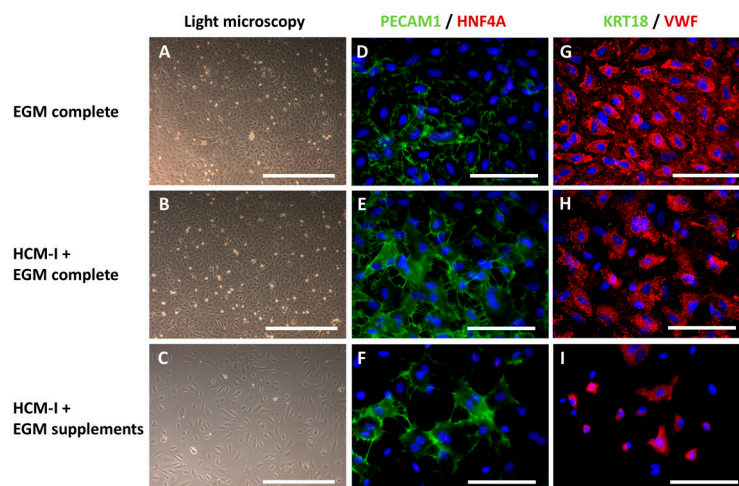


Figure 3. Light microscopy and immunocytochemical staining of mono-cultures of human umbilical vein endothelial cells (HUVEC) after cultivation over 14 days in endothelial cell growth medium, consisting of basal medium and supplements (EGM complete), hepatocyte culture medium and EGM complete mixed at a ratio of 1:1 (HCM-I + EGM complete) or HCM enriched with endothelial cell growth supplements (HCM-I + EGM supplements). The pictures show light microscopic photographs (A–C), staining of the endothelial cell marker platelet endothelial cell adhesion molecule 1 (PECAM1) and the hepatocyte marker hepatocyte nuclear factor 4 α (HNF4A) (D–F), staining of the hepatocyte marker cytokeratin 18 (KRT18) and the endothelial cell marker von Willebrand factor (VWF) (G–I). Nuclei were counter-stained with Dapi (blue). Scale bars correspond to 500 μ m for light microscopy and to 100 μ m for immunofluorescence.

2.2. Hepatic Differentiation of hiPSC-Derived Definitive Endoderm (DE) Cells with or without HUVEC Co-Cultivation Using Different Co-Culture Media

As maintenance and proliferation of endothelial cells might have positive effects on hepatic differentiation of hiPSC, both, HCM-I/II + EGM complete and HCM-I/II + EGM supplements, were tested for their suitability to induce hepatic differentiation in hiPSC-derived DE cells maintained in mono-culture or in co-culture with HUVEC. The results were compared with pure HCM-I/II, used as a positive control. HCM-II is based on HCM-I, but is further supplemented with OSM for the last four days of differentiation.

2.2.1. Morphological Characteristics of hiPSC-Derived Hepatocyte-like Cells (HLC) and Co-Cultured HUVEC

Light microscopic investigation at the end of hepatic differentiation showed that hiPSC-derived HLC maintained without HUVEC co-culture displayed a polygonal shape typical for hepatocytes in all tested media compositions (Figure 4A–C). Use of HCM-I/II + EGM complete resulted in a rather heterogeneous morphology showing large areas of overgrowth (Figure 4B), while HLC differentiated in HCM-I/II or HCM-I/II + EGM supplements appeared more homogeneous (Figure 4A,C). In co-culture experiments, using HCM-I/II + EGM complete or HCM-I/II + EGM supplements as culture media, the HUVEC grew in distinct areas between the hiPSC-derived DE cells until day 7 of the differentiation process (Figure 4D,E). Afterwards, HUVEC progressively infiltrated the hiPSC clusters and at the end of hepatic differentiation (day 17) they could hardly be discriminated from HLC (Figure 4F,G). In both medium conditions, HLC co-cultivated with HUVEC were less homogeneous in their morphology and culture behavior (Figure 4F,G) as compared with the corresponding hiPSC mono-cultures (Figure 4B,C).

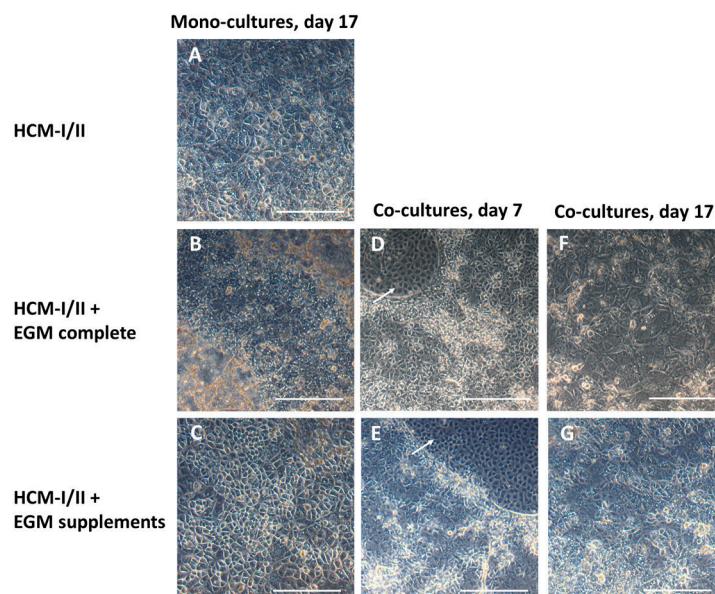


Figure 4. Morphology of human induced pluripotent stem cells (hiPSC) after hepatic differentiation over 17 days in different media and/or in co-culture with human umbilical vein endothelial cells (HUVEC). The pictures show hiPSC after hepatic differentiation in mono-culture over 17 days in hepatocyte culture medium (HCM-I/II) (A), in a 1:1 mixture of hepatocyte culture medium and endothelial cell growth medium EGM, consisting of basal medium and supplements (HCM-I/II + EGM complete) (B) or in HCM enriched with EGM supplements (HCM-I/II + EGM supplements) (C); hiPSC after hepatic differentiation in co-culture with HUVEC on day 7 of differentiation using HCM-I/II + EGM complete (D) or HCM-I/II + EGM supplements (E); hiPSC after hepatic differentiation in co-culture with HUVEC on day 17 of differentiation using HCM-I/II + EGM complete (F) or HCM-I/II + EGM supplements (G). HUVEC were growing in free spaces between the hiPSC (arrows). Scale bars correspond to 300 μ m.

2.2.2. Gene Expression of Stage-Specific and Endothelial Cell Markers

To evaluate the state of differentiation, mRNA expression of stage specific markers in HLC was analyzed relative to undifferentiated hiPSC. HUVEC cultured in EGM complete were used as a positive control for endothelial cell markers (Figure 5). The expression of the pluripotency gene POU domain, class 5, transcription factor 1 (*POU5F1*, Figure 5A) fell to less than 1% relative to undifferentiated hiPSC in all investigated conditions and was lowest in HUVEC mono-cultures. The fetal hepatocyte marker α -fetoprotein (*AFP*) had distinctly increased in all cultures except for the HUVEC. In particular, cultures differentiated in HCM-I/II + EGM supplements showed a distinct up-regulation of *AFP*, amounting to more than 10^7 -fold in both, HLC mono-cultures or co-cultures with HUVEC (Figure 5B). A similar expression pattern was observed for albumin (*ALB*) as a marker for mature hepatocytes, with a more than 10^5 -fold increase in the cultures differentiated in HCM-I/II + EGM supplements with or without HUVEC co-culture (Figure 5C). However, due to large variances in *AFP* and *ALB* expression, the differences between the investigated conditions were not significant (Figure 5B,C). As additional markers for mature hepatocytes, *KRT18* as well as *HNF4A* were investigated (Figure 5D,E). The expression levels of *KRT18* increased by around 10-fold for all tested conditions except for HUVEC mono-cultures which showed a comparable *KRT18* expression as undifferentiated hiPSC. A more pronounced increase by more than 10^4 -fold was observed for *HNF4A* gene expression in the presence of the different test media, which was significantly higher as compared with pure HCM-I/II ($p < 0.05$; Figure 5E). The expression of the endothelial cell marker *PECAM1* was minimally induced in HLC mono-cultures, whereas a more than 200-fold increase in expression was observed in HLC co-cultured with HUVEC, and HUVEC mono-cultures showed a more than 10^4 -fold higher *PECAM1* expression than undifferentiated hiPSC (Figure 5F).

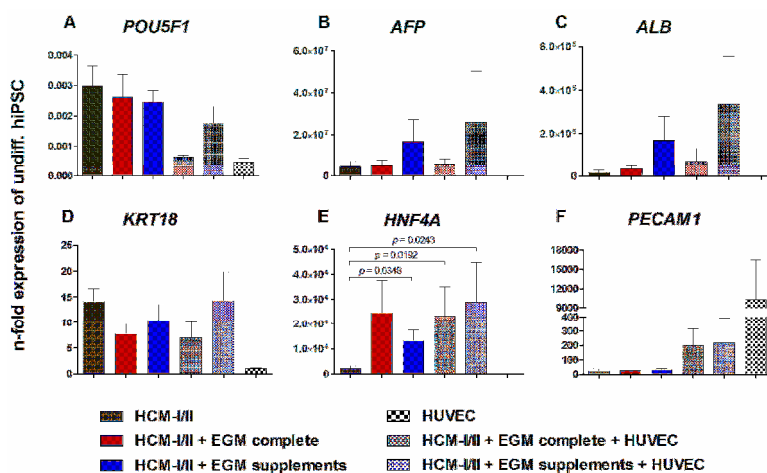


Figure 5. Effect of different media compositions and/or co-culture with human umbilical vein endothelial cells (HUVEC) on mRNA expression of stage-specific markers after hepatic differentiation of human induced pluripotent stem cells (hiPSC). Differentiation of definitive endodermal cells was performed over 14 days using hepatocyte culture medium (HCM-I/II), a 1:1 mixture of hepatocyte culture medium and endothelial cell growth medium, consisting of basal medium and supplements (HCM-I/II + EGM complete) or HCM enriched with endothelial cell growth supplements (HCM-I/II + EGM supplements) with or without HUVEC addition. In addition mRNA expression analysis was performed with HUVEC mono-cultures cultured in EGM complete as control. Graphs show POU class 5 homeobox 1 (*POU5F1*, A), α -fetoprotein (*AFP*, B), albumin (*ALB*, C), cytokeratin 18 (*KRT18*, D), hepatocyte nuclear factor 4 α (*HNF4A*, E) and platelet endothelial cell adhesion molecule 1 (*PECAM1*, F). Fold changes of mRNA expression were calculated relative to undifferentiated hiPSC with normalization to glyceraldehyde-3-phosphate dehydrogenase (*GAPDH*) expression by the $\Delta\Delta C_t$ method. Differences between HCM and all other groups and differences between test media and their corresponding co-cultures were detected with the unpaired, two-tailed Student's *t*-test, $n = 8$; Co-cultures: $n = 3$; mean \pm standard error of the mean.

2.2.3. Immunocytochemical Analysis of Stage-Specific and Endothelial Cell Markers

In order to confirm the results of the mRNA analysis, the protein expression of corresponding stage-specific markers in hiPSC-derived HLC was analyzed using immunocytochemical staining (Figure 6). Relative percentages of stained cells are provided in Table S2. In undifferentiated hiPSC cultures, almost all cells ($99 \pm 3\%$) were positive for the pluripotency marker POU5F1 (Figure 6A), whereas markers of differentiation (KRT18, HNF4A, PECAM1) were not detectable (Figure 6G,M,S). In contrast, the differentiated cultures showed no immunoreactivity for POU5F1 (Figure 6B–F). The hepatocyte marker KRT18 was clearly expressed in all differentiated cultures (Figure 6H–L). However, the percentage of KRT18 positive cells was $80 \pm 6\%$ in cultures incubated with pure HCM-I/II (Figure 6H), whereas in the other experimental groups the proportion of stained cells was distinctly lower, amounting to $60 \pm 17\%$ in HCM-I/II + EGM complete + HUVEC (Figure 6K) and less than 50% in the other groups resulting in a heterogeneous appearance (Figure 6I,J,L). Expression of the hepatocyte marker HNF4A was observed in all differentiated cell cultures with the highest percentage of positive cells ($60 \pm 30\%$) in HCM-I/II cultures (Figure 6N), followed by HCM-I/II + EGM complete cultures with $28 \pm 19\%$ (Figure 6O). All other groups showed 20% or less HNF4A positive cells (Figure 6P–R). The endothelial cell marker PECAM1 was only expressed in HLC cultures differentiated in co-culture with HUVEC (Figure 6W–X), showing a percentage of more than 20% positive cells, while mono-cultures of hiPSC were devoid of PECAM1 (Figure 6S–V).

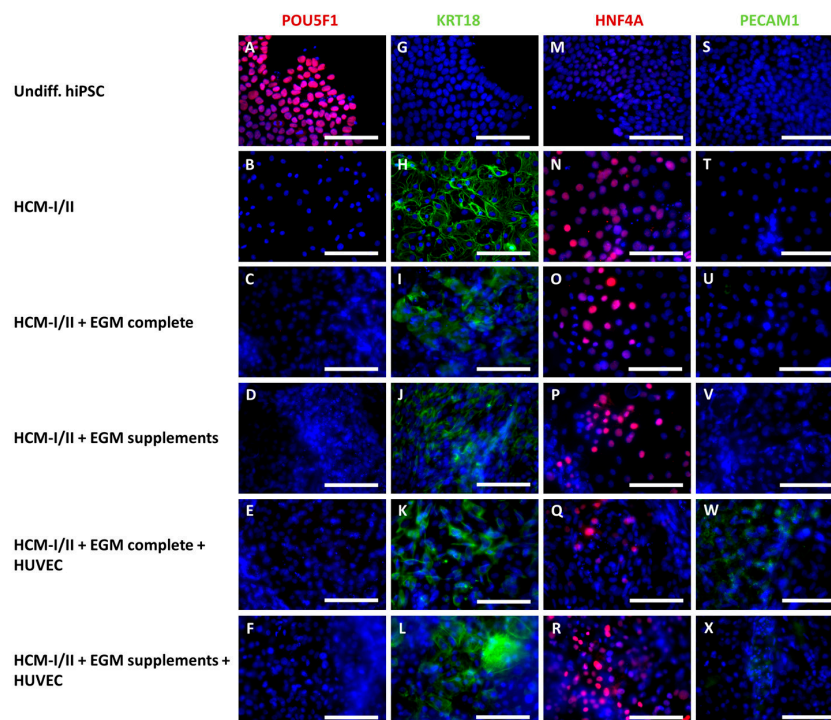


Figure 6. Immunocytochemical staining of human induced pluripotent stem cells (hiPSC) after hepatic differentiation in different media compositions and/or in co-culture with human umbilical vein endothelial cells (HUVEC). Differentiation of definitive endodermal cells was performed over 14 days using hepatocyte culture medium (HCM-I/II), a 1:1 mixture of hepatocyte culture medium and endothelial cell growth medium, consisting of basal medium and supplements (HCM-I/II + EGM complete) or HCM enriched with endothelial cell growth supplements (HCM-I/II + EGM supplements) with or without HUVEC addition. The pictures show the pluripotency marker POU class 5 homeobox 1 (POU5F1, A–F); the hepatocyte markers cytokeratin 18 (KRT18, G–L) and hepatocyte nuclear factor 4 α (HNF4A, M–R) and the endothelial cell marker platelet endothelial cell adhesion molecule 1 (PECAM1, S–X). Nuclei were counter-stained with Dapi (blue). Scale bars correspond to 100 μm .

2.2.4. Secretion of α -Fetoprotein (AFP), Albumin and Urea

The capacity of the cells for synthesis of liver-specific proteins was evaluated by measuring the secretion of the fetal albumin precursor protein AFP and of albumin into the culture supernatant (Figure 7). Secretion of AFP was detectable in all culture conditions from differentiation day 7 onwards (Figure 7A). In the HCM-I/II control culture, AFP secretion increased until day 11 reaching a maximum value of 560 ± 137 ng/h/ 10^6 initial cells and remained stable afterwards. In contrast, a continuous increase of AFP secretion until the end of the differentiation process on day 17 was observed in both, mono-cultures and co-cultures, treated with HCM-I/II + EGM complete or HCM-I/II + EGM supplements. AFP secretion rates over time, as calculated by the area under the curve, significantly ($p < 0.05$) exceeded the release of this protein in HCM-I/II control cultures, amounting to the 6- to 10-fold on day 17 as compared with HCM-I/II. Mean values of the two co-cultures showed a tendency towards higher rates than the corresponding mono-cultures, though there was no significant difference between both groups. Albumin production was detected in all experimental groups from day 9 onwards (Figure 7B). In HCM-I/II control cultures, secretion rates slowly increased up to 2.0 ± 0.4 ng/h/ 10^6 initial cells on day 17, while cultures maintained using the test media clearly showed a steeper increase, attaining 6- to 10-fold higher values as compared with the control. The highest levels of albumin secretion were detected in the co-culture groups with maximal values of 22 ng/h/ 10^6 initial cells on day 17. Cells co-cultured with HUVEC in the presence of HCM-I/II + EGM complete produced significantly more albumin than cells in HCM-I/II control cultures ($p = 0.0058$). As a further parameter to assess the functionality of the differentiated cells, urea secretion was measured over time (Figure 7C). Relatively high values were detected at the beginning of differentiation, which decreased until day 9 and then increased again in all experimental groups until day 17. The highest values of urea secretion were detected in co-cultures with HCM-I/II + EGM supplements. Further, urea secretion was significantly increased in the co-culture with HCM-I/II + EGM complete as compared to the corresponding medium control ($p = 0.0467$).

2.2.5. Functional Analysis of Different Cytochrome P450 (CYP) Isoenzymes

To determine the effect of different culture media and/or co-culture with HUVEC on the functionality of hiPSC-derived HLC, the activity of different pharmacologically relevant CYP isoenzymes was investigated by analyzing isoenzyme-specific product formation rates after application of a substrate cocktail (Figure 8). All measured CYP activities were clearly higher in HCM-I/II + EGM complete or in HCM-I/II + EGM supplements maintained with or without HUVEC as compared with HCM-I/II control cultures. Only for CYP1A2 differentiation with HCM-I/II + EGM complete in co-culture with HUVEC resulted in product formation rates similar to the HCM-I/II control (Figure 8A). And differentiation using HCM-I/II + EGM supplements maintained with or without HUVEC showed higher activities than HCM-I/II + EGM complete. CYP2B6 showed significantly higher activities for HCM-I/II + EGM complete with and without HUVEC and for HCM-I/II + EGM supplements when compared with HCM-I/II control ($p < 0.05$; Figure 8B). Activity patterns for CYP3A4 were similar showing significantly higher activities for both co-cultures and for mono-cultures using HCM-I/II + EGM supplements ($p < 0.05$; Figure 8C).

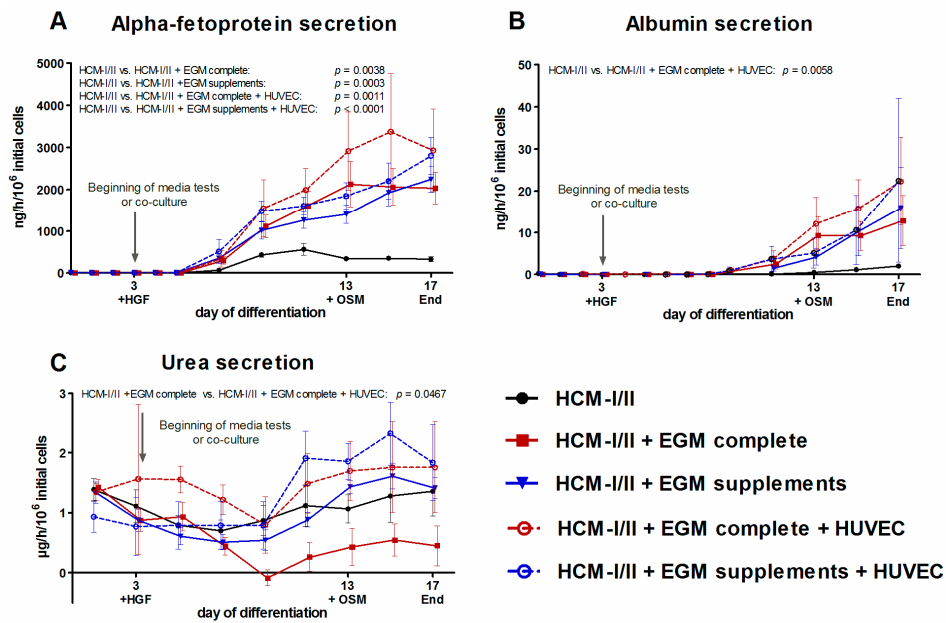


Figure 7. Effect of different media compositions and/or co-culture with human umbilical vein endothelial cells (HUVEC) on secretion of stage-specific markers during differentiation of human induced pluripotent stem cells (hiPSC). Differentiation of definitive endodermal cells was performed over 14 days using hepatocyte culture medium (HCM-I/II), a 1:1 mixture of hepatocyte culture medium and endothelial cell growth medium, consisting of basal medium and supplements (HCM-I/II + EGM complete) or HCM enriched with endothelial cell growth supplements (HCM-I/II + EGM supplements) with or without HUVEC addition. Graphs show the secretion of α -fetoprotein (AFP, A), secretion of albumin (B) and secretion of urea (C). The area under the curve was calculated and differences between HCM and all other groups as well as differences between test media and their corresponding co-cultures were detected using the unpaired, two-tailed Student's *t*-test, $n = 8$; Co-cultures: $n = 3$; mean \pm standard error of the mean.

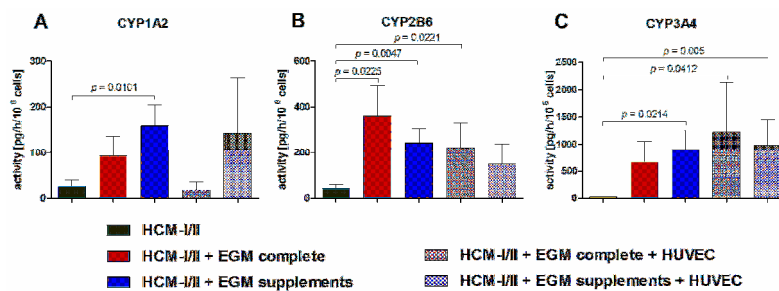


Figure 8. Effect of different media compositions and/or co-culture with human umbilical vein endothelial cells (HUVEC) on activities of cytochrome P450 (CYP) isoenzymes after hepatic differentiation of human induced pluripotent stem cells (hiPSC). Differentiation of definitive endodermal cells was performed over 14 days using hepatocyte culture medium (HCM-I/II), a 1:1 mixture of hepatocyte culture medium and endothelial cell growth medium, consisting of basal medium and supplements (HCM-I/II + EGM complete) or HCM enriched with endothelial cell growth supplements (HCM-I/II + EGM supplements) with or without HUVEC addition. The graphs show activities of CYP1A2 determined by measuring the conversion rates of phenacetin to acetaminophen (A), activities of CYP2B6 determined by measuring the conversion rates of bupropion to 4-OH-bupropion (B) and activities of CYP3A4 determined by measuring the conversion rates of midazolam to 1-OH-midazolam (C) over 6 h. Differences between HCM and all other groups and differences between test media and their corresponding co-cultures were detected using the unpaired, two-tailed Student's *t*-test, HCM: $n = 8$; HCM-I/II + EGM complete and HCM-I/II + EGM Supplements: $n = 7$; co-cultures: $n = 3$; mean \pm standard error of the mean.

3. Discussion

To date, the use of hiPSC-derived HLC in pharmacological drug screening and toxicity testing is limited by their low hepatic functionality due to a heterogeneous phenotype of HLC [26] resembling rather fetal than adult primary human hepatocytes [11]. To improve the differentiation outcome of hiPSC/hESC, several approaches have been focusing on co-culture with non-parenchymal cell types during the differentiation process, using various cell types and culture systems. A major precondition to a functional co-culture system is the use of a suitable culture medium, which meets the requirements of hiPSC as well as those of co-cultured cell types. In the present study, the influence of different culture medium compositions on HUVEC and hiPSC-derived DE cells maintained separately or in co-culture with each other was investigated. Culture media tested included media in use for hiPSC differentiation (HCM), media for HUVEC culture (ECM) and different mixtures of both.

The results from testing different media compositions in HUVEC mono-cultures showed that HUVEC did not survive using pure HCM-I, whereas use of HCM-I + EGM complete resulted in a similar growth behavior as EGM complete, and use of HCM-I + EGM supplements also supported HUVEC growth, although at a reduced level. These findings are in accordance with studies by Takebe et al. [25], who successfully employed HCM and EGM (both from Lonza) for co-culture of hiPSC with HUVEC and mesenchymal stem cells. The observation that HUVEC did not grow in HCM-I can be explained by the fact that this medium lacks some of the ingredients of EGM complete (Table S3), e.g., bovine hypothalamic extract containing the potent endothelial mitogen endothelial cell growth factor (ECGF) [27]. ECGF is even more efficient in combination with heparin [28] also being part of EGM complete, but not being present in HCM. Furthermore, HCM does not contain basic fibroblast growth factor (bFGF), which binds to heparin leading to dimerisation of bFGF receptors [29] and selective induction of endothelial cell proliferation [30]. Insulin, which is included in HCM, but not in EGM complete, is also reported to increase mitosis in endothelial cells [31], but this effect maybe counteracted by other factors. For example, transferrin, which is also part of HCM, was shown to have no influence on endothelial cell proliferation [32], but may play a role in promoting oxidant-induced apoptosis [33]. Furthermore, HCM contains ascorbic acid, which was reported to anticipate oxidative stress-induced apoptosis in endothelial cells [34]. In addition, the reduced proliferation of HUVEC cultivated in HCM-I + EGM supplements compared with cultivation in EGM complete might be associated with the higher glucose concentration of HCM-I + EGM supplements medium (10 mM), as high glucose concentrations have been shown to increase apoptosis and oxidative stress in endothelial cells [35]. In particular constant exposure to glucose levels above 7 mM, which is defined as hyperglycemia in the blood, is not physiological and may harm the endothelium [36].

Based on the results from media testing in HUVEC mono-cultures both, HCM-I/II + EGM complete and HCM-I/II + EGM supplements were tested for their suitability to induce hepatic differentiation in hiPSC-derived DE cells in presence or absence of HUVEC. The results were compared with those from using pure HCM-I/II.

As indicated by stage-specific marker expression and CYP activities, both test media improved the hepatic differentiation of hiPSC as compared with pure HCM-I/II, regardless whether HUVEC were present or not. The favorable effects of EGM complete or EGM supplements on hepatic differentiation of hiPSC may be due to some of the factors contained in those media (Table S3). In particular, the growth factor bFGF contained in EGM supplements has been shown to support the differentiation of DE cells into hepatoblasts in a concentration-dependent manner [37] and has been employed in some studies [17,38]. This may explain the distinctly increased gene expression of the hepatoblast marker *AFP* in cultures treated with HCM-I/II + EGM supplements, since this medium contains the highest amount of bFGF. The secretion of *AFP* was significantly higher in all test groups as compared with the control cultures maintained in pure HCM-I/II. A higher grade of hepatoblast differentiation may consequently lead to an increased hepatic maturation, as indicated by distinctly increased albumin secretion rates in all test groups. The albumin secretion detected in the test groups, when calculated for the same time interval (days), was more than twice as high compared to other

studies [9,16,39,40], while Baxter et al. and Gieseck et al. reported even higher albumin secretion rates of up to 1.5 g/day/10⁶ cells [11,22]. However, it has to be considered that the authors of these studies have been using different cell lines and culture protocols, which might have influenced the differentiation outcome and albumin secretion.

Potential reasons for the observed variability in the present data sets can be seen in influencing factors showing some variations among the experiments, e.g., passage number and seeding efficiency of different cell batches. In addition the usage of different batches of medium compounds may cause some variances. For example, B27 supplement used for the definitive endodermal differentiation step showed substantial variation between specific lots of B27 supplements in neuronal cell cultures [41] and also in hepatic differentiation experiments [42].

The gene expression of the epithelial marker *KRT18* was only slightly increased in differentiated HLC compared with undifferentiated hiPSC; however, immunoreactivity for KRT18 was clearly observed in hiPSC-derived HLC cultures. Both, gene and protein expression of KRT18, were barely influenced by the medium composition or addition of HUVEC. In contrast, the gene expression of the hepatic transcription factor *HNF4A* was distinctly increased in all groups compared with the use of pure HCM-I/II. This observation might again be explained by the effect of bFGF contained in HCM-I/II + EGM complete and HCM-I/II + EGM supplements since gene expression of *HNF4A* was shown to be induced by BMP4/bFGF supplemented media [10,43]. In addition, there are data indicating that the expression of *HNF4A* can be influenced by exposure to glucocorticoids [44], which are contained at a higher level in both test media as compared with pure HCM-I/II. Interestingly there was a discrepancy between protein expression of HNF4A as analyzed by immune fluorescence staining and gene expression of that factor. This could be explained by post-translational modifications of the protein that may reduce the sensitivity of the antibody used for immune fluorescence staining. Yokoyama et al. reported eight different post-translational modifications sites and observed that one of these sites is even changing in response to varying glucose levels [45], as occurring in different culture medium compositions used in this study. The nuclear receptor HNF4A is also responsible for the transcriptional activation of several CYP isoenzymes such as CYP1A2 [46] and CYP3A4 [47]. Both, the significantly increased *HNF4A* expression and the higher hydrocortisone concentration in both test media can explain the significant increase in CYP activities observed in the present study. Glucocorticoids are known to induce CYP2B, CYP2C and CYP3A in humans [48]. CYP activities were significantly increased in cultures differentiated in the optimized co-culture media as compared to the HCM-I/II control group. Maximal activities reached up to 10% of the activities of primary human hepatocytes cultured for 24 h, which were determined in a previous study of the authors [23].

The presence of HUVEC in hiPSC co-cultures could be confirmed by light-microscopy. In addition, HUVEC were detected at the end of hepatic differentiation by gene and protein expression of the endothelial cell marker PECAM1. It was reported that heparin, which is included in EGM supplements, enhances HGF production at a post-transcriptional level in HUVEC [49]. This may promote hepatic maturation [50] and proliferation [10,51] in co-cultures. However, in the present study, no supportive effect of HUVEC on the hepatic differentiation of hiPSC was observed.

An overview of current in vitro co-culture approaches for hepatic differentiation of human pluripotent stem cells is provided in Table 1. So far, the use of HUVEC to support hepatic differentiation of hiPSC was reported only in co-cultures together with either human mesenchymal stem cells [25] or adipose derived stem cells [52]. Takebe and colleagues created highly functional liver buds, which were able to rescue drug-induced lethal liver failure in immunodeficient mice. Additionally they observed that culturing hiPSC-derived HLC with endothelial cells alone failed to form three-dimensional transplantable tissues. Ma and coworkers observed significantly increased *ALB*, *HNF4A* and transthyretin gene expression in their co-culture model compared with hiPSC mono-cultures [52]. Interestingly, in contrast to the present study, both studies [25,52] omitted the epidermal growth factor (EGF) in the HCM used for differentiation. Since EGF was shown to stimulate cell proliferation in HUVEC in a dose-dependent manner [53,54], EGF should not have a negative

effect on HUVEC during co-culture experiments. Another study applied hiPSC-derived endothelial cells for co-culture during hepatic differentiation of hiPSC and was able to show significantly increased albumin secretion [55].

To increase the effect of HUVEC co-culture on hepatic maturation of hiPSC in the here described model, influencing factors such as the number of HUVEC in relation to hiPSC-derived DE cells, and the culture technique should be optimized. For example, Transwells [56] or niches separated by different extracellular matrices [55,57] can be used to provide a larger growth area for HUVEC, in a separate compartment from hiPSC (Table 1). Another approach would be the detachment of hiPSC-derived DE cells, which can then be mixed with HUVEC and reseeded [25,58,59]. These approaches would also enable to add the HUVEC at a later stage of differentiation, namely the hepatic endoderm stage as described *in vitro* by Takebe et al. [25] and *in vivo* by Matsumoto et al. [24]. Since in the present study HUVEC were expected to adhere in free spaces between the DE cells, the co-culture was initiated before spreading of DE cells resulting in a decrease of the available adhesion area for HUVEC.

As becomes apparent in Table 1, the most frequently used cell type in current co-culture approaches for hepatic differentiation of human pluripotent stem cells are murine embryonic fibroblasts [57,59–61], which increased hepatic gene expression and functionality. In the present study HUVEC were chosen as a well-established and standardized cell source for parenchymal-endothelial cell co-cultures. Furthermore, the umbilical vein is the major afferent vessel in the fetal liver [62,63] and HUVEC might thereby be important for the embryonic liver development. In this context, HUVEC were already successfully applied as early supporters of hepatic differentiation in previous studies [25,52]. Another interesting approach would be the usage of tissue-specific endothelial cells for support of hepatic differentiation through the secretion of tissue-specific factors. It was shown for several organs that tissue-specific endothelial cells orchestrate organ development as well as regeneration after injury before building a functional vasculature [64]. Ding et al. could show that liver sinusoidal endothelial cells release factors, which initiate and sustain liver regeneration induced by partial hepatectomy in mice [65]. Furthermore, there is evidence that adult hepatocytes also play a role in stem cell fate decision during liver regeneration by releasing growth factors such as HGF, Wnt and FGFs [66]. Hence, another strategy would be the co-cultivation with primary adult hepatocytes during hepatic differentiation.

In future studies the present findings should be verified using additional hiPSC lines to identify a potential dependency on donor-specific and epigenetic characteristics of individual hiPSC lines. In addition, a closer investigation of individual factors and compounds in the culture media mixtures would be helpful to create well-defined culture media formulations and to facilitate the further improvement of co-culture media.

Table 1. Studies on hepatic differentiation of human induced pluripotent stem cells (hiPSC) or human embryonic stem cells (hESC) in co-culture with different cell types.

Cell Type Used for Co-Culture with hiPSC/hESC	Ratio (hiPSC/hESC-Derived Cells:Co-Cultured Cell Type(s))	Co-Culture Method	Culture Medium Applied	Ref.
Murine hepatic stromal cell line MLSgt20	1:1	Self-aggregation in microwells	DMEM + FBS + differentiation factors	[58]
Murine embryonic fibroblasts (3T3-J2)	0.04:1	Seeding of DE cells onto mitomycin-treated 3T3-J2 feeder cells	Hepatocyte culture medium + FBS	[60]
Murine embryonic fibroblasts (swiss 3T3)	Not specified	Hepatoblast monolayer covered with 3T3 cell sheet	L15 medium + differentiation factors	[61]
HUVEC and mesenchymal stem cells	10:7:2	Spontaneous formation of 3D liver buds	HCM (without EGF) + EGM, 1:1	[25,67]
hiPSC-derived endothelial cells	2 : 1	Multicomponent hydrogel fibers containing galactose for HLC and collagen for endothelial cells	Not specified	[55]
Hepatic stellate cell line TWNT-1	Not specified	Cell inserts	DMEM-F12 + knockout serum replacer + DMSO	[56]
Murine embryonic fibroblasts (3T3-J2)	2:1 or 2.5:1 for cryopreserved HLC	Micropatterned co-culture containing collagen coating and matrigel overlay	RPMI + B27 supplement + differentiation factors	[57]
Murine embryonic fibroblasts (3T3-J2)	2:1	Self-aggregation in microwells	RPMI + B27 supplement + differentiation factors	[59]
Primary rat hepatocytes	1:2	Microfluidic co-culture	DMEM + FBS + maintenance factors and IMDM + FBS + DMSO + differentiation factors	[66]
HUVEC and adipose derived stem cells	1:1:0.02	3D bioprinting of in vivo like liver lobule structures	HCM (without EGF) + EGM-2, 1:1	[52]
HUVEC	2:1	HUVEC grow in free spaces of hiPSC-derived DE cell monolayers	HCM + EGM complete, 1:1 and HCM + EGM Supplements	Present study

4. Materials and Methods

4.1. Culture of HUVEC

Cryopreserved HUVEC (PromoCell GmbH, Heidelberg, Germany) were thawed as recommended by the manufacturer and were cultivated in endothelial cell growth medium (PromoCell GmbH), consisting of basal medium and supplements (EGM complete) and 0.05 mg/mL gentamycin (Merck, Darmstadt, Germany) on cell culture dishes (ThermoScientific, Waltham, MA, USA) at 37 °C in a 5% CO₂ atmosphere. The cells were passaged according to the manufacturer's instructions when they reached around 95% confluence. The composition of EGM complete as provided by the manufacturer is shown in Table S3.

4.2. Culture and Hepatic Differentiation of hiPSC

The hiPSC line DF6-9-9T [68] (WiCell Research Institute, Madison, WI, USA) was cultured under feeder-free conditions on Nunclon™ six-well cell culture plates (ThermoScientific Nunc™, Schwerte, Germany) coated with 8.68 µg/cm² Matrigel (growth factor reduced, Corning, NY, USA). Cells were expanded with mTeSR™1 medium (Stemcell Technologies, Vancouver, BC, Canada) containing 0.05 mg/mL gentamycin (Merck, Darmstadt, Germany).

Hepatic differentiation of hiPSC was performed according to protocols from Hay et al. [15,18,69] with some modifications, as described previously [23]. Briefly, when hiPSC reached a confluence of approximately 70%, differentiation into DE cells was induced with Roswell Park Memorial Institute (RPMI) 1640 culture medium (Merck) supplemented with 100 ng/mL activin A (Peprotech, London, UK), 50 ng/mL Wnt3a (R&D Systems, Minneapolis, MN, USA), 1 µM sodium butyrate (Sigma-Aldrich, St. Louis, MO, USA) and 2% (*v/v*) B27 supplements without insulin (Life Technologies, Carlsbad, CA, USA) for three days. Subsequently DE cells were differentiated into hepatoblasts over 13 days with hepatocyte culture medium consisting of basal medium and single quotes (Lonza, Walkersville, MD, USA) and 10 ng/mL HGF (Peprotech, Rocky Hill, NJ, USA). For further maturation to hepatocyte-like cells 10 ng/mL OSM (Peprotech) were added during the last four days of differentiation. The hepatoblast differentiation medium is referred to as HCM-I and the maturation medium is referred to as HCM-II throughout the whole manuscript. The composition of HCM as provided by the manufacturer is shown in Table S3.

4.3. Culture Medium Testing in Mono-Cultures of HUVEC

For testing of different culture media, HUVEC were seeded at a density of 4×10^3 cells/cm² and cultured over 14 days in the presence of 100% EGM complete (positive control), 100% HCM-I, HCM-I and EGM complete at a ratio of 1:1 (HCM-I + EGM complete) or HCM-I enriched with endothelial cell growth supplements (HCM-I + EGM supplements).

4.4. Co-Culture of hiPSC-Derived DE cells with HUVEC

For co-culture experiments, hiPSC were differentiated into DE cells as described above. Further differentiation was carried out in HCM-I/II + EGM complete or in HCM-I/II + EGM supplements with HUVEC added to the DE cells at a ratio of 1:2 (5×10^5 HUVEC + 1×10^6 DE cells). In parallel, DE cells were differentiated in HCM-I/II + EGM complete or in HCM-I/II + EGM supplements without HUVEC. An overview of culture media and culture medium combinations used for testing in HUVEC or hiPSC cultures is provided in Table 2.

Table 2. Culture media and culture medium combinations used for testing in cultures of human umbilical vein endothelial cells (HUVEC) or human induced pluripotent stem cells (hiPSC).

Component	EGM complete	HCM-I	HCM-II	HCM-I/II + EGM Complete	HCM-I/II + EGM Supplements
Hepatocyte culture medium (HCM) Bullet Kit	-	100% (v/v)		50% (v/v)	97.5% (v/v)
Endothelial cell growth medium (EGM)	97.5% (v/v)	-		48.75% (v/v)	-
EGM Supplements	2.5% (v/v)	-		1.25% (v/v)	2.5% (v/v)
Human hepatocyte growth factor, recombinant	-	10 ng/mL	10 ng/mL	10 ng/mL	10 ng/mL
Human oncostatin M, recombinant	-	-	10 ng/mL	10 ng/mL ¹	10 ng/mL ¹
Gentamycin	0.05 mg/mL	0.05 mg/mL	0.05 mg/mL	0.05 mg/mL	0.05 mg/mL

¹ only added to media containing HCM-II.

4.5. Analyses of Biochemical Parameters

The metabolic activity of HUVEC was assessed by daily measurement of glucose and lactate concentrations with a blood gas analyzer (ABL 700, Radiometer, Copenhagen, Denmark). Potential cell damage was detected by analyzing the release of LDH using an automated clinical chemistry analyzer (Cobas[®] 8000; Roche Diagnostics, Mannheim, Germany). The secretion of the albumin precursor protein AFP and urea during hiPSC differentiation was detected also using an automated clinical chemistry analyzer (Cobas[®] 8000, Roche Diagnostics). Albumin secretion, as a marker for mature hepatocytes, was quantified using an ELISA Quantitation kit and 3',5,5'-tetramethylbenzidine substrate (both from Bethyl Laboratories, Montgomery, TX, USA) according to the manufacturer's instructions.

4.6. Gene Expression Analysis

RNA was isolated from undifferentiated hiPSC, HLC, HUVEC, or HLC-HUVEC co-cultures. Isolation of RNA and subsequent cDNA synthesis were performed as described elsewhere [70], using PureLink[™] RNA Mini Kit (Life Technologies) and High Capacity cDNA Reverse Transcription Kit (Applied Biosystems, Foster City, CA). Each cDNA template was mixed with PCR Master mix (Applied Biosystems) and human-specific primers and probes (TaqMan GeneExpression Assay system, Life Technologies, Table 3). Quantitative real-time PCR (qRT-PCR) was performed using a Realtime cycler (Mastercycler ep Realplex 2, Eppendorf, Hamburg, Germany). The expression of specific genes was normalized to that of the housekeeping gene glyceraldehyde-3-phosphate dehydrogenase (*GAPDH*) and fold changes of expression levels were calculated with the $\Delta\Delta C_t$ method [71].

Table 3. Applied Biosystems TaqMan Gene Expression Assays[®].

Gene Symbol	Gene Name	Assay ID
<i>AFP</i>	α fetoprotein	HS00173490_m1
<i>ALB</i>	albumin	HS00910225_m1
<i>GAPDH</i>	glyceraldehyde-3-phosphate dehydrogenase	HS03929097_g1
<i>HNF4A</i>	Hepatocyte nuclear factor 4, α	Hs00230853_m1
<i>KRT18</i>	Keratin 18	Hs02827483_g1
<i>PECAM1</i>	platelet and endothelial cell adhesion molecule 1	Hs00169777_m1
<i>POU5F1</i>	POU domain, class 5, transcription factor 1	HS00999632_g1
<i>VWF</i>	von Willebrand factor	Hs00169795_m1

4.7. Immunocytochemical Staining

Immunofluorescence staining was performed as described elsewhere [70]. Antibodies used are listed in Table 4. Staining of hiPSC-derived cultures was performed in 24-well plates (lumox[®], Sarstedt, Nümbrecht-Rommelsdorf, Germany), while HUVEC were cultured and subsequently fixed on chamber slides (Thermo Scientific™ Nunc™ Lab-Tek™ II Chamber Slide™ System) for immunocytochemical analysis.

Table 4. Primary and secondary antibodies used for immunofluorescence staining.

Antibody Type and Specificity	Protein Symbol	Species	Manufacturer	Article-No.	Final Conc. (µg/mL)
Primary Antibody					
Cytokeratin 18	CK18	mouse	Santa Cruz	Sc-6259	2
Hepatocyte nuclear factor 4 α	HNF4A	rabbit	Santa Cruz	Sc-8987	4
Platelet endothelial cell adhesion molecule 1	PECAM1	mouse	Abcam	ab24590	5
POU domain, class 5, transcription factor 1	OCT3	rabbit	Santa Cruz	Sc-9081	2
Von Willebrand factor	VWF	rabbit	Abcam	ab6994	35.5
Secondary antibody					
Alexa Fluor®488 anti-mouse		goat	Life Technologies	A-11029	2
Alexa Fluor®594 anti-rabbit		goat	Life Technologies	A-11037	2

Fluorescence microscopic pictures were analysed by means of the open source image processing program ImageJ recording at least 5 visual fields for each group.

4.8. Measurement of Cytochrome P450 (CYP) Isoenzyme Activities

Activities of the pharmacologically relevant CYP isoenzymes CYP1A2, CYP2B6 and CYP3A4 were measured in hiPSC after completion of hepatic differentiation as described previously [23]. Briefly, a cocktail containing the CYP substrates phenacetin (CYP1A2), bupropion (CYP2B6) and midazolam (CYP3A4) was added to the cultures and the formation of the corresponding isoenzyme specific products was analyzed by LC-MS as described previously [23].

4.9. Statistical Evaluation

Experiments were performed in three to eight repeats, as indicated in the figure legends, and results are presented as mean ± standard error of the mean. The area under the curve was calculated for time-courses of biochemical parameters and differences between culture media and/or co-cultures were detected with a subsequent unpaired, two-tailed Student's *t*-test. Differences were judged as significant, if the *p*-value was less than 0.05.

5. Conclusions

In summary, the application of co-cultures to generate functional hiPSC-derived HLC is a relatively new and complex research field. Our study shows that the establishment of a functional co-culture model requires an intense study of surrounding aspects influencing the cell maintenance. Particular attention should be given to the composition of the applied media, as our results show that the effect of the co-culture medium outweighed the effect of the co-culture itself.

Supplementary Materials: Supplementary materials can be found at www.mdpi.com/1422-0067/18/8/1724/s1.

Acknowledgments: The research leading to these results has received support from the Innovative Medicines Initiative Joint Undertaking under grant agreement no. 115439, resources of which are composed of financial contribution from the European Union's Seventh Framework Programme (FP7/2007-2013) and EFPIA companies' in kind contribution. This article reflects only the author's views and neither the IMI JU, EFPIA, nor the European Commission is liable for any use that may be made of the information contained therein.

Author Contributions: Nora Freyer conceived, designed and performed the experiments and wrote the manuscript; Selina Greuel contributed to performance of experiments and writing of the manuscript; Fanny Knöspel contributed to data evaluation, provided useful discussion and revised the manuscript; Nadja Strahl contributed to performance of the experiments and analyzed the experimental data; Leila Amini contributed to performance of the experiments and writing of the manuscript and analyzed the experimental data; Frank Jacobs performed CYP analysis, provided useful discussion and revised the manuscript; Mario Monshouwer contributed to the study design and to the preparation of the manuscript, and Katrin Zeilinger contributed to the design of experiments, evaluation of results and writing of the manuscript.

Conflicts of Interest: The authors declare no conflict of interest.

Abbreviations

AFP	α -fetoprotein
ALB	Albumin
bFGF	Basic fibroblast growth factor
BMP	Bone morphogenetic proteins
CYP	Cytochrome P450
DE	Definitive endoderm
DMEM	Dulbecco's modified eagle's medium
DMSO	Dimethyl sulfoxide
ECGF	Endothelial cell growth factor
EGF	Epidermal growth factor
EGM	Endothelial cell growth medium
FBS	Fetal bovine serum
FGF	Fibroblast growth factor
GAPDH	Glyceraldehyde-3-phosphate dehydrogenase
HCM	Hepatocyte culture medium
hESC	Human embryonic stem cells
HGF	hepatocyte growth factor
hiPSC	Human induced pluripotent stem cells
HLC	Hepatocyte-like cells
HNF4A	Hepatocyte nuclear factor 4 α
HUVEC	Human umbilical vein endothelial cells
KRT18	Cytokeratin 18
L15	Leibovitz's
LDH	Lactate dehydrogenase
OSM	Oncostatin M
PECAM1	Platelet and endothelial cell adhesion molecule 1
POU5F1	POU domain, class 5, transcription factor 1
RPMI	Roswell Park Memorial Institute
VWF	Von Willebrand factor

References

1. Yi, F.; Liu, G.H.; Izpisua Belmonte, J.C. Human induced pluripotent stem cells derived hepatocytes: Rising promise for disease modeling, drug development and cell therapy. *Protein Cell* **2012**, *4*, 246–250. [[CrossRef](#)] [[PubMed](#)]
2. Passier, R.; Orlova, V.; Mummery, C. Complex tissue and disease modeling using hiPSCs. *Cell Stem Cell* **2016**, *18*, 309–321. [[CrossRef](#)] [[PubMed](#)]
3. Suter-Dick, L.; Alves, P.M.; Blaauuboer, B.J.; Bremm, K.D.; Brito, C.; Coecke, S.; Flick, B.; Fowler, P.; Hescheler, J.; Ingelman-Sundberg, M.; et al. Stem cell-derived systems in toxicology assessment. *Stem Cells Dev.* **2015**, *24*, 1284–1296. [[CrossRef](#)] [[PubMed](#)]
4. Larrey, D. Epidemiology and individual susceptibility to adverse drug reactions affecting the liver. *Semin. Liver Dis.* **2002**, *22*, 145–155. [[CrossRef](#)] [[PubMed](#)]

5. Sgro, C.; Clinard, F.; Ouazir, K.; Chanay, H.; Allard, C.; Guilleminet, C.; Lenoir, C.; Lemoine, A.; Hillon, P. Incidence of drug-induced hepatic injuries: A French population-based study. *Hepatology* **2002**, *36*, 451–455. [[CrossRef](#)] [[PubMed](#)]
6. Takayama, K.; Kawabata, K.; Nagamoto, Y.; Kishimoto, K.; Tashiro, K.; Sakurai, F.; Tachibana, M.; Kanda, K.; Hayakawa, T.; Furue, M.K.; et al. 3D spheroid culture of hESC/hiPSC-derived hepatocyte-like cells for drug toxicity testing. *Biomaterials* **2013**, *34*, 1781–1789. [[CrossRef](#)] [[PubMed](#)]
7. Ware, B.R.; Berger, D.R.; Khetani, S.R. Prediction of drug-induced liver injury in Micropatterned Co-cultures Containing iPSC-Derived Human Hepatocytes. *Toxicol. Sci.* **2015**, *145*, 252–262. [[CrossRef](#)] [[PubMed](#)]
8. Yu, Y.; Liu, H.; Ikeda, Y.; Amiot, B.P.; Rinaldo, P.; Duncan, S.A.; Nyberg, S.L. Hepatocyte-like cells differentiated from human induced pluripotent stem cells: Relevance to cellular therapies. *Stem Cell Res.* **2012**, *9*, 196–207. [[CrossRef](#)] [[PubMed](#)]
9. Song, Z.; Cai, J.; Liu, Y.; Zhao, D.; Yong, J.; Duo, S.; Song, X.; Guo, Y.; Zhao, Y.; Qin, H.; et al. Efficient generation of hepatocyte-like cells from human induced pluripotent stem cells. *Cell Res.* **2009**, *19*, 1233–1242. [[CrossRef](#)] [[PubMed](#)]
10. Si-Tayeb, K.; Noto, F.K.; Nagaoka, M.; Li, J.; Battle, M.A.; Duris, C.; North, P.E.; Dalton, S.; Duncan, S.A. Highly efficient generation of human hepatocyte-like cells from induced pluripotent stem cells. *Hepatology* **2010**, *51*, 297–305. [[CrossRef](#)] [[PubMed](#)]
11. Baxter, M.; Withey, S.; Harrison, S.; Segeritz, C.P.; Zhang, F.; Atkinson-Dell, R.; Rowe, C.; Gerrard, D.T.; Sison-Young, R.; Jenkins, R.; et al. Phenotypic and functional analyses show stem cell-derived hepatocyte-like cells better mimic fetal rather than adult hepatocytes. *J. Hepatol.* **2015**, *62*, 581–589. [[CrossRef](#)] [[PubMed](#)]
12. Takayama, K.; Mizuguchi, H. Generation of human pluripotent stem cell-derived hepatocyte-like cells for drug toxicity screening. *Drug Metab. Pharmacokinet.* **2017**, *32*, 12–20. [[CrossRef](#)] [[PubMed](#)]
13. Sullivan, G.J.; Hay, D.C.; Park, I.H.; Fletcher, J.; Hannoun, Z.; Payne, C.M.; Dalgetty, D.; Black, J.R.; Ross, J.A.; Samuel, K.; et al. Generation of functional human hepatic endoderm from human induced pluripotent stem cells. *Hepatology* **2010**, *51*, 329–335. [[CrossRef](#)] [[PubMed](#)]
14. Vosough, M.; Omidinia, E.; Kadivar, M.; Shokrgozar, M.A.; Pournasr, B.; Aghdami, N.; Baharvand, H. Generation of functional hepatocyte-like cells from human pluripotent stem cells in a scalable suspension culture. *Stem Cells Dev.* **2013**, *22*, 2693–2705. [[CrossRef](#)] [[PubMed](#)]
15. Hay, D.C.; Fletcher, J.; Payne, C.; Terrace, J.D.; Gallagher, R.C.; Snoeys, J.; Black, J.R.; Wojtacha, D.; Samuel, K.; Hannoun, Z.; et al. Highly efficient differentiation of hESCs to functional hepatic endoderm requires ActivinA and Wnt3a signaling. *Proc. Natl. Acad. Sci. USA* **2008**, *105*, 12301–12306. [[CrossRef](#)] [[PubMed](#)]
16. Cai, J.; Zhao, Y.; Liu, Y.; Ye, F.; Song, Z.; Qin, H.; Meng, S.; Chen, Y.; Zhou, R.; Song, X.; et al. Directed differentiation of human embryonic stem cells into functional hepatic cells. *Hepatology* **2007**, *45*, 1229–1239. [[CrossRef](#)] [[PubMed](#)]
17. Brolén, G.; Sivertsson, L.; Björquist, P.; Eriksson, G.; Ek, M.; Semb, H.; Johansson, I.; Andersson, T.B.; Ingelman-Sundberg, M.; Heins, N. Hepatocyte-like cells derived from human embryonic stem cells specifically via definitive endoderm and a progenitor stage. *J. Biotechnol.* **2010**, *145*, 284–294. [[CrossRef](#)] [[PubMed](#)]
18. Hay, D.C.; Zhao, D.; Fletcher, J.; Hewitt, Z.A.; McLean, D.; Urruticochea-Uriguen, A.; Black, J.R.; Elcombe, C.; Ross, J.A.; Wolf, R.; et al. Efficient differentiation of hepatocytes from human embryonic stem cells exhibiting markers recapitulating liver development in vivo. *Stem Cells* **2008**, *26*, 894–902. [[CrossRef](#)] [[PubMed](#)]
19. Takayama, K.; Inamura, M.; Kawabata, K.; Katayama, K.; Higuchi, M.; Tashiro, K.; Nonaka, A.; Sakurai, F.; Hayakawa, T.; Furue, M.K.; et al. Efficient generation of functional hepatocytes from human embryonic stem cells and induced pluripotent stem cells by HNF4 α transduction. *Mol. Ther.* **2012**, *20*, 127–137. [[CrossRef](#)] [[PubMed](#)]
20. Doddapaneni, R.; Chawla, Y.K.; Das, A.; Kalra, J.K.; Ghosh, S.; Chakraborti, A. Overexpression of microRNA-122 enhances in vitro hepatic differentiation of fetal liver-derived stem/progenitor cells. *J. Cell Biochem.* **2013**, *114*, 1575–1583. [[CrossRef](#)] [[PubMed](#)]
21. Deng, X.G.; Qiu, R.L.; Wu, Y.H.; Li, Z.X.; Xie, P.; Zhang, J.; Zhou, J.J.; Zeng, L.X.; Tang, J.; Maharjan, A.; et al. Overexpression of miR-122 promotes the hepatic differentiation and maturation of mouse ESCs through a miR-122/FoxA1/HNF4a-positive feedback loop. *Liver Int.* **2014**, *34*, 281–295. [[CrossRef](#)] [[PubMed](#)]

22. Gieseck, R.L., III; Hannan, N.R.; Bort, R.; Hanley, N.A.; Drake, R.A.; Cameron, G.W.; Wynn, T.A.; Vallier, L. Maturation of induced pluripotent stem cell derived hepatocytes by 3D-culture. *PLoS ONE* **2014**, *9*, e86372. [[CrossRef](#)] [[PubMed](#)]
23. Freyer, N.; Knöspel, F.; Strahl, N.; Amini, L.; Schrade, P.; Bachmann, S.; Damm, G.; Seehofer, D.; Jacobs, F.; Monshouwer, M.; et al. Hepatic differentiation of human induced pluripotent stem cells in a perfused three-dimensional multicompartiment bioreactor. *BioRes. Open Access* **2016**, *5*, 235–248. [[CrossRef](#)] [[PubMed](#)]
24. Matsumoto, K.; Yoshitomi, H.; Rossant, J.; Zaret, K.S. Liver organogenesis promoted by endothelial cells prior to vascular function. *Science* **2001**, *294*, 559–563. [[CrossRef](#)] [[PubMed](#)]
25. Takebe, T.; Sekine, K.; Enomura, M.; Koike, H.; Kimura, M.; Ogaeri, T.; Zhang, R.R.; Ueno, Y.; Zheng, Y.W.; Koike, N.; et al. Vascularized and functional human liver from an iPSC-derived organ bud transplant. *Nature* **2013**, *499*, 481–484. [[CrossRef](#)] [[PubMed](#)]
26. Godoy, P.; Schmidt-Heck, W.; Natarajan, K.; Lucendo-Villarín, B.; Szkolnicka, D.; Asplund, A.; Björquist, P.; Widera, A.; Stöber, R.; Campos, G.; et al. Gene networks and transcription factor motifs defining the differentiation of stem cells into hepatocyte-like cells. *J. Hepatol.* **2015**, *63*, 934–942. [[CrossRef](#)] [[PubMed](#)]
27. Maciag, T.; Cerundolo, J.; Ilsley, S.; Kelley, P.R.; Forand, R. An endothelial cell growth factor from bovine hypothalamus: Identification and partial characterization. *Proc. Natl. Acad. Sci. USA* **1979**, *76*, 5674–5678. [[CrossRef](#)] [[PubMed](#)]
28. Thornton, S.C.; Mueller, S.N.; Levine, E.M. Human endothelial cells: Use of heparin in cloning and long-term serial cultivation. *Science* **1983**, *222*, 623–625. [[CrossRef](#)] [[PubMed](#)]
29. Spivak-Kroizman, T.; Lemmon, M.A.; Dikic, I.; Ladbury, J.E.; Pinchasi, D.; Huang, J.; Jaye, M.; Crumley, G.; Schlessinger, J.; Lax, I. Heparin-induced oligomerization of FGF molecules is responsible for FGF receptor dimerization, activation, and cell proliferation. *Cell* **1994**, *79*, 1015–1024. [[CrossRef](#)]
30. Kang, S.S.; Gosselin, C.; Ren, D.; Greisler, H.P. Selective stimulation of endothelial cell proliferation with inhibition of smooth muscle cell proliferation by fibroblast growth factor-1 plus heparin delivered from fibrin glue suspensions. *Surgery* **1995**, *118*, 280–286. [[CrossRef](#)]
31. Montagnani, M.; Golovchenko, I.; Kim, I.; Koh, G.Y.; Goalstone, M.L.; Mundhekar, A.N.; Johansen, M.; Kucik, D.F.; Quon, M.J.; Draznin, B. Inhibition of phosphatidylinositol 3-kinase enhances mitogenic actions of insulin in endothelial cells. *J. Biol. Chem.* **2002**, *277*, 1794–1799. [[CrossRef](#)] [[PubMed](#)]
32. Carlevaro, M.F.; Albini, A.; Ribatti, D.; Gentili, C.; Benelli, R.; Cermelli, S.; Cancedda, R.; Cancedda, F.D. Transferrin promotes endothelial cell migration and invasion: implication in cartilage neovascularization. *J. Cell. Biol.* **1997**, *136*, 1375–1384. [[CrossRef](#)] [[PubMed](#)]
33. Kotamraju, S.; Chitambar, C.R.; Kalivendi, S.V.; Joseph, J.; Kalyanaraman, B. Transferrin receptor-dependent iron uptake is responsible for doxorubicin-mediated apoptosis in endothelial cells: Role of oxidant-induced iron signaling in apoptosis. *J. Biol. Chem.* **2002**, *277*, 17179–17187. [[CrossRef](#)] [[PubMed](#)]
34. Dhar-Masareño, M.; Cárcamo, J.M.; Golde, D.W. Hypoxia-reoxygenation-induced mitochondrial damage and apoptosis in human endothelial cells are inhibited by vitamin C. *Free Radic. Biol. Med.* **2005**, *38*, 1311–1322. [[CrossRef](#)] [[PubMed](#)]
35. Piconi, L.; Quagliaro, L.; Assaloni, R.; Da Ros, R.; Maier, A.; Zuodar, G.; Ceriello, A. Constant and intermittent high glucose enhances endothelial cell apoptosis through mitochondrial superoxide overproduction. *Diabetes Metab. Res. Rev.* **2006**, *22*, 198–203. [[CrossRef](#)] [[PubMed](#)]
36. Tanaka, M.; Gong, J.; Zhang, J.; Yamada, Y.; Borgeld, H.J.; Yagi, K. Mitochondrial genotype associated with longevity and its inhibitory effect on mutagenesis. *Mech. Ageing Dev.* **2000**, *116*, 65–76. [[CrossRef](#)]
37. Ameri, J.; Ståhlberg, A.; Pedersen, J.; Johansson, J.K.; Johannesson, M.M.; Artner, I.; Semb, H. FGF2 specifies hESC-derived definitive endoderm into foregut/midgut cell lineages in a concentration-dependent manner. *Stem Cells* **2010**, *28*, 45–56. [[CrossRef](#)] [[PubMed](#)]
38. Touboul, T.; Hannan, N.R.; Corbinau, S.; Martinez, A.; Martinet, C.; Branchereau, S.; Mainot, S.; Strick-Marchand, H.; Pedersen, R.; Di Santo, J.; et al. Generation of functional hepatocytes from human embryonic stem cells under chemically defined conditions that recapitulate liver development. *Hepatology* **2010**, *51*, 1754–1765. [[CrossRef](#)] [[PubMed](#)]
39. Kim, J.H.; Jang, Y.J.; An, S.Y.; Son, J.; Lee, J.; Lee, G.; Park, J.Y.; Park, H.J.; Hwang, D.Y.; Kim, J.H.; et al. Enhanced Metabolizing Activity of Human ES Cell-Derived Hepatocytes Using a 3D Culture System with Repeated Exposures to Xenobiotics. *Toxicol. Sci.* **2015**, *147*, 190–206. [[CrossRef](#)] [[PubMed](#)]

40. Tasnim, F.; Phan, D.; Toh, Y.C.; Yu, H. Cost-effective differentiation of hepatocyte-like cells from human pluripotent stem cells using small molecules. *Biomaterials* **2015**, *70*, 115–125. [[CrossRef](#)] [[PubMed](#)]
41. Chen, Y.; Stevens, B.; Chang, J.; Milbrandt, J.; Barres, B.A.; Hell, J.W. NS21: Re-defined and modified supplement B27 for neuronal cultures. *J. Neurosci. Methods*. **2008**, *171*, 239–247. [[CrossRef](#)] [[PubMed](#)]
42. Cai, J.; DeLaForest, A.; Fisher, J.; Urick, A.; Wagner, T.; Twaroski, K.; Cayo, M.; Nagaoka, M.; Duncan, S.A. Protocol for Directed Differentiation of Human Pluripotent Stem Cells toward a Hepatocyte Fate. StemBook. 2012. Available online: <http://www.ncbi.nlm.nih.gov/books/NBK133278/PubMed> (accessed on 2 August 2017).
43. DeLaForest, A.; Nagaoka, M.; Si-Tayeb, K.; Noto, F.K.; Konopka, G.; Battle, M.A.; Duncan, S.A. HNF4A is essential for specification of hepatic progenitors from human pluripotent stem cells. *Development* **2011**, *138*, 4143–4153. [[CrossRef](#)] [[PubMed](#)]
44. Dean, S.; Tang, J.I.; Seckl, J.R.; Nyirenda, M.J. Developmental and tissue-specific regulation of hepatocyte nuclear factor 4-alpha (HNF4-alpha) isoforms in rodents. *Gene Expr.* **2010**, *14*, 337–344. [[CrossRef](#)] [[PubMed](#)]
45. Yokoyama, A.; Katsura, S.; Ito, R.; Hashiba, W.; Sekine, H.; Fujiki, R.; Kato, S. Multiple post-translational modifications in hepatocyte nuclear factor 4 α . *Biochem. Biophys. Res. Commun.* **2011**, *410*, 749–753. [[CrossRef](#)] [[PubMed](#)]
46. Martínez-Jiménez, C.P.; Castell, J.V.; Gómez-Lechón, M.J.; Jover, R. Transcriptional activation of CYP2C9, CYP1A1, and CYP1A2 by hepatocyte nuclear factor 4alpha requires coactivators peroxisomal proliferator activated receptor-gamma coactivator 1alpha and steroid receptor coactivator 1. *Mol. Pharmacol.* **2006**, *70*, 1681–1692. [[CrossRef](#)] [[PubMed](#)]
47. Tirona, R.G.; Lee, W.; Leake, B.F.; Lan, L.B.; Cline, C.B.; Lamba, V.; Parviz, F.; Duncan, S.A.; Inoue, Y.; Gonzalez, F.J.; et al. The orphan nuclear receptor HNF4alpha determines PXR- and CAR-mediated xenobiotic induction of CYP3A4. *Nat. Med.* **2003**, *9*, 220–224. [[CrossRef](#)] [[PubMed](#)]
48. Pascussi, J.M.; Gerbal-Chaloin, S.; Drocourt, L.; Maurel, P.; Vilarem, M.J. The expression of CYP2B6, CYP2C9 and CYP3A4 genes: A tangle of networks of nuclear and steroid receptors. *Biochim. Biophys. Acta* **2003**, *1619*, 243–253. [[CrossRef](#)]
49. Matsumoto, K.; Nakamura, T. Heparin functions as a hepatotrophic factor by inducing production of hepatocyte growth factor. *Biochem. Biophys. Res. Commun.* **1996**, *227*, 455–461. [[CrossRef](#)] [[PubMed](#)]
50. Behbahan, I.S.; Duan, Y.; Lam, A.; Khoobyari, S.; Ma, X.; Ahuja, T.P.; Zern, M.A. New approaches in the differentiation of human embryonic stem cells and induced pluripotent stem cells toward hepatocytes. *Stem Cell Rev.* **2011**, *7*, 748–759. [[CrossRef](#)] [[PubMed](#)]
51. Kang, L.I.; Mars, W.M.; Michalopoulos, G.K. Signals and cells involved in regulating liver regeneration. *Cells* **2012**, *1*, 1261–1292. [[CrossRef](#)] [[PubMed](#)]
52. Ma, X.; Qu, X.; Zhu, W.; Li, Y.S.; Yuan, S.; Zhang, H.; Liu, J.; Wang, P.; Lai, C.S.; Zanella, F.; et al. Deterministically patterned biomimetic human iPSC-derived hepatic model via rapid 3D bioprinting. *Proc. Natl. Acad. Sci. USA* **2016**, *113*, 2206–2211. [[CrossRef](#)] [[PubMed](#)]
53. Nakamura, M.; Nishida, T. Differential effects of epidermal growth factor and interleukin 6 on corneal epithelial cells and vascular endothelial cells. *Cornea* **1999**, *18*, 452–458. [[CrossRef](#)] [[PubMed](#)]
54. Gentilini, G.; Kirschbaum, N.E.; Augustine, J.A.; Aster, R.H.; Visentin, G.P. Inhibition of human umbilical vein endothelial cell proliferation by the CXC chemokine, platelet factor 4 (PF4), is associated with impaired downregulation of p21(Cip1/WAF1). *Blood* **1999**, *93*, 25–33. [[PubMed](#)]
55. Du, C.; Narayanan, K.; Leong, M.F.; Wan, A.C. Induced pluripotent stem cell-derived hepatocytes and endothelial cells in multi-component hydrogel fibers for liver tissue engineering. *Biomaterials* **2014**, *35*, 6006–6014. [[CrossRef](#)] [[PubMed](#)]
56. Javed, M.S.; Yaqoob, N.; Iwamuro, M.; Kobayashi, N.; Fujiwara, T. Generation of hepatocyte-like cells from human induced pluripotent stem (iPS) cells by co-culturing embryoid body cells with liver non-parenchymal cell line TWNT-1. *J. Coll. Physicians Surg. Pak.* **2014**, *24*, 91–96. [[PubMed](#)]
57. Berger, D.R.; Ware, B.R.; Davidson, M.D.; Allsup, S.R.; Khetani, S.R. Enhancing the functional maturity of induced pluripotent stem cell-derived human hepatocytes by controlled presentation of cell-cell interactions in vitro. *Hepatology* **2015**, *61*, 1370–1381. [[CrossRef](#)] [[PubMed](#)]

58. Ishii, T.; Yasuchika, K.; Fukumitsu, K.; Kawamoto, T.; Kawamura-Saitoh, M.; Amagai, Y.; Ikai, I.; Uemoto, S.; Kawase, E.; Suemori, H.; et al. In vitro hepatic maturation of human embryonic stem cells by using a mesenchymal cell line derived from murine fetal livers. *Cell Tissue Res.* **2010**, *339*, 505–512. [[CrossRef](#)] [[PubMed](#)]
59. Song, W.; Lu, Y.C.; Frankel, A.S.; An, D.; Schwartz, R.E.; Ma, M. Engraftment of human induced pluripotent stem cell-derived hepatocytes in immunocompetent mice via 3D co-aggregation and encapsulation. *Sci. Rep.* **2015**, *5*, 16884. [[CrossRef](#)] [[PubMed](#)]
60. Yu, Y.D.; Kim, K.H.; Lee, S.G.; Choi, S.Y.; Kim, Y.C.; Byun, K.S.; Cha, I.H.; Park, K.Y.; Cho, C.H.; Choi, D.H. Hepatic differentiation from human embryonic stem cells using stromal cells. *J. Surg. Res.* **2011**, *170*, 253–261. [[CrossRef](#)] [[PubMed](#)]
61. Nagamoto, Y.; Tashiro, K.; Takayama, K.; Ohashi, K.; Kawabata, K.; Sakurai, F.; Tachibana, M.; Hayakawa, T.; Furue, M.K.; Mizuguchi, H. The promotion of hepatic maturation of human pluripotent stem cells in 3D co-culture using type I collagen and Swiss 3T3 cell sheets. *Biomaterials* **2012**, *33*, 4526–4534. [[CrossRef](#)] [[PubMed](#)]
62. Collardeau-Frachon, S.; Scoazec, J.Y. Vascular development and differentiation during human liver organogenesis. *Anat. Rec.* **2008**, *291*, 614–627. [[CrossRef](#)] [[PubMed](#)]
63. Si-Tayeb, K.; Lemaigre, F.P.; Duncan, S.A. Organogenesis and development of the liver. *Dev. Cell* **2010**, *18*, 175–189. [[CrossRef](#)] [[PubMed](#)]
64. Rafii, S.; Butler, J.M.; Ding, B.S. Angiocrine functions of organ-specific endothelial cells. *Nature* **2016**, *529*, 316–325. [[CrossRef](#)] [[PubMed](#)]
65. Ding, B.S.; Nolan, D.J.; Butler, J.M.; James, D.; Babazadeh, A.O.; Rosenwaks, Z.; Mittal, V.; Kobayashi, H.; Shido, K.; Lyden, D.; et al. Inductive angiocrine signals from sinusoidal endothelium are required for liver regeneration. *Nature* **2010**, *468*, 310–315. [[CrossRef](#)] [[PubMed](#)]
66. Haque, A.; Gheibi, P.; Stybayeva, G.; Gao, Y.; Torok, N.; Revzin, A. Ductular reaction-on-a-chip: Microfluidic co-cultures to study stem cell fate selection during liver injury. *Sci. Rep.* **2016**, *6*. [[CrossRef](#)] [[PubMed](#)]
67. Takebe, T.; Zhang, R.R.; Koike, H.; Kimura, M.; Yoshizawa, E.; Enomura, M.; Koike, N.; Sekine, K.; Taniguchi, H. Generation of a vascularized and functional human liver from an iPSC-derived organ bud transplant. *Nat. Protoc.* **2014**, *9*, 396–409. [[CrossRef](#)] [[PubMed](#)]
68. Yu, J.; Hu, K.; Smuga-Otto, K.; Tian, S.; Stewart, R.; Slukvin, I.I.; Thomson, J.A. Human induced pluripotent stem cells free of vector and transgene sequences. *Science* **2009**, *324*, 797–801. [[CrossRef](#)] [[PubMed](#)]
69. Hay, D.C.; Zhao, D.; Ross, A.; Mandalam, R.; Lebkowski, J.; Cui, W. Direct differentiation of human embryonic stem cells to hepatocyte-like cells exhibiting functional activities. *Cloning Stem Cells* **2007**, *9*, 51–62. [[CrossRef](#)] [[PubMed](#)]
70. Knöspel, F.; Freyer, N.; Stecklum, M.; Gerlach, J.C.; Zeilinger, K. Periodic harvesting of embryonic stem cells from a hollow-fiber membrane based four-compartment bioreactor. *Biotechnol. Prog.* **2016**, *32*, 141–151. [[CrossRef](#)] [[PubMed](#)]
71. Livak, K.J.; Schmittgen, T.D. Analysis of relative gene expression data using real-time quantitative PCR and the 2(-Delta Delta C(T)) Method. *Methods* **2001**, *25*, 402–408. [[CrossRef](#)] [[PubMed](#)]



LEBENS LAUF

Mein Lebenslauf wird aus datenschutzrechtlichen Gründen in der elektronischen Version meiner Arbeit nicht veröffentlicht.

Mein Lebenslauf wird aus datenschutzrechtlichen Gründen in der elektronischen Version meiner Arbeit nicht veröffentlicht.

KOMPLETTE PUBLIKATIONSLISTE

Meier F*, **Freyer N***, Brzeszczynska J, Knöspel F, Armstrong L, Lako M, Damm G, Ludwig-Schwellinger E, Deschl U, Ross JA, Beilmann M, Zeilinger K. Hepatic differentiation of human iPSC in different 3D models: a comparative study. *Int J mol med*, 40:1759-1771. IF: 2.341

Freyer N, Greuel S, Knöspel F, Amini L, Schrade P, Bachmann S, Damm G, Seehofer D, Jacobs F, Monshouwer M, Zeilinger K Effects of Co-Culture Media on Hepatic Differentiation of hiPSC with or without HUVEC Co-Culture. *Int J Mol Sci*, 2017; 18:pii: E1724 2017. IF: 3.226

Cipriano M, **Freyer N**, Knöspel F, Oliveira NG, Barcia R, Cruz PE, Cruz H, Castro M, Santos JM, Zeilinger K, Miranda JP. Self-assembled 3D spheroids and hollow-fibre bioreactors improve MSC-derived hepatocyte-like cell maturation in vitro. *Arch Toxicol*, 2017; 91:1815-1832. IF: 5.901

Montacir H, **Freyer N**, Knoespel F, Urbaniak T, Dedova T, Berger M, Damm G, Tauber R, Zeilinger K, Blanchard V. The N-glycome of embryonic stem cells and thereof differentiated hepatic cells. *Chembiochem*, 2017; 18:1234-1241. IF: 2.847

Schmidt-Heck W, Wönne EC, Hiller T, Menzel U, Koczan D, Damm G, Seehofer D, Knöspel F, **Freyer N**, Guthke R, Dooley S, Zeilinger K. Global transcriptional response of human liver cells to ethanol stress of different strength reveals hormetic behavior. *Alcohol Clin Exp Res*, 2017; 41:883-894. IF: 2.716

Freyer N, Knöspel F, Strahl N, Amini L, Schrade P, Bachmann S, Damm G, Seehofer D, Jacobs F, Monshouwer M, Zeilinger K. Hepatic Differentiation of Human Induced Pluripotent Stem Cells in a Perfused Three-Dimensional Multicompartment Bioreactor. *Biores Open Access*, 2016; 5:235-248. IF: none

Zeilinger K, **Freyer N**, Damm G, Seehofer D, Knöspel F. Cell sources for in vitro human liver cell culture models. *Exp Biol Med (Maywood)*, 2016; 241:1684-98. [Review] IF: 2.688

Deharde D, Schneider C, Hiller T, Fischer N, Kegel V, Lübberstedt M, **Freyer N**, Hengstler JG, Andersson TB, Seehofer D, Pratschke J, Zeilinger K, Damm G. Bile canaliculi formation and biliary transport in 3D sandwich-cultured hepatocytes in dependence of the extracellular matrix composition. *Arch Toxicol*, 2016; 90:2497-511. IF: 5.901

Knöspel F, Jacobs F, **Freyer N**, Damm G, De Bondt A, van den Wyngaert I, Snoeys J, Monshouwer M, Richter M, Strahl N, Seehofer D, Zeilinger K. In vitro model for hepatotoxicity studies based on Primary Human Hepatocyte Cultivation in a Perfused 3D Bioreactor System. *Int J Mol Sci*, 2016; 17:584. IF: 3.226

Knöspel F*, **Freyer N***, Stecklum M, Gerlach JC, Zeilinger K. Periodic harvesting of embryonic stem cells from a hollow-fiber membrane based four-compartment bioreactor. *Biotechnol Prog*, 2016; 32:141-51. IF: 1.986

*These authors contributed equally to this study.

DANKSAGUNG

Die vorliegende Arbeit wurde in der Arbeitsgruppe von Frau Dr. Katrin Zeilinger am Berlin-Brandenburger Centrum für Regenerative Therapien (BCRT) in der Zeit von Juni 2013 bis August 2017 angefertigt. Die Forschung, die zu den beschriebenen Ergebnissen führte, wurde durch das *Innovative Medicines Initiative Joint Undertaking* (IMI JU) unter der Fördervertragsnummer n° 115439 gefördert, deren Ressourcen sich aus dem siebenten Europäischen Rahmenprogramm (FP7/2007-2013) und Sachbeiträgen der EFPIA Unternehmen zusammensetzen. Diese Arbeit gibt lediglich die Ansichten des Autors wieder und weder die IMI JU noch EFPIA noch die Europäische Kommission haften für die etwaige Benutzung der darin gemachten Angaben.

An dieser Stelle möchte ich all Jenen danken, die mich in den letzten vier Jahren der Forschung und in meinem Promotionsvorhaben unterstützt haben.

Zu aller Erst möchte ich mich daher bei Dr. Katrin Zeilinger für die Möglichkeit, diese Arbeit in ihrer Forschungsgruppe durchführen zu dürfen, bedanken. Ich habe die freundliche und vertrauensvolle Atmosphäre sehr geschätzt, in der es immer Spaß machte die Fortschritte aber auch Probleme der Forschungsarbeit jederzeit offen zu diskutieren.

Auch Prof. Dr. Michael Sittinger möchte ich für die Zeit danken, die er sich genommen hat, um meine Arbeit zu betreuen.

Außerdem möchte ich mich bei allen momentanen und ehemaligen Mitgliedern der AG Zeilinger bedanken, die genauso zu einer angenehmen Arbeitsatmosphäre beigetragen haben, sodass ich mich immer gerne auf den Weg zur Arbeit machte. Dr. Fanny Knöspel wies mich in die Bioreaktortechnologie und die Stammzellkultur ein und hat mir sehr viele praktische Tipps und Tricks gezeigt und Dr. Thomas Urbaniak lehrte mich die hepatische Differenzierung von Stammzellen. Bei Selina Greuel möchte ich mich für die schöne Zeit im Labor und die hervorragende Zusammenarbeit bedanken. Außerdem danke ich Nadja Strahl und Leila Amini, deren Bachelor bzw. Masterarbeiten auch zum Gelingen dieser Arbeit beigetragen haben und deren Betreuung mir sehr viel Spaß gemacht hat und für mich auch eine lehrreiche Zeit waren. Auch Christin Schneider, Dr. Marco Richter und Dr. Madalena Cipriano möchte ich sehr danken für die schöne Zeit in der AG, lange Labortage, die zusammenschweißten ebenso wie die unterhaltsamen Mittagspausen oder gemeinsame Kanufahrten.

Ein weiterer großer Dank gilt außerdem allen Ko-Autoren meiner Publikationen, ohne die diese Arbeit in der vorliegenden Form nicht möglich gewesen wäre. Dr. Florian Meier danke ich für die hervorragende Zusammenarbeit und den regen Austausch in langen Telefonaten während der

Vorbereitung unserer gemeinsamen Publikation. Für die Isolierung und Bereitstellung der primären humanen Hepatozyten danke ich Dr. Georg Damm. Bei Dr. Frank Jacobs möchte ich mich für die massenspektrometrische Messung der Medikamentenmetabolite sowie die konstruktiven Denkanstöße bedanken. Prof. Dr. Jim Ross und Dr. Joanna Brzeszczynska hießen mich für eine Woche in Ihrem Labor willkommen und wir nahmen gemeinsam mit Dr. Florian Meier das Projekt zum Vergleich der verschiedenen Kultursysteme in Angriff. Bei Jim Black möchte ich mich für die technische Unterstützung und die Durchführung der ELISAs bedanken. Petra Schrade danke ich für die Aufarbeitung meiner Bioreaktorproben für die Transmissionselektronenmikroskopie und die Einweisung in das beeindruckende Mikroskop. Besonders danken möchte ich meinen Eltern Wolfgang und Dorette Freyer sowie meinem kleinen Bruder Alexander Freyer, die mir immer Sicherheit und Rückhalt geboten und viele gute Ratschläge gegeben haben. Mein größter Dank gilt meinem Freund Marco Stahl, der mich durch alle Höhen und Tiefen dieser Arbeit begleitet und immer unterstützt hat.